Santa Paula Creek Watershed Planning Project: Geomorphology and Channel Stability Assessment

FINAL REPORT

Prepared for
Santa Paula Creek Fish Ladder Joint Powers Authority
California Department of Fish and Game

Prepared by
Stillwater Sciences
2855 Telegraph Avenue, Suite 400
Berkeley, CA 94705

November 2007

Stillwater Sciences

Suggested citation:
Stillwater Sciences. 2007. Santa Paula Creek watershed planning project: geomorphology and channel stability assessment. Prepared for California Fish and Game, Santa Paula Creek Fish Ladder Joint Powers Authority.

Table of Contents

Tables

List of Figures

List of Appendices

1 INTRODUCTION

1.1 Project and Report Overview

Santa Paula Creek, in southwest Ventura County, California, is one of three main historical spawning tributaries for the endangered southern steelhead (*Oncorhynchus mykiss*). The creek holds approximately 30 km (18.5 mi) of habitat once accessible to steelhead (Stoecker and Kelley 2005) but now blocked by in-channel structures that act as migration barriers. Prior mitigation of these barriers has included construction of fish ladders and drop structures. The recent record floods of January and February 2005 severely damaged these fish-passage facilities and caused major channel incision and bank erosion in the lower reaches of Santa Paula Creek, increasing the severity of existing blockages to the upstream steelhead migration corridor. Damaged and non-functioning facilities include the fish ladder at the upstream end of the U.S. Army Corps of Engineers channelization project in lower Santa Paula Creek, the Harvey Diversion fish ladder just above the confluence with Mud Creek, and the Highway 150 drop structure downstream of the confluence of Santa Paula and Sisar creeks (Figure 1-1). Failure of past fish passage structures, as well as damage to the natural functions and resources of the watershed, has been due in part to the lack of accounting for local- and watershed-scale geomorphic processes into structure design (M. Whitman, *pers. comm.*, 2007). This recognition has motivated the need for a more concentrated focus on large-scale, watershed-forming processes in future fish passage solutions.

In an effort to improve fish passage along Santa Paula Creek, the Santa Paula Creek Fish Ladder Joint Powers Authority, in coordination with the California Department of Fish and Game, is sponsoring the Santa Paula Creek Watershed Planning Project. The project is being conducted by RBF Consulting Inc. and Stillwater Sciences. The overall goal of the project is to produce a detailed watershed assessment and a set of restoration alternatives with site-specific, prioritized recommendations for future work leading to restoration of southern steelhead passage throughout historically accessible reaches in the Santa Paula Creek watershed. First-phase project objectives include the following:

- Develop a detailed watershed-scale geomorphic assessment as background to design of improved fish passage and diversion facilities
- Perform a detailed hydrologic and hydraulic analysis for current conditions, future land use conditions, and proposed modified channel conditions for each restoration alternative
- Conducted focused studies of southern steelhead and resident *O. mykiss* behavior, habitat, and population to support the provision of adequate passage and expand upon knowledge gained in previous studies

Together, the in-depth understanding of both watershed geomorphology and steelhead ecology will guide the development of appropriate, long-term engineering solutions for improved fish passage in Santa Paula Creek while maintaining existing water-diversion rights.

To assess the geomorphic conditions in the watershed, Stillwater Sciences was tasked with assessing watershed geomorphic processes from both an historical and present-day perspective. The overall purpose of the resulting geomorphic assessment is to: 1) synthesize existing and newly collected data to better describe the watershed sediment transport and deposition dynamics under existing conditions; and 2) help guide restoration strategies that meet the goal improved fish passage, flood control, and streambed and bank stabilization upstream from the north end of

the U.S. Army Corp of Engineers (USACE) Fish Ladder on lower Santa Paula Creek. This assessment should also contribute significantly to the broader understanding of geomorphic processes and sediment transport in the Santa Clara River watershed (of which Santa Paula Creek is a tributary).

This study constitutes Phase I of the Project and reports quantitative estimates of sediment delivery dynamics and describes elements of historic geomorphic change to advance the understanding of the impacts to future channel conditions. These results will then be integrated into the suite of restoration alternatives for Santa Paula Creek, to be devised in a later Project phase. Results from the hydrology and hydraulics analysis and steelhead studies are presented in companion reports.

This report examines geomorphic processes across the Santa Paula Creek watershed at both the hillslope and mainstem channel scale. At the hillslope scale, field observations combined with literature values were used to construct estimates of average annual hillslope sediment production and delivery to the channel network, based on land cover, geology, and topographic relief. This sediment production is ultimately driven by tectonic uplift across the watershed, with uplift rates determined by prior studies that are reviewed here for context. The calculated rate of sediment production, in turn, can be constrained by empirical data on historic sediment removal in the lower reaches of Santa Paula Creek, which provides a check on the likely accuracy of the methodology we have used. Within the mainstem channel, channel morphologic evolution over the past century was assessed using historic and current aerial photography and topography. Mainstem sediment transport dynamics were then assessed based on current hydrology, bed sediment size, and channel morphologic characteristics. The results from both hillslope and in-channel analyses have then been combined to determine the primary historic and current impacts on sediment transport and delivery within the watershed (both natural and anthropogenic) and develop a conceptual model of geomorphic processes in the lower Santa Paula Creek. The conceptual understanding is then used to summarize important geomorphic characteristics that should inform appropriate future management decisions.

1.2 Regional Setting

Santa Paula Creek is a major tributary to the Santa Clara River, draining approximately 166.5 km^2 (Figure 1-1). The headwaters of the creek are located within the actively uplifting, steep south-facing slopes of the Topatopa Mountains where the maximum watershed elevation is over 2,000 m above mean sea level [MSL]. In the upper watershed, the creek flows through narrow bedrock canyons with steep channel gradients (>6%) and contains large bed particles (dominated by boulders and cobbles). Lower in the watershed, the creek flows through bedrock (narrow reaches) and cobble-dominant alluvial deposits (wide reaches) before entering into the Santa Clara River at the town of Santa Paula. Channel gradients in the lower watershed range from 1.5–2.5% and the channel has incised up to 10 m relative to the adjacent terrace with many reaches showing evidence of active incision and active channel widening. The major tributaries within the lower Santa Paula Creek watershed include (from upstream to downstream) Sisar Creek (29.7 km^2 watershed), Anlauf Canyon (3.7 km^2 watershed), and Mud Creek (7.0 km^2 watershed).

Santa Paula Creek experiences a high degree of annual flow variability, multi-year droughts, and extreme seasonal flooding. Annual precipitation within the watershed ranges from approximately 914 mm within the Topatopa Mountains to approximately 457 mm at the mouth, with over 90% of the annual precipitation occurring within 6 months at both locations (November to April)

(USACE 1995). At the mouth of Santa Paula Creek, annual precipitation ranged from 168 mm (1961) to 1,137 mm (1998) over the past 80 years (VCWPD 2007). Extreme precipitation events (as recorded at the mouth of Santa Paula Creek) occurred in January 1969 (416 mm in 9 days), February 1969 (118 mm in 5 days), February 1978 (214 mm in 8 days), January 2005 (355 mm in 9 days), and February 2005 (242 mm in 6 days) (VCWPD 2007).

Land use within the Santa Paula Creek watershed remains undeveloped compared to other Southern California coastal watersheds to the south. Land use/vegetation cover within the watershed includes scrub/chaparral (52.1% of total area), mixed evergreen/deciduous forest (35.5% of total area), agriculture/herbaceous grasslands (10.5% of total area), and developed/residential (0.8% of total area) (NOAA 2000). The northern portion of the watershed is within the Los Padres National Forest (approximately 65% of total area) and the vegetation cover is entirely chaparral/scrub and mixed forest. The agricultural/developed areas within the watershed are primarily along the mainstem Santa Paula Creek downstream of the Sisar Creek confluence, and within Anlauf Canyon and Mud Creek. Agriculture is dominated by citrus orchards and avocado fields (USACE 1995).

2 HILLSLOPE GEOMORPHIC PROCESSES

2.1 Overview

Soil production and hillslope sediment transport are difficult to quantify, because they are driven by the episodic and commonly transient effects of rainstorms, windstorms, fires, earthquakes, and human and other disturbances (Benda and Dunne 1997, Gabet and Dunne 2003). The inherently episodic nature of erosional processes results in substantial year-to-year variability and makes any assessment of sediment-transport rates sensitive to the timescales over which they are averaged (Kirchner *et al.* 2001). For example, if the basin-wide erosion rate is averaged over a relatively dry 10-year period, it might be considerably lower than if it were averaged over a 10-year period that included several wet years. Although long-term averages cannot predict the sediment load for any given year, they nevertheless can be useful in assessing the long-term consequences of alternative management actions.

As the first step in understanding and quantifying the magnitude of sediment flux down the channel of Santa Paula Creek, this section evaluates the production of hillslope sediment across the watershed, and the delivery of that sediment into the channel network. The rates of sediment production and delivery have been estimated using a variety of techniques, over a variety of temporal and spatial scales, because different scales of analysis can provide more robust and reliable estimates than any single method alone. Over long timescales, best represented by the geologic record of the past several million years, the likely rate of sediment production can be approximated from the rate of overall landscape uplift. This provides a coarse indication of the likely range of average sediment-delivery rates across the watershed as a whole, and one that is completely independent of other methods. Over shorter, more human timescales, rates of sediment production can be assessed using a "process-domain" approach, in which different parts of the watershed are assumed to erode at different rates due to differences in their physical characteristics. The degree to which these two estimates agree with each other, and with additional data that assess rates of in-channel sediment transport directly, provides a measure of the reliability of these results.

2.2 Rates of Sediment Production from Geologic Evidence

Watershed topography reflects the interplay between uplift (if any) due to tectonic processes, and the sculpting and wearing away of slopes by erosion. In general, high steep mountains occur in areas that have been subjected to sustained rapid uplift, whereas gently sloping terrain is found where uplift is slow or has been followed by long periods of denudation. The linkages between uplift, slope steepness, and erosion imply that slopes should tend to contribute sediment in proportion to their uplift rates over the long term (Burbank *et al.* 1996). Uplift rates, in turn, are directly related to the tectonic setting and deformation history of the landscape.

2.2.1 Tectonic setting

The Santa Paula watershed lies in the middle of a distinctive geologic province of California known as the Transverse Ranges. Unlike the Coast Ranges to the north and the Peninsular Ranges to the south, both of whose major ridges and intervening valleys trend generally NW–SE, the Transverse Ranges are oriented almost exactly east–west and form a marked disruption to the

overall grain of California topography (Figure 2-1). Santa Paula Creek drains the south-facing flank of one of these east–west ridges, the Topatopa Mountains.

The regional tectonic activity of California over the last 6 million years has created this unusual topographic and geologic setting. Both north and south of this area, the 1000-km-long (600-mile-long) San Andreas Fault (SAF) separates the northwest-moving Pacific plate from the (relatively) stationary North American plate. Where the SAF is straight, these plates slide past each other as a "transform plate boundary," with either continuous motion (at rates of a few centimeters per year) or stick–slip motion where movement is episodic (and expressed as earthquakes when it occurs). The SAF is deflected from its straight trend, however, at its intersection with a NE–SW trending cross-cutting fault, the Garlock Fault, about 50 km south of Bakersfield. Where the SAF is bent, the Pacific and North American plates cannot simply slip past each other. Because the underlying plate motion continues, the north-migrating rocks of the Pacific Plate "pile up" in the region south of the San Andreas Fault's bend. The crustal shortening that results from this underlying plate movement provides an ideal setting for rapid rates of landscape uplift.

In the Santa Paula Creek watershed, one fault expresses this north–south compression most prominently, the San Cayetano fault, which cuts west-to-east across the watershed just north of lower Sisar Creek and continues east across the headwaters of Anlauf Canyon and Mud Creek. It is a north-dipping thrust fault, where the upper block (north of the fault plane) has slid up the fault plane relative to the rocks of the lower block (south of the fault plane). In the watershed, the San Cayetano fault separates a sequence of hard sandstone and shale (mainly, the Matilija and Coldwater sandstones and the Cozy Dell Shale), all of Eocene age (*i.e.*, about 50 million years old), that has been thrust over the much younger Pico, Santa Barbara, Las Posas, and Saugus formations, all shales and claystones less than 6 million years old. Rockwell (1988) estimates as much as 9 km (5.6 mi) of net vertical offset along this fault. The offset is distributed between a number of closely spaced, sub-parallel fault strands in a zone of deformation about 1 km wide in which rocks have been pervasively shattered and sheared. Where exposures on the ground are good these strands have been mapped in some detail (*e.g.*, Tan and Irvine 2005). Where exposures are poor, individual strands are not shown on published geologic maps, but a similar degree of complexity is assumed to occur along the entire extent of the fault.

A second extensive, but less significant, fault system is the Sulphur Mountain–Sisar fault, which also cuts the Santa Paula watershed along a trend roughly parallel to that of the San Cayetano fault. Although alternate mappings and interpretations of the of the faults' traces have been proposed (Dibblee 1990, Tan and Irvine 2005), all recognize a fault zone that splays west from the San Cayetano fault under or east of the alluvium filling the valley floor of Anlauf Canyon and continues west, to the south of lower Sisar Creek, beyond the boundaries of the watershed as two (or more) separate but sub-parallel strands.

Both the San Cayetano and the Sulphur Mountain–Sisar faults maintain the same gross sense of motion, with rocks on the north side of each fault moving up relative to those of the south. Strands of the Sulphur Mountain–Sisar fault system, however, have steeper orientation (based on their topographic expression) and significantly less total offset (based on the relative age of adjacent rocks) than do those across the San Cayetano fault. The most recent published geologic map (Tan and Irvine 2005) also identifies at least one strand with an opposite sense of motion (*i.e.,* north side down) that cuts the valley of Santa Paula Creek a few hundred meters upstream of the Sisar Creek confluence.

These mapped faults are one expression of the crustal deformation that involves the Santa Paula watershed, and that has resulted in substantial, rapid uplift of the ridges and valleys constituting

the topography of the watershed. The rate of this uplift, in turn, can be determined in several ways, and the evidence for each are explored in the following sections:

(1) Slip rates across faults, which are generally measured in the direction of movement but can also be translated into vertical (*i.e.,* uplift) rates;
(2) Geomorphic features of known age and distinctive environments of formation (such as dated marine terraces that were originally created at sea level), which can provide a direct measure of uplift since their formation; and
(3) Direct geodetic measurements using precisely located benchmarks, which can provide year-to-year determination of movement, both lateral and vertical, of the earth's surface.

Each of these methods have application in the vicinity of the Santa Paula watershed, and they all contribute to a broadly consistent picture of uplift rates. These data sources and results are described in some detail below, because they provide indirect but independent constraints on watershed erosion rates and ultimately sediment-delivery rates to Santa Paula Creek.

2.2.2 Rates of fault slip

Reported rates of fault slip in and around the Santa Paula watershed vary from place to place but they are everywhere rapid. In the Santa Paula watershed itself, many uplifted river terraces provide direct evidence of movement on the San Cayetano fault. One, near the main tributary of Sisar Creek, now lies 13 m above the level of modern fluvial deposition. Rockwell (1988) assigned an age of 15,000–20,000 years based on dated landforms elsewhere in the region with equivalent soil-weathering profiles; this yields an uplift rate between 0.65–0.87 mm a^{-1}. One km east, a younger alluvial fan (estimated age 8,000–12,000 a) shows about 9 m of vertical offset, giving a rate of 0.6–1.2 mm a^{-1}. In this same area but using older landforms, he also inferred an uplift rate of as much as 1.6 ± 0.2 mm a^{-1} over the past 80,000–100,000 years. At the head of Mud Creek, a strand of the San Cayetano fault has produced about 32 m of offset in an alluvial fan of indeterminate age, but estimated by Rockwell (1988) to range between 8,000–20,000 a. Uplift rates inferred from this feature thus lie between about 2–4 mm a^{-1}. Along the trace of the fault, features as young as about 4,000 years old are offset, suggesting that these rates are not only "recent" from a geologic perspective but also probably apply to the modern-day tectonic regime as well. Rockwell's data and interpretations suggest that (1) uplift rates increase to the east along the 40-km-trace of the San Cayetano fault, and (2) rates predicted from older offset deposits may be greater than those predicted from younger deposits, suggesting a reduction in rate over the last 1 million years.

Uplifted features within the watershed also demonstrate differential uplift, with somewhat greater values to the north that tend to increase the gradient of Santa Paula Creek. Although the change is unlikely to be important over human timescales, the north-to-south tilt of the landscape has increased by about 1 degree in the last 10,000 years (Rockwell 1988).

Çemen (1989) also evaluated uplift rates on the San Cayetano fault, but his focus was farther east than that of Rockwell (1988), between the towns of Fillmore and Piru. He found a minimum of 7,300 m of offset in the direction of movement, which for the presumed fault inclination would translate into about 5 km of uplift. The duration over which this movement has occurred is somewhat indeterminate but no greater than about 1,000,000 years, suggesting an uplift rate in this eastern segment of 5+ mm a^{-1}.

Yeats (1988) evaluated evidence for long-term uplift rates on the Oak Ridge fault, which runs roughly parallel to the San Cayetano fault but on the south side of the Santa Clara valley, about 10 km distant. Both faults have formed under the same north–south compressional regime, and

Yeats argues that they should have slip rates of the same general magnitude. Offset bedrock contacts across the Oak Ridge fault, with an (uncertain) age range of 200,000–400,000 a, indicate vertical uplift of 6–12 mm a^{-1} over this time period, higher than the rates found by Rockwell (1988) for the western part of the San Cayetano fault through the Santa Paula watershed but similar to the rates on that fault farther east (see below). Molnar (1991, as cited in Petersen and Wesnousky 1994) reinterpreted some of Yeats' and Rockwell's cross-sections and inferred slightly slower maximum slip rates (7 mm a^{-1}; equivalent to an uplift rate of about 5 mm a^{-1}).

Huftile and Yeats (1995) evaluated overall shortening across the Transverse Ranges in the vicinity of the Santa Paula watershed, relying on some of the same stratigraphic markers as earlier studies. They concluded that the magnitude of shortening across the region was most likely about 5 km in the last 500,000 years, of which about 1/3 was taken up across the San Cayetano fault. This yields a horizontal shortening rate across the fault of 3–4 mm a^{-1}; because the fault angle is about 45^{o}, the resulting uplift rate is of equivalent magnitude.

2.2.3 Rates of uplift from geologic inference

Independent of the fault-slip studies discussed above, uplift rates in the Santa Paula Creek watershed have not been directly assessed. At least three other studies, however, provide direct evidence of uplift rates from regions to the southeast and west of the watershed. In the San Gabriel Mountains, about 60 km SE of Santa Paula, Blythe *et al.* (2000) looked at the cooling history of mineral grains, which can indicate the age at which rocks now at the surface were buried at least several kilometers deep in the crust. The younger that age, the more rapid has been the exhumation of the overlying material. Based on such data, Blyth *et al.* determined likely uplift rates averaging as high as about 1 mm a^{-1} in the eastern San Gabriel Mountains, with less well-determined but significantly lower rates in the western San Gabriel Mountains.

To the west and south of the Santa Paula Creek watershed, uplifted marine terraces along the Pacific Ocean coastline from Santa Barbara south past Ventura and Malibu provide additional constraints. On the well-developed flight of Mesa Hills terraces in the city of Santa Barbara, Trecker *et al.* (1998) determined an overall uplift rate of 0.55 ± 0.05 mm a^{-1}. In the Ventura area, Lajoie *et al.* (1991) determined uplift rates of between 1 and 10 mm a^{-1} for terraces between 1800 and 80,000 years in age. Orme (1998) interpreted these data to show a four-fold decline in uplift rates over the last 200,000 years, ranging from 20 mm a^{-1} at the beginning of this period to 5 mm a^{-1} for the most recent 30,000 years. He also noted that rates decline substantially to the south, with estimates of only about 0.3 mm a^{-1}on terraces flanking the Santa Monica Mountains, about 50 km to the south-southeast.

2.2.4 Recent geodetic uplift measurements

Geologic evidence of uplift must average the inferred rates over periods determined by the age of the rocks or landforms being assessed, which range from a minimum of several thousand years to a maximum of more than a million years. In contrast, Global Positioning System (GPS) networks can make direct measurements of crustal movement over a period of just a few years. Although there are no assurances that short-term rates should equal long-term rates, they can provide independent verification of the general magnitude of each method. Donnallan *et al.* (1993) conducted one such GPS campaign over a 4.6-year period across the Ventura basin to obtain modern rates of north–south convergence. Across their network, spanning a region from about 25 km south of the Santa Clara River valley to just north of the San Cayetano fault, the convergence rates measured by Donnallan *et al.* (1993) were 7–10 mm a^{-1}. Two of their stations straddled the San Cayetano fault directly; they suggest a convergence across that structure of about 2 mm a^{-1}

(although uncertainties in the measurements are of the same magnitude as the measurements themselves). As with the analysis of Huftile and Yeats (1995), horizontal convergence rates on a 45^{o}-dipping fault result in an equal magnitude of uplift.

A second 4-year GPS campaign (Argus *et al.* 1999), focused more to the southeast in the Los Angeles basin but including stations across the Ventura basin, came to very similar conclusions. The Ventura basin displays north–south shortening at rates of about 6 mm a^{-1}, with measured displacements taken up primarily by the Oak Ridge and San Cayetano faults. Although instrument locations were inadequate to separate the relative degrees of motion across these two structures, Yeats (1988) had previously argued that their respective offsets should be approximately equivalent and thus in the range of 3 mm a^{-1}.

2.2.5 Summary of watershed uplift and erosion rates in the Santa Paula Creek watershed

In summary, published rates of crustal uplift in and surrounding the Santa Paula watershed range from about 0.5 mm per year to about ten times this value. Over the last 1 million years, estimates of rates range between 1 and 4 mm a^{-1}, with modest increases both east and west of the watershed and possibly reduced uplift rates over the last several thousand to tens of thousands of years. Uplift is certainly continuing into modern time, and the magnitude of vertical change is about 1–2 meters per thousand years.

"Uplift rates," however, do not directly correlate with erosion rates, and the geomorphic evidence from the Santa Paula Creek watershed indicates that these uplift rates are probably an upper bound on the actual rate of hillslope erosion here. This evidence is primarily in the form of relict uplifted landforms, because faster degradation rates would presumably have consumed these features (Burbank et al. 1996). A line of terraces on the upthrown (northern) block of the San Cayetano fault are particularly prominent in the Santa Paula watershed; the best developed of these is the "Bear Canyon surface" of Rockwell (1988) (Figure 2-2), with an estimated age of 80,000–105,000 years. Correlative surfaces are visible a few km to both the east and west, and they indicate that fluvial downcutting and associated hillslope erosion have not entirely consumed these remnant terrace surfaces. We expect that the actual erosion rate, therefore, is probably between 0.5 and 1 mm per year.

2.3 Coarse and Fine Sediment Production and Delivery

2.3.1 Lithology, erosion, and channel sediment

With rapid landscape uplift to drive hillslope processes and large areas of young, poorly consolidated sediments now hundreds of meters above the valley bottoms, the Santa Paula watershed has geologic characteristics commonly associated with high rates of erosion. The eroded sediment is derived from two distinct sources:

1. Easily eroded siltstone and mudstone, which makes up nearly all of the southern (and topographically lower) part of the watershed and about half of the northern (upper) part of the watershed; and
2. Highly durable sandstone, which is very sparse in the lower watershed but underlies most of the prominent high ridges of the upper watershed. Sandstone boulders also mantle many of the younger terraces that flank Santa Paula Creek but are no longer being transported by the modern channel.

This two-part division into fine-grained (*e.g.*, siltstone) and coarse-grained (sandstone) bedrock components is central to understanding the present behavior, and predicting the future behavior, of Santa Paula Creek. By analogy to other rivers world-wide, the fine-grained load represents the majority of sediment that is delivered by hillslopes into the channel, and transported by the channel down to the trunk valley of the Santa Clara River. Qualitative identification of areas displaying rapid hillslope erosion is uniformly underlain by siltstone and mudstone. The most rapid zones of channel incision also correlate to bedrock lithology; for example, over one meter of bedrock incision in lower Santa Paula Creek just below the Harvey Diversion Dam occurred during a single high-discharge event in 2005. In contrast, the few exposures of sandstone bedrock along the lower channel are consistently zones of minimal erosion.

Delivery of sandstone, however, from hillslopes to channels is also important. The sandstone clasts are resistant to mechanical breakdown during fluvial transport—although they become rounded within a short distance of their initial entry into the stream channel network, they persist throughout their passage down the network, which in many cases requires more than 10 km of transport. Duvall *et al.* (2004) found more than a five-fold difference in rock strength between the two main rock types in the Santa Paula watershed (Matilija sandstone and Pico siltstone). Based on observations along the channel of Santa Paula Creek, this probably underestimates their relative durability to fluvial transport (Figure 2-3). Because of the persistence and dominance of sandstone-derived gravel and boulders in the coarse fraction of bedload sediment, channel morphology is largely determined by the delivery, transport, and floodplain deposition of these clasts. The presence or absence of this sediment in the channel also determines whether any given reach will be alluvial, with a mantle of bed sediment, or non-alluvial, with a scoured channel bottom that exposes the underlying bedrock to potentially erosive streamflow.

The transport of sediment down the channel network is important for assessing potential and actual impacts of that sediment on human infrastructure in the lower watershed. Sediment that enters a low-order tributary does not move steadily downstream; indeed, some sediment may never move into lower reaches at all. This partial decoupling of initial delivery of hillslope sediment from subsequent fluvial sediment transport is particularly important for coarse-grained clasts and will be revisited in greater detail below.

2.3.2 Observed processes of sediment production and delivery in the Santa Paula Watershed

The processes and rates by which sediment is eroded off of hillslopes, and subsequently delivered to the channel network, vary substantially across the watershed. Given the profound differences in mechanical properties of the shale and sandstone bedrock, the processes affecting each must be considered distinctly.

2.3.2.1 Fine sediment production and delivery

Thin-bedded shaley rocks of the Pico, Sisquoc, and Cozy Dell formation cover more than half of the Santa Paula watershed, particularly downstream of the Sisar–Santa Paula confluence, and make the largest contribution to fine sediment production. In this region, the once-horizontally bedded marine sediments of the Pliocene-age (about 2–5 million years ago) Pico Formation has been tipped up to (and beyond) vertical, reflecting many kilometers of crustal shortening since their original deposition. The rock is very weakly indurated and is transported into adjacent stream channels by virtually all known hillslope processes, including creep, rainsplash, rilling, gullying, landslides, and debris flows. The catchment of Mud Creek best displays the hillslope

morphology associated with these rocks (Figure 2-4), and the channel runs turbid at all discharges. A particularly voluminous, slow-moving earthflow encroaches on the channel about two kilometers upstream of the mouth, but areas of sediment input are pervasive wherever these rocks are exposed at the ground surface. Owing to unstable ground and lower annual rainfall at the lower elevations associated with this part of the watershed, vegetation cover is generally sparse and locally absent altogether, further increasing the rates of sediment erosion and delivery from this source.

Higher in the watershed, the Eocene-age Cozy Dell Shale (about 42 million years old [Prothero 2001]) and slightly older fine-grained facies of the Matilija and Juncal formations crop out from elevations of about 600 m (2,000 ft) up to more than 1,800 m (6,000 ft). Although many millions of years older than the Pico Formation and originally deposited in deep marine waters, these rocks now lie atop the Pico formation due to thrusting along the San Cayetano fault (and its subsidiaries). Outside of the fault zone they are much less deformed than the overridden younger rocks, with gentle dips between 10–30^{o} to the southeast, east, and northeast. Although clearly incised by the drainage network, the intensity of hillslope erosion on these older, better vegetated fine-grained units (Figure 2-5) is significantly less than for the younger shales of the Pico Formation.

By analogy to other studies, rates of fine sediment delivery from these rock types should depend on several factors, of which hillslope gradient and vegetation cover are generally the most important (Reid and Dunne 1996). Observations in the Santa Paula watershed affirm this principle, recognizing that vegetation cover is both a cause and an effect of relative hillslope stability. Lack of vegetation cover enhances the rate of sediment delivery; but where the ground is unstable or eroding rapidly, vegetation does not grow well. Gradients are generally moderate in areas underlain by these rocks, because they are not strong enough to stand steeply without rapidly degrading (Schmidt and Montgomery 1995). Over time, nearly all of the broad areas that maintain steep slopes are underlain by active landslides, bounded by rapidly eroding stream channels, or both. Locally, the shale can maintain vertical stream-valley walls, but these areas are of limited extent and owe their existence to relatively recent channel downcutting or lateral erosion.

2.3.2.2 Coarse sediment delivery

Well-indurated sandstone (*i.e.*, well-cemented and very hard), primarily associated with the Eocene-age rocks of the northern Santa Paula watershed (Juncal and Matilija formations) but also locally present as interbeds in the shale-dominated deposits, display characteristic modes of hillslope erosion and channel delivery that are very different from those of the fine-grained deposits. These rocks are quite resistant to surface erosion; unconsolidated soils are generally thin, and so downslope transport by rainsplash, rills, or shallow landsliding is volumetrically limited. In contrast, the rock itself is well-bedded and locally fractured by cross-cutting joints, and so steep bluffs are prone to rockfalls. Accumulations of talus at the base these slopes are susceptible to mass transport or to gullying; the alluvial fan deposits at the base of such channels are commonly choked with coarse, subangular blocks (Figure 2-6).

Sandstone bluffs are preferentially found on west-facing slopes in the north-central and northeastern parts of the watershed. This distribution reflects the predominant gentle east dips of the strata in those parts of the upper watershed outside of the San Cayetano fault zone—where channels here have incised, their valleys will tend to have a gentle slope on the west that follows the dip surface (Figure 2-7) and a steep east wall that crosscuts the primary bedding. The best example of this in the watershed is Topatopa Bluff (Figure 2-8), with its steep western face

overlooking the Sisar Canyon and the surrounding landscape. The gentle slopes on the back side of the bluff, forming the west wall of adjacent upper Santa Paula Canyon, in contrast, supports a mature forest and no significant sediment delivery at all.

The most effective delivery of sandstone blocks into the channel network occurs where oversteepened bedrock slopes abut large channels and rockfalls provide direct input (Figure 2-9). These conditions are only present in a few locales across the Santa Paula watershed, but those locations display a marked upstream-to-downstream change in channel characteristics (Figure 2-10a, b) that demonstrates the importance of these sites to sandstone delivery. These relatively limited locations are primary, perhaps even the dominant, sources of coarse sediment into the channel; even though they are all located upstream of the confluence of Sisar and Santa Paula creeks, they likely supply most of the coarse sediment load for the entire system downstream to the Santa Clara River.

2.3.3 Quantifying sediment delivery locations and rates

No matter how complete the description of processes that move sediment from hillslopes to river channels, a complete reconstruction of sediment-delivery rates over time and space is infeasible. As discussed above, delivery is controlled by such conditions as vegetation cover, rainfall, and the physical properties and topography of the hillslope deposit itself. These conditions, however, can be relatively steady through time, or they can reflect unpredictable external events, which in this part of California are most commonly intense rainstorms, vegetation-destroying fires, and earthquakes (see Stillwater Sciences 2007). As a result, some delivery processes have fairly constant rates (such as soil creep), but many are unpredictably episodic (such a debris flows or rockfalls).

Despite this fundamental uncertainty, different parts of the landscape can be readily identified as to their relative sediment-delivery potential. Given the fortuitous availability of sediment-accumulation data in this region (see Section 2.3), we can also estimate time-averaged rates for these zones of relative sediment production with an opportunity to corroborate these predictions. The value of making such estimates is three-fold: first, the relative contribution of different tributaries and subwatersheds can be identified more precisely; second, the potential influence of vegetation-removing fire can be estimated in a spatial context; and third, a calculated magnitude of sediment flux can be used in the context of future management options for in-channel management actions or structures.

Our approach was to begin with a relative, but qualitative, assessment of process domains. We then determined numeric values for the different categories of sediment production that appear to be regionally appropriate on an annual, unit-area basis. For this quantitative assessment, we relied on data compiled for the earlier study of the Santa Clara River watershed as a whole (Stillwater Sciences 2007), augmented with an updated report of local debris-basin sediment volumes.

2.3.3.1 Relative rates of sediment production

Although many factors determine sediment-production rates from hillslopes, this study focused on three that were judged to impose the greatest range of variability over the Santa Paula watershed: rock type, hillslope gradient, and vegetation cover. Data sources for each were compiled in a GIS environment over the entire watershed at a resolution determined by the coarsest dataset (30 m). Rock types were based on the available 1:24,000-scale geologic maps of the region, emphasizing the maps of Dibblee (1990, 1992) over those of Tan and Irvine (2005)

because the latter displays a much greater cover of shallow landslide deposits that obscure the underlying bedrock material. Mapped units were grouped into categories of "shale," "sandstone," and "unconsolidated Quaternary deposits," reflecting their qualitatively observed erodibility and likelihood of producing coarse sandstone blocks. Slopes were generated directly from the digital elevation model, which in turn was a product of a LiDAR survey across all but the northern-most part of the watershed. Based on observed ranges of relative erosion and slope instability, the continuous range of hillslope gradients was categorized into three groups: 0–10%, 10–20%, and steeper than 20%.

Lastly, land cover was based on a classified Landsat image at 30-m resolution previously developed for the entire Santa Clara River watershed. By an automated classification system, five grouped categories were identified; they largely correspond to vegetation covers of forest, scrub, and agriculture and/or grassland; developed land; and miscellaneous (which included water of the river channel itself, where wide enough to register at this scale, and bare rock).

These three factors (geology, slope, and land cover) could theoretically overlap into 45 possible "process domains"—that is, areas that each have a unique combination of these factors that are the major determinants of hillslope sediment production. In fact, nearly every combination of these factors was represented in the watershed (42 of 45), but one third of the watershed is included in just three types: Shale Scrub 10–20%, Sandstone Scrub 10–20%, and Sandstone Forest 10–20%, and only 18 of the possible combinations cover more than one percent of the total watershed area (Table 2-1).

Maps of the classified slope, geology, and land cover are included in Appendix A.

Table 2-1. Process domains over percent as a percent of total watershed area (representation = 95.5% of the watershed).

Process domains	% of watershed
Shale Scrub 10–20%	12.5%
Sandstone Scrub 10–20%	10.7%
Sandstone Forest 10–20%	9.2%
Shale Forest 10–20%	8.7%
Sandstone Scrub 20–171%	6.5%
Shale Scrub 0–10%	6.2%
Shale Scrub 20–171%	5.3%
Unconsolidated Ag/grass 0–10%	4.8%
Sandstone Scrub 0–10%	4.8%
Sandstone Forest 0–10%	4.6%
Sandstone Forest 20–171%	4.5%
Shale Forest 0–10%	4.1%
Unconsolidated Scrub 0–10%	3.9%
Shale Forest 20–171%	3.3%
Unconsolidated Scrub 10–20%	1.8%
Shale Ag/grass 10–20%	1.7%
Unconsolidated Forest 0–10%	1.5%
Shale Ag/grass 0–10%	1.4%

Representative areas in each of the major categories were visited in the field and categorized into a limited number of relative sediment-delivery rates, based on observed indications of erosion and mass-wasting processes. Although not a direct quantification of those rates, the relative differences between process domains were dramatic, lending confidence to the three-fold division of relative rates. Figure 2-11 demonstrates the significant influence of vegetation on relative sediment yields.

Final assignments of relative sediment yield by type of process domain are listed in Table 2-2.

Table 2-2. Relative sediment production by process domain type.

Process domain	Relative sediment production
Unconsolidated Ag/grass 0–10%	Low
Unconsolidated Forest 0–10%	Low
Unconsolidated Forest 10–20%	Low
Unconsolidated Scrub 0–10%	Low
Shale Ag/grass 0–10%	Low
Shale Forest 0–10%	Low
Shale Forest 10–20%	Low
Shale Forest 20–171%	Low
Sandstone Ag/grass 0–10%	Low
Sandstone Forest 0–10%	Low
Sandstone Forest 10–20%	Low
Sandstone Forest 20–171%	Low
Sandstone Scrub 0–10%	Low
Unconsolidated Misc. 0–10%	Medium
Unconsolidated Misc. 10–20%	Medium
Unconsolidated Misc. 20–171%	Medium
Unconsolidated Developed 0–10%	Medium
Unconsolidated Developed 10–20%	Medium
Unconsolidated Developed 20–171%	Medium
Unconsolidated Forest 20–171%	Medium
Unconsolidated Scrub 10–20%	Medium
Shale Misc. 0–10%	Medium
Shale Misc. 10–20%	Medium
Shale Misc. 20–171%	Medium
Shale Developed 0–10%	Medium
Shale Developed 10–20%	Medium
Shale Scrub 0–10%	Medium
Shale Scrub 10–20%	Medium
Shale Scrub 20–171%	Medium
Sandstone Misc. 0–10%	Medium
Sandstone Misc. 10–20%	Medium
Sandstone Misc. 20–171%	Medium
Sandstone Developed 0–10%	Medium
Sandstone Developed 10–20%	Medium
Sandstone Developed 20–171%	Medium
Sandstone Scrub 10–20%	Medium
Sandstone Scrub 20–171%	Medium

Process domain	Relative sediment production
Unconsolidated Ag/grass 10–20%	High
Unconsolidated Ag/grass 20–171%	High
Unconsolidated Scrub 20–171%	High
Shale Ag/grass 10–20%	High
Shale Ag/grass 20–171%	High
Sandstone Ag/grass 10–20%	High
Sandstone Ag/grass 20–171%	High

A map showing the distribution of the 42 process domain categories across the entire watershed is displayed in Appendix A; their distribution by relative sediment-delivery category from Table 2-2 is shown in Figure 2-12.

This map represents, in effect, a prediction of the relative production of sediment from every part of the watershed. Some of those predictions can be tested directly, which can provide independent evaluation of this approach. For example, the greatest density of pixels representing high-production process domains lies in the subwatershed of Mud Creek; and, distinct of any other channel in the entire watershed, lower Mud Creek in fact runs turbid under all flow conditions. Other lower-watershed tributaries with high predicted sediment-producing areas also display massive valley fills (*e.g.*, Anlauf Canyon) or voluminous alluvial fans at their mouths that flank the Santa Paula Creek floodplain along its eastern margin. Farther up-watershed, sources are more uniformly distributed across the landscape, but the particularly dense clustering of "high" and "medium" areas along the west-central watershed boundary feed sediment to the voluminous alluvial fan that has developed at the emergence of Sisar Creek from the rangefront of the Topatopa Mountains (Figure 2-13).

2.3.3.2 Quantified rates of sediment delivery

Although this qualitative, systematic assessment of sediment-production zones is useful for understanding how the watershed behaves, numeric values for the rates of production and, ultimately, downstream sediment delivery are particularly valuable for applied studies. They can be used to assess the magnitude of downstream sediment loads and the potential consequences of vegetation changes (*e.g.*, by fire or land clearing), and they can also inform the locations where greatest management attention should be invested.

Ventura County Watershed Protection District (VCWPD 2005) has reported the volumes of excavated sediment in their debris basins, including a measured or estimated remaining volume, as of summer 2005. To determine typical delivery rates over the period(s) spanned by these records, we selected a subset of the basins previously evaluated in Stillwater Sciences (2005), all in the general vicinity of Santa Paula Creek across a range of contributing watershed areas. We tallied only those years of accumulation following the first recorded excavation of the basin (so the beginning and ending times were under equivalent, empty conditions). With one exception, all had one to several decades of record (Table 2-3).

Table 2-3. Ventura County debris basin characteristics.

Name	Contrib. area (km^2)	Annual Average Sediment Yield ($m^3\ a^{-1}$)*	Sediment Yield per Unit Area ($t\ km^{-2}\ a^{-1}$)	Years evaluated[a]	Notes
Coyote Canyon Debris Basin	17.8	4,848	517	1969–2005	Back side of South Mountain
Fox Barranca Debris Basin	12.5	4,095	620	1973–2005	Adjacent to Coyote Canyon
Adams Barranca Debris Basin	21.8	22,160	1,931	1998–2005	Just west of SPC
Gabbert Canyon Debris Basin	9.5	10,438	2,085	1969–2005	East of Fox/Coyote
Fagan Canyon	7.5	10,136	2,564	1994–2005	Just west of SPC
Real Wash	0.6	6,487	19,034	1969–2005	Small basin, E of Santa Paula

*Source: VCWPD (2005)

Not surprisingly, the order of annual unit-area sediment accumulation rates is inversely related to drainage area. This is a common outcome of sediment-yield studies, reflecting the "dilution" of high-yield areas with a broader spectrum of process domains and the greater opportunity for storage of sediment (*e.g.*, longer hillslopes, broader floodplains) in larger river systems, which results in lower rates of downstream delivery for a given rate of hillslope production. Because our analysis is based on pixel-scale discriminations in the Santa Paula watershed, maximum delivery rates are probably best represented by the smallest measured areas (in this case, the data from Real Wash). However, the "true" delivery of sediment down the tributaries of Santa Paula Creek also includes the effects of within-watershed storage, and so those measured debris basins with slower filling rates, reflecting (in part) less efficient sediment delivery off of hillslopes into channels, will also be relevant when reconciling different types of sediment-production data.

Assigning specific numeric values to the relative categories of "high," "medium," and "low" sediment delivery is therefore not well constrained. Warrick (2002) calculated an integrated sediment delivery value for the lower Santa Clara River watershed (including Santa Paula Creek) of 2800 $t\ km^{-2}\ a^{-1}$ for suspended load (crudely, the fine sediment contribution). This value is modestly greater than the median value from the debris-basin data above. A combinination of these two estimates suggests a value of 2400 $t\ km^{-2}\ a^{-1}$ for the "medium" category sediment yield, used in the following calculations. A value of 300 $t\ km^{-2}\ a^{-1}$ is used for the "low" category, representative of the lowest yielding Ventura County basins as calculated in Stillwater Sciences (2005). A "high" value of 22,000 $t\ km^{-2}\ a^{-1}$ is used, the maximum of calculated rates for Real Wash (Table 2-3 and Stillwater Sciences [2005], which differ by 10% over somewhat different periods of record).

Although by convention these rates are all expressed on a "per year" basis, both geomorphic theory and common sense acknowledge that actual sediment production is highly episodic, with many years of relatively little production punctuated by erratic pulses of very high delivery associated with large storms. These values are averaged over the period of debris-basin records, namely a few decades, and so they have significant uncertainty—truly extreme rainfall (or rain following fire) events are not included, nor are multi-decadal droughts. There is no basis to assume that they are inherently biased (either too high or too low), but every reason to expect that

year-to-year variability may be of the same order, or more, as the predicted "annual" values themselves.

The results of these assignments, integrated over the individual tributary subwatersheds of Santa Paula Creek, are displayed in the Appendix. Noteworthy results from the major tributaries are presented in Table 2-4.

Table 2-4. Santa Paula Creek sediment yield.

Tributary	Total annual load ($t\ a^{-1}$)	Annual load ($t\ km^{-2}\ a^{-1}$)	Landscape lowering rate ($mm\ a^{-1}$)
Sisar Creek	44,000	2,300	0.9
Upper Santa Paula Creek (to Sisar Ck. confluence)	73,000	1,700	0.7
SPC at Harvey Diversion Dam	146,000	2,100	0.8
Mud Creek	24,000	5,800	2.2
Santa Paula Creek at mouth (*i.e.,* whole watershed)	252,000	2,200	0.8

The overall reliability of these calculations is best evaluated in the context of other, independent data. In tectonically active regions, the rate of landscape lowering through hillslope erosion and fluvial transport is strongly influenced by the rate of landscape uplift. Over long periods of geologic time, these two rates must crudely balance (*e.g.*, Willett and Brandon 2002)—if they did not, either mountains would grow without bounds or topographic relief would be obliterated altogether. Long-term uplift rates can also constrain interpretations of how certain landscape features have formed, particularly river terraces that stand above the level of the modern fluvial system. The previous discussion of uplift rates, as determined by a variety of fault studies and geodetic measurements, indicates a likely watershed-wide rate between 1 and 2 mm a^{-1}. That discussion also noted the morphologic indicators that suggest this is probably an upper bound on the corresponding rate of landscape lowering, because features of uplifted but as-yet uneroded topography are still visible in the watershed. These inferences are consistent with the calculated sediment-production rate here, which corresponds to 0.8 mm a^{-1} of landscape lowering.

Additional data are available from USACE (1995), which reported a long-term average annual sediment deposition rate in their "excavated reach" (extending just upstream of the in-channel fish ladder down to the Railroad bridge) of 45,000 $yd^3\ a^{-1}$ (~65,000 t a^{-1}, assuming a bulk density of 1,900 kg/m^3). During the period 1965–1992, sediment removal volumes ranged from 350,000 yd^3 [500,000 t] (Feb 1978) to 100,000 yd^3 [140,000 t] (Nov 1990 and Nov 1992). These values compare to a calculated average annual load of 252,000 tonnes, suggesting that about one quarter of the predicted total load is deposited in this reach. There is little basis to evaluate the credibility of this prediction, except to note that it is the correct order of magnitude (*e.g.*, the amount deposited does not exceed the predicted total transport amount). If most of the deposited sediment was bedload (presumably just a modest fraction of otherwise suspended load would be trapped in the interstices of the coarser particles), this would imply a bedload-to-total-load ratio of 20–25% and that most if not all of the bedload is trapped in this reach. This bedload ratio is high by the standards of most alluvial rivers, including limited measurements on other channels in the region (see Stillwater Sciences 2005), but it is not implausible. Alternatively, the calculated production of total load from the watershed may be low.

2.3.4 Delivery rates of coarse sediment

Analogous to the procedure for fine sediment, the process domains across the Santa Paula watershed can be evaluated for their relative contribution of coarse sandstone blocks into the channel. This component of the sediment load is highlighted because of the overriding influence of this resistant lithology on the bedload and morphology of the lower river. With the exception of poorly vegetated (*i.e.,* "Ag/grass" land-cover category) unconsolidated deposits, only those areas mapped as having sandstone-dominated lithology were included. This probably results in a modest under-representation of actual sandstone-contributing areas, because unconsolidated deposits under other land covers locally include fluvially transported gravel and boulders from up-basin (Figure 2-14), and because even the shaley units include interbeds of sandstone that were observed to constitute as much as about 10 percent of the deposit (Figure 2-15).

The final assignment of process domains into sandstone-delivery categories are listed in Table 2-5. Their spatial distribution across the watershed is displayed in Figure 2-16.

Table 2-5. Sandstone-delivery by process domain.

Process domain	Sandstone sediment production
Unconsolidated Ag/grass 0–10%	Low
Sandstone Ag/grass 0–10%	Low
Sandstone Misc. 0–10%	Low
Sandstone Developed 0–10%	Low
Sandstone Developed 10–20%	Low
Sandstone Forest 0–10%	Low
Sandstone Forest 10–20%	Low
Sandstone Forest 20–171%	Low
Sandstone Scrub 0–10%	Low
Unconsolidated Ag/grass 10–20%	Medium
Unconsolidated Ag/grass 20–171%	Medium
Sandstone Misc. 10–20%	Medium
Sandstone Developed 20–171%	Medium
Sandstone Scrub 10–20%	Medium
Sandstone Scrub 20–171%	Medium
Sandstone Ag/grass 10–20%	High
Sandstone Ag/grass 20–171%	High
Sandstone Misc. 20–171%	High

The process domain map for sandstone-producing areas emphasizes several features of the sandstone sources. First, landforms expressive of voluminous sediment accumulation do not correspond well to the distribution of high sandstone-production zones. This affirms the common recognition that the coarse load of a channel network, although important for channel morphology and dynamics, is not volumetrically the most significant component of the total load. Second, the areas of "high" production are quite limited, and they correspond well with field-observed localities of abundant sandstone sediment production (see, for example, Figure 2-9). Last, the distribution of sandstone-producing process domains is relatively uniform across the

subwatersheds of Sisar Creek and Upper Santa Paula Creek; conversely, these areas are almost entirely absent from the lower watershed.

Unlike the movement of fine sediment, which tends to correspond closely to the flow of water down the channel network, coarse bedload sediment moves only episodically and is subject to the vagaries of local flow competency, long-term floodplain storage, and hydraulic constrictions. Thus the "coarse sediment connectivity" (Hooke 2003) of a channel network can influence the downstream flux of bedload material as significantly as the initial hillslope supply itself.

The channel network of the Santa Paula Creek watershed displays several examples of this phenomenon. The most prominent observed disconnection of coarse sediment transport occurs at the mouth of the north fork of Little Santa Paula Creek, where a bedrock slot gorge appears to severely constrict the downstream transport of sandstone boulders, effectively eliminating the northernmost watershed from supplying a significant amount of coarse sediment to the downstream system. A less dramatic, but still readily apparent, loss of downstream-moving boulders is imposed by the channel crossing of successive strands of the San Cayetano fault in lower Little Santa Paula Creek. Each is accompanied by a valley constriction, marked by bedrock along the channel banks (and, in one location, mid-valley), and presumably an initial change in the imposed gradient; the fluvial response has obscured any such gradient changes, but the local channel morphology clearly displays a net accumulation of coarse sediment upstream and a reduction in the load farther downstream (Figure 2-17).

This imposed transport reduction in bedload-transport capacity, a consequence of both faulting and hydraulic constriction by the Highway 150 bridge, results in roughly equivalent boulder loads observed in Sisar Creek and Santa Paula Creek at their confluence, despite a three-fold difference in drainage areas and in contributing sources of sandstone.

Anthropogenic influences on coarse sediment connectivity are even more dramatic farther downstream. The lower Highway 150 bridge crossing appears to impose a significant, additional impediment to boulder transport; in consequence, the channel immediately downstream has scoured down several meters and exposes bedrock in the channel banks (Figure 2-18a). The next location in the channel where an equivalent degree of scour occurs is, not coincidentally, immediately downstream of the next significant blockage to boulder transport, the Harvey Diversion Dam (Figure 2-18b).

2.4 Potential Effects of Fire, Vegetation Changes, and Extreme Storms on Sediment Delivery

2.4.1 Fire and vegetation changes

Wildfires are a major contributor to hillslope erosion throughout the arid American West and are particularly devastating in California, where expanding urbanization and fire suppression (which often increases the availability of highly flammable, natural fuels) have been the norm for nearly a century (see Booker 1998 and references therein). Historical records indicate that much of the Santa Clara River watershed has burned at least once since the late 19th century, with many areas of the lower watershed, including South Mountain and the lower Sespe, Hopper, and Piru creek watersheds, burning up to 7 times since 1878. Most of the Santa Paula watershed has burned at least twice in this interval, with some areas seeing as many as five recorded episodes (CDF 2004).

Wildfires often contribute to drastically accelerated rates of sediment supply in subsequent years: hillslopes in steep, arid lands during the post-fire period can respond to winter rains with increased runoff and accelerated erosion, which results in debris flows, landslides, and floods—thus completing what has been dubbed the "fire-flood" sequence (USDA Forest Service 1954).

Literally dozens of studies have been made of the changes in runoff and sediment yield following fire, most recently compiled by Shakesby and Doerr (2006). Most of the work has been concentrated in semi-arid regions of the world with vegetative and climatic characteristics similar to Southern California, and so many of the results have broad applicability to the Santa Paula Creek watershed. From local studies, De Koff *et al.* (2006) measured a 6.6-fold increase in sediment yield from a prescribed burn in chaparral-covered Southern California; Wells (1981) documented up to ten- to hundred-fold increases in sediment transport rates in woodlands of the San Gabriel Mountains. Most of these increases can be attributed to increases in dry raveling rates, both during and immediately after fires, and increases in sediment delivery along post-fire rills (Wells *et al.* 1987; Wells 1987). Reported rates tend to decline rapidly following the first year of post-fine rains, although one study that assessed coarse sediment production separately found elevated rates for at least five years following a burn (Reneau *et al.* 2007). Most reported studies, however, cannot calculate the proportional increase in sediment production because they have limited or no data on pre-fire sediment rates (but well-measured post-fire rates). The compilation of Shakesby and Doerr (2006, their Table 3) lists 25 separate 1st-year post-fire measurements, with rates ranging between 0–414 t ha^{-1} and a median value of about 60 t ha^{-1} (6,000 t km^{-2}). The lone San Gabriel Mountain study reported in this compilation (from Krammes and Osborne 1969) measured 19,700 t km^{-2}.

These published, field-measured values invite a comparison with our modeled sediment-production rates across the Santa Paula Creek watershed, because the existing land-cover conditions can be easily altered to crudely simulate a burned condition. Changes in land cover, in turn, will change the unit-area contribution of sediment to the channel network. This can be simulated by changing each land-cover category in the process-domain analysis to rating appropriate for a minimal level of vegetation cover (Table 2-6). Inserting these sediment-production categories in turn results in a seven-fold increase in predicted sediment production across the watershed as a whole (Table 2-7).

Table 2-6. Categories of relative rates of sediment production assigned for the post-fire scenario.

Process domain	Original sediment-production rating*	Fire scenario sediment-production rating
Sandstone Ag/grass 0–10%	Low	Low
Sandstone Ag/grass 10–20%	High	High
Sandstone Ag/grass 20–171%	High	High
Sandstone Developed 0–10%	Medium	Medium
Sandstone Developed 10–20%	Medium	Medium
Sandstone Developed 20–171%	Medium	Medium
Sandstone Forest 0–10%	Low	Low
Sandstone Forest 10–20%	Low	High
Sandstone Forest 20–171%	Low	High
Sandstone Misc. 0–10%	Medium	Medium
Sandstone Misc. 10–20%	Medium	High
Sandstone Misc. 20–171%	Medium	High
Sandstone Scrub 0–10%	Low	Low

Process domain	Original sediment-production rating*	Fire scenario sediment-production rating
Sandstone Scrub 10–20%	Medium	High
Sandstone Scrub 20–171%	Medium	High
Shale Ag/grass 0–10%	Low	Low
Shale Ag/grass 10–20%	High	High
Shale Ag/grass 20–171%	High	High
Shale Developed 0–10%	Medium	Medium
Shale Developed 10–20%	Medium	Medium
Shale Forest 0–10%	Low	Low
Shale Forest 10–20%	Low	High
Shale Forest 20–171%	Low	High
Shale Misc. 0–10%	Medium	Medium
Shale Misc. 10–20%	Medium	High
Shale Misc. 20–171%	Medium	High
Shale Scrub 0–10%	Medium	Medium
Shale Scrub 10–20%	Medium	High
Shale Scrub 20–171%	Medium	High
Unconsolidated Ag/grass 0–10%	Low	Low
Unconsolidated Ag/grass 10–20%	High	High
Unconsolidated Ag/grass 20–171%	High	High
Unconsolidated Developed 0–10%	Medium	Medium
Unconsolidated Developed 10–20%	Medium	Medium
Unconsolidated Developed 20–171%	Medium	Medium
Unconsolidated Forest 0–10%	Low	Low
Unconsolidated Forest 10–20%	Low	High
Unconsolidated Forest 20–171%	Medium	High
Unconsolidated Misc. 0–10%	Medium	Medium
Unconsolidated Misc. 10–20%	Medium	High
Unconsolidated Misc. 20–171%	Medium	High
Unconsolidated Scrub 0–10%	Low	Low
Unconsolidated Scrub 10–20%	Medium	High
Unconsolidated Scrub 20–171%	High	High

*Values reproduced from Table 2-2.

NOTE: Shaded categories are those altered between the two scenarios. Except for the "Developed" land cover, fire is presumed to raise all sediment yields to that equivalent to "Ag/grass," *i.e.*, "Low" for slopes <10% and "High" for all others, except where a higher non-fire rating has already been applied (namely the "Miscellaneous" category). These are likely conservative assumptions, and so the quantitative estimate is a lower bound on probable first-year sediment increases (assuming rainfall is abundant).

Table 2-7. Changes in predicted land area by sediment-production category and in total sediment yield.

	Current land-cover scenario	Post-fire scenario	Change
By total area (km^2):			
High	4.8	78.5	16-fold increase
Medium	51.6	8.4	6-fold decrease
Low	60.4	29.8	2-fold decrease
By percent watershed area:			
High	4.1%	67.3%	
Medium	44.2%	7.2%	
Low	51.7%	25.5%	
By relative contribution to watershed sediment yield:			
High	41.7%	98.3%	
Medium	51.1%	1.2%	
Low	7.2%	0.5%	
Total Sediment Yield:	**2,160 t km^{-2} a^{-1}**	**15,000 t km^{-2} a^{-1}**	**7-fold increase**

NOTE: Based on the fire-scenario assignments in Table 2-6 and assuming a complete burn of the watershed area. The predicted annual post-fire sediment yield is equivalent to 150 t ha^{-1}, remarkably close to that measured from burned plots in the San Gabriel Mountains (197 t ha^{-1}) by Krammes and Osborn (1969). This rate is equivalent to landscape lowering of almost 6 mm a^{-1}, well in excess of tectonic uplift rates across the watershed, and if achieved would only persist for relatively few years.

This scenario assumes that the entire watershed burns and that a mobilizing rainfall occurs before vegetation recovery, and so from this perspective it is almost certainly a limiting condition. Nearly two-thirds of the watershed has a "High" sediment production rate, with these areas responsible for virtually all sediment. Net watershed-averaged yield is about 15,000 t km^{-2} — well within the range (although significantly above the median) of reported values, world-wide, and entirely consistent with studies more specifically from Southern California. These comparisons offer some confidence in the order-of-magnitude results of this approach, and they would support the future use of the process-domain analysis to explore the consequences of more limited burns in any chosen part of the watershed.

This analysis also carries a cautionary note for any prediction of post-fire erosion. Published literature, and common sense, indicates that the stochastic interplay of summertime burns and subsequent rains will determine the actual consequence of a given fire on the sediment loads. After just a single year the magnitude of sediment-production increases should substantially decline; and after no more than a few years the effect may be nearly indiscernible. Erosion rates of 5 mm a^{-1} (*i.e.*, the lowering rate equivalent to a post-fire sediment yield of 15,000 t km^{-2} a^{-1} from Table 2.7) are not sustainable across this landscape; as vegetation regrows, those rates would return to values more typical of the long-term averages predicted by the process-domain analysis.

2.4.2 Extreme storms

Insofar as sediment delivery in the Santa Paula Creek watershed is event-driven (*i.e.*, most sediment is delivered over short time periods by intense storms), the sediment yield during high-magnitude, infrequent storm events can be as important as assessing average annual sediment delivery for understanding sediment transport dynamics, geomorphic evolution, and the response of engineered structures. Following the 1969 flood events in southern California, Scott and Williams (1978) analyzed the storm-induced sediment yield for Transverse Range watersheds in Los Angeles and Ventura County (which included drainages in and adjacent to the Santa Paula

Creek watershed). We revisited this analysis to assess the magnitude of sediment delivery that could be expected in the Santa Paula Creek watershed during such a significant storm event.

The equation devised by Scott and Williams (1978) for calculating sediment yield for the 1969 flood event (>50-yr return) was derived from multiple regression analysis of watershed characteristics, storm conditions, and measured sediment accumulation in debris basins. Their equation for predicting the sediment delivered in the 1969 storm event, calibrated on data from the region including the Santa Paula Creek watershed, is:

$$\log Sy = 1.244 + 0.828(\log A) + 1.382(\log ER) + 0.375(\log SF) + 0.251(\log FF) + 0.840(\log K)$$

where Sy = sediment yield (yd^3),
A = drainage area (mi^2),
ER = watershed elongation ratio (ratio of the diameter of a circle, having an area equal to the watershed area, to the maximum watershed length parallel to the channel),
SF = area of slope failures ($acres/mi^2$),
FF = a fire factor (product of the area of land not revegetated since the last major fire and the percent of the watershed burned), and
K = a storm factor (measure of antecedent soil moisture conditions and the peak intensity of the storm).

This equation was then used to determine sediment yield from the 1969 storm events for over thirty watersheds throughout Ventura and Los Angeles County. For our application, three catchments were chosen for examination: the Mud Creek Canyon (located in the Santa Paula Creek drainage); Orcutt Canyon (located in the Santa Paula Creek drainage); and Aliso Canyon (located in the next major drainage west of Santa Paula Creek).

The Scott and Williams (1978) analysis for these three watersheds predicts an average sediment yield of about 11,000 t/km^2, five times the average annual Santa Paula Creek watershed sediment yield (as determined in Section 2.3.3.2 of this report). Sediment delivery varies by an order of magnitude between the three sample watersheds (normalized by contributing watershed area), with Mud Creek displaying the highest unit-area sediment yield in accord with our observations (and annual average calculations) there.

This equation also invites an alternative approach to predicting the influence of fire, based on their calibration data set. The "FF" term influences the final result by approximately the one-quarter root of its value (*i.e.*, $FF^{0.251}$). Thus, a 10,000-fold increase in this factor would increase the total predicted sediment yield ten-fold, which approximates the order-of-magnitude change in the sediment production reported from recently and fully burned watersheds (including those reported in Scott and Williams 1978). However, the FF term in this equation only varies between 1 and 100, permitting at most a 3-fold increase in rates as predicted by this equation. This highlights one of the serious shortcomings of regression equations—conditions of interest (*e.g.*, a large watershed burn) that require extrapolation from the actual conditions used to calibrate the equation are likely to yield results that have little physical meaning or applicability.

3 CHANNEL MORPHOLOGY AND SEDIMENT TRANSPORT DYNAMICS

3.1 Overview

The overall understanding of channel geomorphic evolution is driven by characterization of hillslope and fluvial sediment production and transport and channel morpholgic dynamics. These dynamics are influenced by factors that include geologic and topographic controls, climatic conditions, vegetation cover and land use, and channel alteration. Within Southern California watersheds, high rates of tectonic uplift and the semi-arid envrionment result in extremely high sediment production rates and frequent high-intensity, short duration storm events. These two factors contribute to naturally high rates of sediment transport (and watershed sediment yield, see last section) and channel morphologic change. Further, channel modifications that occur (*e.g.*, in-channel sediment removal, bank armoring, building of in-channel structures) can significantly impact sediment transport and morphologic dynamics, thereby causing channel destabilization and accelerated rates of channel incision, aggradation, and bank erosion (*e.g.*, lower Santa Clara river [Stillwater Sciences 2007]).

In an effort to better understand the channel geomorphic evolution of Santa Paula Creek, this section presents an analysis of current and historic fluvial geomorphic characteristics. Current channel geomorphic condition is discussed in the context of flow dynamics, climatic forcing, geologic controls, and in-channel structures and modification. Sediment transport dynamics for current channel conditions are then analyzed to determine the frequency with which the entire bed is mobilized and significant channel geomorphic change occurs. Finally, channel geomorphic change over the past century is assessed to identify the key controls on historic morphologic evolution and inform the projected trojectory future channel morphology. These results will be crucial in guiding the developent of management solutions for improved fish passage in Santa Paula Creek while maintaining existing water-diversion rights.

3.2 Channel Characteristics

3.2.1 Hydrology

Discharge within Santa Paula creek is characterized by long durations of little to no flow punctuated by flood events triggered by short-duration, high-intensity precipitation events that travel relatively quickly through the watershed (see Table 3-1). The annual maximum discharge for Santa Paula Creek, measured at USGS gage 11113500 approximately 2.3 km upstream of the Mud Creek confluence, has ranged over approximately 3 order of magnitude (1 to 780 $m^3 s^{-1}$ [35 to 27,500 cfs]) over the past 73 years (1933 to 2006), with the largest annual maximum flows occurring during WY ("Water Year," from October through the following September) 1969 and 2005 (Figure 3-1). Compiling the annual maximum data show that the discharge expected to be equaled or exceeded at least once in one-half of all years (*i.e.,* $Q_{2\text{-yr}}$) is approximately 36 $m^3 s^{-1}$ (1,254 cfs) (Figure 3-2). Mean daily discharge data (WY 1927–2006) show that, on average, the annual daily mean flow stays below 14 $m^3 s^{-1}$ (500 cfs) (Figure 3-3), most (approximately 99%) of the daily mean flow values over the period of record were at or below 5.7 $m^3 s^{-1}$ (202 cfs), and over 2/3 (approximately 70%) of daily mean discharge values for the entire period of record were at or below 0.3 $m^3 s^{-1}$1 (10 cfs) (Figure 3-4). Mean daily discharge during days with the highest

peak discharge values for the period of record (1969, 1978, and 2005) was well above 142 $m^3 s^{-1}$ (5,000 cfs).

Flood flows within the watershed are extremely 'flashy,' meaning that there is a rapid increase in discharge over a short time period with a quickly developed peak discharge in relation to normal base flow (Ward 1978). A measurement of 'flashiness' is the ratio of the annual maximum instantaneous discharge to the associated daily mean discharge for the day in which the annual maximum instantaneous discharge occurred. Within Santa Paula Creek, this ratio averages 3.6 (range = 1.6 to 8.4 from WY 1933–2005), where as ratios for other coastal watersheds of similar size can be much less. For comparison, the unregulated and undeveloped Big Sur River watershed (Monterey County, CA) has an average 'flashiness' ratio of 2.4. The difference in the 'flashiness' ratios among these watersheds is a function of local storm intensity, topographic relief, geology and soil development, and land use (*i.e.*, vegetation type and distribution, extent of impervious surfaces).

Table 3-1. Largest flood events on record (peak discharge >10,000 cfs).

Date	Peak Discharge (cfs)	Peak Discharge ($m^3 s^{-1}$)
Winter 1884	>10,000a	>319.3
March 2, 1938	13,500	431.1
January 22, 1943	10,000	319.3
January 25, 1969	19,000	606.7
February 25, 1969	21,000	670.6
February 10, 1978	16,000	510.9
February 16, 1980	11,800	376.8
February 12, 1992	10,000	319.3
January 10, 2005	27,500 (maximum of record)	878.2 (maximum of record)

[a] Value estimated from precipitation record and accounts of flood damage.

Periodicity in the pattern of the wet/dry years in the Santa Paula Creek watershed is correlated to the El Niño–Southern Oscillation (ENSO) climatic phenomenon. ENSO is characterized by warming and cooling cycles (oscillations) in the waters of the eastern equatorial Pacific Ocean. ENSO cycles have a 1–1.5 year duration and a 3–8 year recurrence interval. They are related to changes in atmospheric circulation, rainfall, and upper ocean heat content (see Deser *et al.* 2004 and references contained therein). In Southern California, ENSO years are characterized by relatively high rainfall intensities, with rivers and streams exhibiting higher annual peak flow magnitudes than they do in non-ENSO years (Cayan *et al.* 1999, Andrews *et al.* 2004). Santa Paula Creek displays this difference in flow magnitude, shown quantitatively in an analysis of the instantaneous peak flow record for ENSO and non-ENSO years between 1933 and 2005 (Figure 3-5). For ENSO years, there is a greater than 60% probability of peak flow exceeding 142 $m^3 s^{-1}$ (5,000 cfs), whereas for a non-ENSO year there is a less than 7% probability of peak flow exceeding 142 $m^3 s^{-1}$ (5,000 cfs).

ENSO-induced climate change occurs on a multi-decadal time scale that is consistent with the recent shift from a relatively dry climate (averaged over the period 1944–1968) to a relatively wet

climate (averaged over the period 1969–1995) in the North America's Pacific region (Inman and Jenkins 1999). The recent wet period of the ENSO cycle, which likely still continues, is marked by strong El Niño years every 3–7 years, and mean sediment fluxes for Southern California rivers (from Pajaro south to Tijuana) that were approximately 5 times greater than during the preceding dry period (1944–1968) (Inman and Jenkins 1999). Within Santa Paula Creek, this recent wet period appears to be evident within the average annual discharge record pre- and post 1960. Comparison of WY cumulative precipitation (in) and cumulative discharge (ft^3) within Santa Paula Creek shows that there has been more cumulative annual discharge for the same amount of cumulative annual precipitation after WY 1960 (Figure 3-6). As land-use change in the upper watershed upstream of the Santa Paula gage has been moderate since 1933, and there were over twice as many ENSO years from 1961 to 2005 as from 1933 to 1960, an increased storm intensity mechanism (associated with ENSO years) is suggested to be associated with the increased WY cumulative discharge (*i.e.*, increased storm intensity results in less infiltration and relative increase in runoff).

3.2.2 Current channel geomorphic condition

In general, Santa Paula Creek is characterized by very steep, narrow channel within the upper watershed transitioning to a less steep, widening channel within the lower watershed. Within the study area for this project (Highway 150 bridge crossing down to the USACE fish ladder structure), the channel alternates between 'alluvial reaches' (*i.e.,* reaches in which the bed and banks are composed of alluvial material previously transported by the channel) and 'confined reaches' (*i.e.,* reaches in which the bed and banks are composed of bedrock with at most a thin alluvial deposit) that vary in local slope, channel width, and bed particle size. In-channel infrastructure and modifications within Santa Paula Creek further influence the channel geomorphology within these alluvial and confined reaches.

To characterize and better understand current channel geomorphic condition at this local scale, the study area was divided into 8 distinct channel reaches based on alluvial/bedrock-confined setting and infrastructure influence (Figure 3-7) and current (2005) reach geomorphic characteristics were determined (Table 3-2). In general, the reaches have variable, but consistently steep channel gradient ranging from 0.0145 (directly downstream of Harvey Diversion Dam) to 0.0229 (directly downstream of the Highway 150 bridge). Channel width varies considerably, ranging over a factor of 5 from approximately 20.1 m through a the confined reach just downstream of Harvey Diversion Dam to approximately 108.8 m through the alluvial reach adjacent to the northern extent of the town of Santa Paula. Channel bed substrate is relatively coarse, dominated by coarse cobble deposits with exposed bedrock within several confined reaches. Specific detail pertaining to the geomorphic characteristics of each reach is given below.

Table 3-2. Santa Paula Creek Reach characteristics.

Reach ID	Type	Length (m)	Channel gradient[a]	Average channel width[b] (m)	Average channel depth (from terrace)[c] (m)	Facies distribution (% of reach channel area)[d]
R1	Confined	610	0.0229	32.6	10.3	BGC/bedrock (25%) GBC (20%) GBC/bedrock (55%)
R2	Alluvial	1,250	0.0203	60.8	11.2	GC (27%) BGC (55%) GBC (18%)
R3	Confined	215	0.0152	45.9	12.4	BGC (100%)
R4	Alluvial	1,070	0.0216	74.7	6.3	GC (23%) BGC (49%) GBC (28%)
R5	Confined	945	0.0202	65.1	5.7	GC/bedrock (1%) BGC (33%) GBC (66%)
R6	Confined	1,005	0.0145	20.2	11.5	BGC (70%) GBC (9%) GBC/bedrock (20%)
R7	Alluvial	1,190	0.0174	108.8	7.1	BGC (100%)
R8	Confined	955	0.0208	75.4	7.9	BGC (53%) BGC/bedrock (47%)

[a] Slope from thalweg elevation (2005 LiDAR)
[b] Width measured every 150 m (2005 aerial photograph)
[c] Channel depth taken approximately every 240 m (range of 30-850 m) along thalweg trace (2005 LiDAR)
[d] Facies data compiled from channel facies mapping and particle size distribution data (2006). GC = gravelly-cobble, BGC = bouldery-gravelly-cobble [cobble dominates], GBC = gravelly-bouldery-cobble. BGC/bedrock means bouldery-gravelly-cobble over outcropping bedrock. See Buffington and Montgomery (1997) for more detail.

Reach 1 is a confined reach (*i.e.,* bedrock-dominant bank material) whose upstream boundary is the Highway 150 bridge crossing and downstream boundary is a transition in dominant bank material from bedrock to alluvium very close to the confluence with Anlauf Canyon (Figure 3-8),. The channel through this reach has a relatively steep channel gradient (0.0230), narrow average channel width (32.6 m), and is incised down to bedrock in several locations (average depth of channel is 10.4 m below the adjacent left bank terrace). The bed substrate is coarse, transitioning from a shallow very coarse cobble deposits (gravely-bouldery-cobble [GBC]) (D_{50}=72 mm, D_{84}=154 mm) overlying shale bedrock of the Pico Formation at the upstream end to a deeper very coarse cobble deposit at the downstream end (see Appendix B for information on facies designation). The channel bed is organized into a plane-bed morphology at the upstream end of the reach that transitions to a quasi pool-riffle structure at the downstream end of the reach (see Montgomery and Buffington 1997, for channel classification definitions). Along the banks, the alluvial terrace deposit overlying the shale bedrock is relatively shallow, ranging in depth from approximately 1.5–2.5 m. The downstream end of this reach is marked by the channel crossing of the Sulphur Mountain fault, which has uplifted bedrock on the north side relative to the south. At this location, Tertiary bedrock is thrust against Quaternary alluvium, and the left-bank terrace surface is warped down more than a meter across the fault zone.

Reach 2 is a long, alluvial reach that starts at the bottom of Reach 1 and continues downstream to a reemergence of bedrock as the bank material (Figure 3-9). Midway through this reach, the

channel enters a wide, unconfined valley that allows active thalweg migration. The channel through this reach has a relatively moderate gradient (0.0200) and is wide (average width of 70.0 m). Although the channel within this reach is incised (average depth of 11.3 m below the left-bank terrace), the downstream section of the reach is presently depositional, with active channel widening. The bed substrate transitions from very coarse cobble deposit (D_{50}=150 mm; D_{84}=290 mm) into a fine cobble deposit (gravelly-cobble [GC]) (D_{50}=85 mm, D_{84}=130 mm) at the upstream end, then from a coarse cobble deposit (bouldery-gravelly-cobble [BGC]) into a fine cobble deposit at the downstream end. The channel bed is organized into a pool-riffle morphology, with localized incision through bar deposits. Channel widening within this reach provides a local source of both coarse and fine sediment available for local deposition and downstream transport.

Reach 3 is a short, and exclusively bedrock-bounded confined reach that ends at the Steckel Park bridge (Figure 3-10). The reach has a relatively gentle channel gradient (0.015) and an average channel width of 45.7 m, and is very incised below the left bank terrace (average depth of 12.5 m). The substrate through this reach is a coarse cobble deposit, with the bed arranged into a plane-bed morphology. The alluvial terrace deposits through this reach are approximately 3 m thick at the upstream end and become thicker downstream, with large boulders in the alluvial deposit. The emergence of bedrock at the upstream end is likely an expression of dip-slip movement along an unmapped fault that crosses Santa Paula Creek.

Similar to Reach 2, Reach 4 is an alluvial reach whose downstream end is marked by the reemergence of bedrock (Figure 3-10). The reach, located in Steckel Park, transitions from a locally narrow channel at the upstream end to a wider channel at the downstream end with active thalweg migration (Figure 3-11). The channel through this reach is steep (0.022) and relatively wide (average channel width of 74.7 m), and it has aggraded relative to the left bank terrace (average depth is 6.4 m). The substrate is very coarse cobble at the upstream end of the reach and then changes to a coarse cobble to fine cobble bed within the mid-reach depositional zone. The substrate then transitions to very coarse cobble at the downstream end. The bed is organized into a plane-bed morphology in the upstream portion of the reach, and into a quasi pool-riffle morphology at the downstream, more alluvial portion of the reach. There is bank erosion within this reach, resulting in a local source of coarse and fine sediment available for local deposition and downstream transport. There is a bedrock outcrop that marks the downstream end of this reach that tends to backwater flow during high discharges, thus inducing upstream deposition and downstream erosion.

Reach 5 is a confined reach that begins in Steckel Park and ends at Harvey Diversion Dam (Figure 3-12). The channel through this reach has a relatively moderate channel gradient (0.020), is relatively wide (average width of 65.2 m), and is relatively shallow (average channel depth of 5.8 m from left bank terrace). The substrate is relatively coarse, ranging from coarse cobble to very coarse cobble at the downstream end of the reach. The bed is organized into a plane-bed morphology, with a quasi pool-riffle morphology within the low-flow channel and channel banks that are actively widening through the shale bedrock. This reach is the depositional zone for the sediment impounded behind Harvey Diversion Dam.

Reach 6 is a confined reach whose upstream boundary is the Harvey Diversion Dam/Mud Creek confluence and ends where dominant bank material changes from bedrock to alluvium (Figure 3-13). Through this reach, the channel has the most gentle channel gradient of the study area (0.014), is the narrowest (average width of 20.1 m), and is deeply incised (average channel depth of 11.6 m below the left bank terrace). The substrate through the channel is coarse, transitioning from a shallow deposit of very coarse cobble (D_{50}=138 mm; D_{84}=370 mm) over exposed bedrock

directly downstream of the Harvey Diversion Dam/Mud Creek confluence to coarse cobble through the remainder of the reach. The bed is organized into a plane-bed morphology through most of the reach, with a quasi pool-riffle morphology for a short section at the downstream end. The alluvial deposit on top of the floodplain terrace within this reach is relatively thin (approximately 1.5–2.5 m) and is a local source of fine and coarse sediment available for local deposition and downstream transport. Shale bedrock banks are a local source of fine sediment; however, the channel does not appear to be actively widening, so the fine sediment contribution from the bedrock banks is limited. The fine sediment veneer over the coarse bed substrate suggests that this reach is a depositional zone for the sediment load delivered from Mud Creek during events that do not cause significant scour. During large storm events, significant scour can occur within this reach. For example, the WY 2005 flood event caused over 1 m of bed incision, which resulted in the exposure of dam abutments and disconnection of the fish ladder from the channel bed.

Reach 7 is an alluvial reach that, similar to upstream alluvial reaches, is defined at the upstream and downstream boundaries by a transition in dominant bank material (bedrock to alluvium at the upstream end and alluvium to bedrock at the downstream end) and transitions from a locally narrow channel at the upstream end to a wider channel at the downstream end that permits active thalweg migration (Figure 3-14). The reach begins approximately 150 m downstream of the Bridge Street bridge and continues downstream approximately 1,300 m along the northern boundary of the town of Santa Paula, where it ends at a break in channel slope. The channel through this reach has a relatively shallow channel gradient (0.017), is wide (108.8 m), and is aggraded compared to the left bank terrace (average depth of 7.0 m). The substrate through this reach is coarse cobble and the channel morphology is plane bed with an actively migrating thalweg (although frequent channel modification has an impact on in-channel morphology [see next section]). The channel is actively widening in this section during major storms, making the banks a local supply of coarse and fine sediment for downstream transport (see next section).

Reach 8 is an actively incising reach that ends at the USACE fish ladder/channel stabilization structure (Figure 3-15). The dominant bank material within this reach transitions from alluvium to bedrock, with the upstream and downstream extents of Reach 8 marked by significant breaks in channel slope. The channel through this reach is relatively steep (0.0208), relatively wide (average width of 75.3 m), and has a relatively shallow depth (average depth of 7.9 m from left bank terrace). The substrate within the reach transitions from a deeper deposit of coarse cobble at the upstream end to a shallow deposit of coarse cobble where the channel is incised into bedrock. The bed at the upstream end is organized into a plane bed morphology that transitions to a quasi step-pool morphology through the steep, incising, downstream bedrock portion of the reach.

3.2.3 Infrastructure and channel modification

In-channel structures and artificial modifications to the channel (*e.g.*, channelization, sediment removal, and bank alteration) can have significant and long-term effects on channel geomorphic conditions. Permanent structures within the channel affect local and reach-scale flood hydraulics, thereby impacting zones of in-channel and floodplain sediment deposition as well as areas of bed and bank erosion. Removal of in-channel sediment and/or the straightening and armoring of channel banks can destabilize channel gradients, causing channels to incise and local knickpoints to migrate upstream. This section describes the current channel infrastructure through the study reach that have the potential to affect long-term local and reach-scale geomorphic conditions within Santa Paula Creek.

3.2.3.1 Major bridges

Highway 150 bridges/grade control

The Highway 150 bridge (at the upstream end of the study reach) is approximately 55 m long and is over 6 m above the current channel thalweg (Figure 3-16). The bridge was built in the current location sometime after the flood events of January 1969 (the 1947 USGS topographic map shows a smaller bridge upstream of the current location and that the current bridge location was once part of the right bank terrace). Concrete in-channel structures upstream and directly downstream of the bridge were installed as grade control; however, it is not known the date of installation of these structures as it was not possible to obtain detailed bridge information from the California Department of Transportation (Caltrans). Upstream of the bridge, the channel appears to be actively aggrading; downstream, the channel has incised over 2 m below the concrete in-channel structure (Figure 3-17) (aerial photographs suggest that the channel was not incised at this location in 1978). This bridge appears to restricting flow during storm events, causing coarse sediment deposition upstream of the bridge and associated coarse sediment depletion and localized scour downstream of the bridge.

SPTC Railroad truss bridge & Telegraph Road bridge

Within the lower portion of Santa Paula Creek (adjacent to the town of Santa Paula), the Southern Pacific Transportation Company (SPTC) truss bridge and Telegraph Rd bridge have been shown to impact flow hydraulics and sediment transport dynamics during high flow events (Figure 3-18 and Figure 3-19). The SPTC truss bridge was constructed in 1912 as a 30.5-m (100-ft) span with a channel capacity of approximately 283 m^3s^{-1} (10,000 cfs) (i.e., the peak discharge for an 18-year flow event). This bridge span has been identified as the most critical flow constriction along the lower reach of Santa Paula Creek (USACE 1995). For example, the bridge caused significant flow impoundment and subsequent upstream flooding during the January 1969 flood event. The Telegraph Road bridge (approximately 0.4 km downstream of the SPTC truss bridge) was constructed sometime after 1960 and has a 36.6-m (120-ft) span. Its capacity is larger than the SPTC truss bridge but it has been identified as the second most critical flow constriction in the lower reach of Santa Paula Creek, also contributing to localized flooding in Santa Paula during past flood events (USACE 1995).

3.2.3.2 Major In-channel Structures

Harvey Diversion Dam

The Harvey Diversion Dam is an agricultural diversion dam operated by Santa Paula Water Works that currently diverts between 500 to 1,800 acre-feet of water per year for use by Canyon Irrigation District (formerly Farmer's Irrigation District) (USACE 1995). The original structure was built 1.8 m (6 ft) high in 1910 and increased to 7.0 m (23 ft) by 1923 (NMFS Southwest Regional Office website [http://swr.nmfs.noaa.gov/hcd/soCalDistrib.htm]). Repairs were made to the dam in 1928, the dam was rebuilt in 1941, and additional cap repairs were made after major storm events in 1966, 1969, and 1987 (USACE 1995). Recently, sediment transported over the dam during the 2005 storm event scoured a notch at the top of the dam (approximately area = 2.3 m^2) (Figure 3-20), prompting emergency repairs and an additional increase in dam height of approximately 1.5 m (based on field observations). The fish ladder on the right-bank side of the dam was initially constructed in 1939, rebuilt in 1950, and rebuilt again in 2000 to increase fish passage (USACE 1995, NMFS Southwest Regional Office website [http://swr.nmfs.noaa.gov/hcd/soCalHistoric.htm]). Subsequent storm events following construction of the new fish ladder in-filled the lower portion of the ladder with sediment and caused associated structural damage. Until recently, the fish ladder was disconnected from the river during all but moderate to high storm flows as a consequence of the 2005 storm; further in-

channel work has presently reestablished both upstream and downstream connections (Figure 3-21).

USACE fish ladder/channel bed stabilization

The USACE fish ladder was constructed in 2002 as part of the inlet stabilization (*i.e.,* grade control to prevent headcutting and incision) for the downstream USACE-designed flood control project (discussed in the next section) (Figure 3-22). The fish ladder (located approximately 3 km downstream from the Harvey Diversion Dam) is built on bedrock, is approximately 198.1 m (650 ft) long, has a 2:1 side slope (top width = 7.8 m [25.5 ft], bottom width = 4.1 m [13.5 ft]), and has a invert slope of 0.074 (13.5:1) (USACE 1995). The fish ladder suffered structural damage during the 2003 and 2005 storm events.

3.2.3.3 Channelization/sediment excavation

Due to concerns about damage to property and infrastructure during flood events, major channel modifications have occurred between Bridge Road and the SPTC truss bridge over the last 35 years. Flooding as a result of the January and February 1969 storm events motivated regular sediment removal and/or redistribution within this lower portion of Santa Paula Creek. Between Bridge Road and the USACE fish ladder (*i.e.*, R7 and R8), the channel thalweg was until recently maintained at a 1977 channel thalweg elevation, which resulted in approximately 6,500 t a^{-1} of sediment that was excavated and placed at the channel margins to provide some protection to the eroding banks. In the past, channel excavation has been required only after flows exceeding 255 m^3 s^{-1} (9,000 cfs) and/or when the channel thalweg elevation is on average higher than the 1977 channel thalweg elevation (USACE 1995). Under these conditions, the channel can convey the 5-year flood event (HDR 2006). The damage from the recent 2005 flood event within this reach has resulted in a more long-term stabilization of the channel through channel re-design and installation of spur dikes (see HDR 2006).

Between the USACE fish ladder and the Telegraph Road bridge ('channelized reach'), Ventura County has awarded gravel mining contracts to remove sediment deposited during flood events (Table 3-3) (USACE 1995). As in the upstream reach, sediment is removed to maintain the1977 thalweg elevation. Assuming a sediment bulk density of 1,900 kg m^{-3}, the average annual sediment removal rate between WY 1969 and 1992 was approximately 115,000 t a^{-1} and the long-term average annual sediment deposition within this reach is estimated to be approximately 65,000 t a^{-1} (USACE 1995). This long-term deposition rate represents approximately 25% of the total sediment load predicted by the analysis of hillslope sediment production (Section 2.3); the remaining 75% of the predicted total sediment load is presumably transported downstream to the Santa Clara River. The channel within this reach was redesigned in 2000 as part of the USACE flood control project (USACE 1995). The redesigned channel in the channelized reach has 2:1 side slopes, a maintained channel invert slope of 0.0135, and a depth of excavation ranging from 3.7 m [12 ft] (at the downstream end) to 11.0 m [36 ft] (at the upstream end). Following the 2005 flood event, the channel was excavated to convey the 5-year flood event (USACE Los Angeles District website [http://www.spl.usace.army.mil/cms]).

Table 3-3. Sediment removal from the Santa Paula Creek 'Channelized Reach.'

Date	Volume of sediment removed[a] (yd^3)	Mass of sediment removed[b] (t)	Maximum discharge prior to sediment removal (cfs)	Maximum discharge prior to sediment removal (m^3s^{-1})
February 1969	300,000	436,000	22,510[b]	718.8
March 1969	300,000	436,000	21,000	670.6
March 1973	119,000	173,000	13,400	427.9
February 1978	350,000	508,000	11,112[c]	354.8
March 1978	150,000	218,000	16,000	510.9
March 1980	150,000	218,000	11,800	376.8
May 1983	185,000	269,000	4,750	151.7
November 1990	100,000	145,000	3,550 (February 1986)	113.4 (February 1986)
November 1991	150,000	218,000	1,010	32.3
November 1992	100,000	145,000	1,0000	319.3
TOTAL	**1,904,000**	**2,766,000**		
AVERAGE ANNUAL	**79,333**	**115,250**		

[a] from USACE (1995)
[b] assuming a sediment bulk density of 1,900 kg m^{-3}
[c] determined from relationship between daily annual maximum discharge and associated daily mean discharge.

The recent 2005 flood event has prompted in-channel modifications within other reaches of Santa Paula Creek. Within R4, large spur dikes (approximately 2 m high and 15–35 m long) were constructed directly following the 2005 storm event along the right bank where the bank is coming close to undermining infrastructure on the adjacent terrace (Figure 3-23). Within R5, the channel has been re-aligned and deposited sediment has been redistributed in an effort to divert flow away from Highway 150 and to increase the sediment deposition capacity behind Harvey Diversion Dam (Figure 3-24). Immediately downstream of Harvey Diversion Dam in Reach 6, large boulder steps have been installed to act as grade control in an effort to protect the dam structure, decrease localized channel incision, and promote sediment deposition (Figure 3-25)

3.3 Sediment Transport Dynamics

Understanding sediment transport dynamics at the local and reach scale is a crucial component in determining long-term changes to channel morphology. In particular, understanding the relationship between flow and sediment discharge, and the associated magnitude and frequency of sediment-transporting events, allows for the determination of short-term (individual storm) and long-term (cumulative over time) watershed sediment yield, and can also indicate the channel 'dominant discharge' (*i.e.*, the channel-forming discharge that transports the most sediment) (Wolman and Miller 1960). Determining the discharge required to mobilize the coarser fraction of bed sediment ("incipient motion") can indicate when the majority of bed sediment is in mobilized, which has implications for local bed incision and aggradation dynamics (see Buffington and Montgomery [1997] for detailed discussion) and is therefore critical in devising practical, long-term engineering design solutions for in-channel structures and maintenance measures.

In order to understand the sediment-transport dynamics of lower Santa Paula Creek, two analyses were conducted: 1) an analysis of sediment discharge dynamics above the Mud Creek confluence

over the past 77 years; and 2) an analysis of the critical threshold discharge required to mobilize cobble- to boulder-sized sediment (Q_{crit}), and the associated return period of Q_{crit}, at several locations within the study reach. Combined, these analyses elucidate both spatial and temporal trends in sediment transport dynamics within Santa Paula Creek.

3.3.1 Sediment discharge

Sediment discharge dynamics in Santa Paula Creek was examined in two ways. First, the daily mean flow record for Santa Paula Creek was combined with a watershed sediment-rating curve to determine sediment yield for both individual storm events and on an annual basis. Secondly, the watershed sediment-rating curve was combined with the distribution of daily mean flows (*i.e.*, flow frequency) to determine the magnitude and frequency of sediment transporting flows within the watershed and investigate the 'dominant discharge' in Santa Paula Creek.

Flow and sediment discharge data used in the analysis were derived from data for the Santa Paula Creek watershed and an adjacent watershed with similar characteristics. The daily mean flow data was compiled from the Santa Paula Creek gage upstream of the Mud Creek confluence (USGS gage 11113500) for WY 1928–2006 (see Figure 3-3) and flow frequency was determined by dividing the daily mean flow into log-based bins (*i.e.*, bins were defined by increasing the exponent by 0.1) ranging from 10^{-1} (0.1 cfs) to 10^{4} (10,000 cfs) and fitting a regression through the relationship. The sediment discharge rating curve was calculated as a combination of the suspended sediment load and bedload. As there is no known sediment discharge data available for Santa Paula Creek, the sediment discharge rating curve for the adjacent Sespe Creek watershed (derived in Stillwater Sciences 2005) was used in this analysis due to the similarity in watershed land use (chaparral dominant in both watersheds), geology (Eocene sandstone and shale is dominant in both watersheds), and topography (similar drainage density and topographic relief) (see Warrick 2002). The suspended sediment discharge data (and the associated flow data) for the Sespe data was compiled and a regression was fitted through the relationship. Bedload discharge at the Sespe Creek gage was calculated as 10% of the total suspended load (as suggested by Williams [1979] for Southern California Rivers) and a regression was fitted through the data [see Stillwater Sciences 2005]. This 10% value was assumed in a previous analysis of sediment transport dynamics in the Santa Clara River watershed (Stillwater Science 2007) and although lower than the 20–25% value for the bedload to total load ratio estimated in Section 2.3.3.2, it is an appropriately more conservative value for use in subsequent applications. The suspended rating curve and bedload rating curve where combined to give an overall sediment rating curve for Sespe Creek that was then applied to Santa Paula Creek (Figure 3-26).

Although there are many similarities in watershed characteristics between Sespe Creek and Santa Paula Creek, there are significant limitations in using the Sespe Creek sediment rating curve as a surrogate sediment rating curve for Santa Paula Creek. Sediment rating curves are site-specific, taking into account watershed-scale variables (upstream geology, land use, topographic relief, and watershed size) as well as local in-channel impacts that affect local channel aggradation and incision dynamics. In this case, even though land use, geology, and topography are similar between the two watersheds, there is a large difference in watershed size that affects scaling of runoff rate and sediment transport dynamics and leads to inherently different values of sediment discharge for the same flow. There are also differences in the size and extent of in-channel impacts to sediment transport dynamics (in-channel structures, bedrock constrictions) between the two watersheds that will also cause differences in sediment transport for the same flow. Although these differences prohibit use of the Sespe Creek rating curve to get actual values of sediment discharge from Santa Paula Creek, trends in sediment discharge can still be assessed assuming a similarity in sediment rating curve slope for two watersheds. This assumption

appears validated by the similarity in sediment rating curve slope for Sespe Creek and two other locations in the Santa Clara River watershed (see Stillwater Sciences 2005). Therefore, the Sespe Creek sediment rating curve is used within the analysis to determine relative variability in annual sediment discharge and to identify patterns in the long-term record of individual sediment discharge events.

The annual sediment yield estimate for WY 1928–2006 within Santa Paula Creek upstream of the Mud Creek confluence (as a fraction of the long-term average) is shown in Figure 3-27. Sediment discharge is estimated to have ranged from 0.25% of the long-term average (WY 1951) to approximately 2400% of the long-term average (WY 1969), with 3 years (WY 1969, 1978, and 2005) accounting for over half of the total sediment yield over the period of record. Examination of the sediment yield from Santa Paula Creek within the context of the regional ENSO signal within Southern California rivers shows that sediment delivery within ENSO years has accounted for nearly all of the sediment delivery over the period of record (WY 1928–2006). Furthermore, the data show that average annual sediment yield has been over 5 times higher in the recent wetter period (post-1960).

The magnitude-frequency analysis of sediment transport (using daily mean discharge) is shown in Figure 3-28. These data show that the majority of sediment transport in Santa Paula Creek occurs during very brief intervals. These data also show that the "dominant discharge" is in fact the highest flow on record (*i.e.,* the daily mean discharge that has delivered the most sediment over the entire period of record is the single day with the highest daily mean discharge) (see Figure 3-3). This trend matches the results for other Santa Clara River watershed locations (see Stillwater Sciences 2005) but contrasts significantly to the observations for alluvial rivers in more humid environments. In humid environments, the dominant discharge is the flow that, over the long-term average, performs the most work in terms of sediment transport and is similar in magnitude to the bankfull discharge (Wolman and Miller 1960). Because the "dominant discharge" corresponds to the largest flow on record, Santa Paula Creek will not behave like a classic alluvial river and will not exhibit equilibrium tendencies, with small, year-to-year fluctuations around a long-term average condition. Instead, the channel and its floodplain are prone to dramatic changes due to episodically high flows that change the dynamics of the entire system with the potential to completely alter roughness and channel shape, with significant fluctuations in local channel bed elevation.

3.3.2 Threshold for coarse sediment mobility

The overall approach for determining the threshold discharge for mobilizing coarse sediment (*Qcrit*) within Santa Paula Creek was to first determine the critical depth of flow (H_{crit}) required to mobilize the coarsest fraction of bed particles (D_{90}) and then to use $Hcrit_{D90}$ to determine the associated critical discharge (by two separate methods) and return interval. The critical threshold for coarse sediment mobility was calculated at seven locations throughout the study reach (Figure 3-7). The locations were selected in reaches that are relatively uniform and therefore most likely to have steady flow during storm events, and, for the most part, where particle-size distributions were measured. In order to integrate the results of incipient motion analysis with the parallel study of flow hydraulics for this project, the specific locations were also chosen to correspond to stations in the HEC-RAS hydraulic model.

The equation used for calculating $Hcrit_{D90}$ was derived from the boundary shear stress equation ($\tau = \rho_w gHS$),

$$Hcrit_{D90} = \frac{\tau_{critD90}}{(\rho_w g S)} \quad (1)$$

where ρ_w= 1,000 kg/m^3 (density of water), g = 9.81 m/s^2 (gravitational acceleration), S = reach-scale slope, and $\tau_{critD90}$ is the critical shear stress required to mobilize D_{90} (the particle size that is larger than 90% of the surface particles present [m]), which can be calculated by the Shields stress equation (Shields 1936),

$$\tau_{critD90} = \tau^*_{critD90}(\rho s - \rho w) g D_{90} \quad (2)$$

where ρ_s = 2,650 kg/m^3 (assumed bed particle density), and $\tau^*_{critD90}$ is the dimensionless Shields stress. Substituting (2) into (1) yields

$$Hcrit_{D90} = \frac{[(\tau^*_{critD90})(\rho_s - \rho_w)(D_{90})]}{(\rho_w)(S)} \quad (3)$$

The input values used for D_{90}, S, and $\tau^*_{critD90}$ are shown in Table 3-4. The values for D_{90} came from the particle size distribution and facies data, S values are from the 2005 LiDAR data (compiled for R1 through R5, R6, and R7), and $\tau^*_{critD90}$ was derived from the equation given by Ferguson (1994) for the Roaring River

$$\tau^*_{crit_i} = 0.074\left(\frac{D_i}{D_{50}}\right)^{-0.87} \quad (4)$$

where, for this analysis, D_i is D_{90} and $D_{50,}$ the median grain size from particle-size distribution and facies data. The equation for the Roaring River was chosen due to the similar hydraulic conditions as Santa Paula Creek (*i.e.*, similar D_{50} values and reach slope). The exponent in Equation (4) is a 'hiding factor' where a value closer to -1 indicates a lower degree of bed particle embeddedness and a similarity in the discharge required to move all of the bed particles (*i.e.*, equal mobility) (Parker 1990). The bed particles in Santa Paula Creek are not very embedded relative to other river systems and the coarse bed particles in particular are, for the most part, located either on top of bedrock or other finer sediment, or as exposed bar deposits within the active channel. It is therefore assumed that the 'hiding factor' derived for the Roaring River is a high value for Santa Paula Creek (*i.e.*, the Santa Paula Creek value is likely closer to -1) and that the calculated values for $\tau^*_{critD90}$ and $Hcrit_{D90}$ are relatively high estimates (see Table 3-4 for values).

Table 3-4. Summary of the threshold discharge for coarse sediment mobility (Q_{crit}) analysis.

		Sediment Transport Location (HEC-RAS Cross-section)						
		1 (32799.65)	**2** (31651.29)	**3** (30399.71)	**4** (27199.77)	**5** (19199.85)	**6** (14397.72)	**7** (11197.76)
Input Variables	Facies type	BGC	GBC	GC	BGC	GBC	BGC	BGC
	Pebble count location?	Y	Y	Y	N	Y	N	N
	D_{50} (m)	0.072	0.150	0.085	0.072[a]	0.138	0.072[a]	0.072[a]
	D_{90} (m)	0.230	0.310	0.165	0.230[a]	0.390	0.230[a]	0.230[a]
	Estimated Manning's *n*	0.050	0.050	0.050	0.050	0.050	0.050	0.050
	$\tau^* crit_{D50}$	0.074	0.074	0.074	0.074	0.074	0.074	0.074
	Slope (*S*)	0.0205[b]	0.0205[b]	0.0205[b]	0.0205[b]	0.016[c]	0.016[c]	0.0208[d]
Output Variables	$\tau^* crit_{D90}$	0.027	0.039	0.042	0.027	0.030	0.027	0.027
	$Hcrit_{D90}$ (m)	0.5	1.0	0.6	0.5	1.2	0.6	0.5
	width at $Hcrit_{D90}$ (m)	15.2	30.5	32.6	27.4	18.3	18.3	14.0
Mannings Equation Results	$Acrit_{D90}$ (m^2)	4.8	21.4	6.8	12.9	20.7	16.7	5.3
	$Qcrit_{D90}$ ($m^3 s^{-1}$)	8.6	60.5	13.1	23.2	59.2	31.4	9.5
	$Qcrit_{D90}$ ($ft^3 s^{-1}$)	303	2,135	464	818	2,090	1,110	335
Unit Critical Discharge Results	$qcrit_{D90}$ ($m^2 s^{-1}$)	1.0	2.7	1.1	1.0	3.6	1.4	1.0
	$wcrit_{D90}$ (m)	9.6	21.8	12.4	25.8	17.1	26.2	10.7
	$Qcrit_{D90}$ ($m^3 s^{-1}$)	9.4	59.0	14.1	25.3	61.1	36.1	10.3
	$Qcrit_{D90}$ ($ft^3 s^{-1}$)	331	2,085	499	893	2,158	1,273	364
Recurrence of $Qcrit_{D90}$ (yrs)		**1.23–1.25**	**2.65–2.75**	**1.36–1.39**	**1.65–1.70**	**< 2.65–2.75**	**< 1.88–2.02**	**< 1.25–1.28**

[a] from particle size distribution data at locations with the same facies type
[b] from 2005 thalweg elevation (R1 through R5)
[c] from 2005 thalweg elevation (R6 through R7)
[d] form 2005 thalweg elevation (R8)

The $Qcrit_{D90}$ at each location was then determined by two separate methods: the Manning's Equation and the Unit Critical Discharge Equation (Bathurst 1987, Ferguson 1994). Manning's Equation derived $Q_{critD90}$ as function of $Hcrit_{D90}$, channel roughness, slope and area:

$$Qcrit_{D90} = \frac{1}{n}\left[H^{2/3} S^{1/2} \right] * Acrit_{D90} \quad (5)$$

where *n* is Manning's roughness coefficient (Manning's n) and $Acrit_{D90}$ is the cross-sectional critical flow area (see Table 3-4 for values). The value for Manning's n used in the analysis was 0.050 for all of the locations and was estimated from information on rivers with similar flow hydraulics and particle sizes (Barnes 1967). The critical flow area ($Acrit_{D90}$) was determined by combining the $Hcrit_{D90}$ values with the channel elevation data (taken from the RBF HEC-RAS model) and calculating the flow area under the $Qcrit_{D90}$ water surface at each location. The return period (recurrence interval) for the $Qcrit_{D90}$ values was then derived from the flood frequency curve for the gage on Santa Paula Creek upstream of the Mud Creek confluence (USGS gage 11113500)

The Unit Critical Discharge Equation derives $Qcrit_{D90}$ as a function of $Hcrit_{D90}$, bed particle size, slope, and effective flow width:

$$Qcrit_{D90} = \frac{a \cdot (D_{50})^{1.5} \left(\frac{D_{90}}{D_{50}} \right)^{0.19}}{S^{1.37}} * (w_{critD90}) \quad (6)$$

where $a = 0.198$ and is a function of the product of $Hcrit_{D90}$ and $\tau^*_{critD50}$ (0.074 from equation (4)) and includes the hiding factor that takes accounts for the effect of bed particle embeddedness on sediment mobility (see Ferguson [1994] for more detailed derivation). Effective critical flow width ($w_{critD90}$) was then calculated by dividing $Acrit_{D90}$ by $Hcrit_{D90}$. The return period (recurrence interval) for the $Qcrit_{D90}$ values was then derived from the flood frequency curve for the gage on Santa Paula Creek upstream of the Mud Creek confluence (USGS gage 11113500)

The $Qcrit_{D90}$ values derived from each method (and the associated recurrence interval) are shown in Table 3-4. In general, both methods for calculating $Qcrit_{D90}$ produced very similar values at individual stations, suggesting that assumptions inherent in both methods had the same effect on calculated value of $Qcrit_{D90}$. The calculated $Qcrit_{D90}$ values ranged from 8.6 $m^3 s^{-1}$ (recurrence interval of 1.23 years) to 60.5 $m^3 s^{-1}$ (recurrence interval of 2.75 years). The locations where D_{90} is within the coarse cobble range have $Qcrit_{D90}$ values with a recurrence interval less than 2 years, while the locations where D_{90} is in the boulder range have $Qcrit_{D90}$ recurrence interval values that range between 2 and 3 years. These data suggest that coarse size fraction of the bed (and therefore the majority of bed sediment) is mobilized under fairly frequently occurring flows. Overall, the steep reach slopes within Santa Paula Creek act to promote entire bed mobilization throughout the study reach for flows statistically expected to occur (over a long time period) at least once every 3 years under the current slope and bed particle size conditions. These results seem consistent both with the highly changeable morphology of the channel bed in the lower Santa Paula Creek and with the fairly frequent damage caused to the crest of the Harvey Diversion Dam by large particles in transport.

3.4 Channel Morphologic Evolution (1901-2005)

Understanding the historic changes to channel morphology can be important in determining the expected future trajectory for channel evolution. In particular, determining how a channel has responded to watershed perturbations such as major storm events, changes in sediment and/or water input, and in-channel modifications (*e.g.*, in-channel structures and sediment removal) can give insight into how the channel will continue to adjust to existing conditions and how it will subsequently respond to future watershed perturbations. In an effort to elucidate causes for geomorphic change and inform future geomorphic conditions, channel morphologic characteristics (channel thalweg location, channel thalweg elevation/slope, and channel width) in Santa Paula Creek were compared over the past 100 years. Data sources included orthorectified topographic maps from 1901, 1947, and 2005, and aerial photography from 1969, 1998, and 2005. Although the 1969 and 2005 data were collected directly after the 2 largest storm events on record, these data are still considered useful in making an assessment on overall channel geomorphic evolution. In order to characterize upstream and downstream geomorphic impacts of in-channel structures, the portion of Santa Paula Creek of interest within this project was divided into two geomorphic zones: Sisar Creek confluence/Highway 150 bridge to Mud Creek confluence/Harvey Diversion Dam (R1–R5), and Mud Creek confluence/Harvey Diversion Dam to lower Santa Paula Creek (R6–'channelized reach'). Changes in channel morphology and factors affecting the geomorphic change are presented below.

3.4.1 Recorded morphological changes

Over the past 100 years, Santa Paula Creek between the Sisar Creek confluence/Highway 150 bridge and the Mud Creek confluence/Harvey Diversion Dam has migrated within an active channel valley with pronounced incision at the upstream end followed by pronounced channel downstream aggradation and localized channel widening in downstream portion of the zone (Figure 3-29 and Figure 3-30). Specific historical changes include the following:

- Between 1947 and 2005, channel thalweg position changed within R2, decreasing local sinuosity, and stayed relatively static through reaches 1, 3, and 5. Channel thalweg position in 1901 is suggested to be on the current left bank terrace through R1 and at the downstream end of R5, starting just upstream of the Mud Creek confluence (however, there is no evidence of the historic channel on the left bank terrace in the 1969, 1998, or 2005 aerial photographs).

- Comparison of the channel thalweg data from 1901/1947 and 2005 shows approximately 4.6 m (15 ft) of incision through R1 and approximately 4.6 m of average aggradation within R2 through R4 (with an associated decrease in thalweg slope from 0.0231 to 0.0205) (Figure 3-30). Within R5, the 2005 channel thalweg elevation shows approximately 3 to 6 m (10 to 20 ft) of aggradation compared to 1947 (when the channel was in the same location) and is at same approximate elevation as the 1901 channel thalweg (when it is thought that the channel was located on the current left bank terrace).

- The decreased channel slope and increased channel aggradation within R2–R5 resulted in increasing bank erosion and channel widening within alluvial reaches: between 1969 and 2005, the average channel width within the downstream section of R2 increased approximately 10 m (Figure 3-31a).

Compared to the upstream geomorphic zone, Santa Paula Creek downstream of the Mud Creek confluence/Harvey Diversion Dam shows significant variations in position, elevation, and width from 1901 to 2005 (Figure 3-29 and Figure 3-30). Specifically, this geomorphic zone is characterized by a long depositional reach characterized by channel slope decrease and local widening located between reaches with significant channel incision. Specific historical changes include the following:

- The 1947 channel thalweg is essentially in the same location as the current (2005) channel thalweg. However the 1901 channel thalweg was shown to be on the left bank terrace at the Mud Creek confluence, was within the current channel location through R6, and was again on the left bank terrace through R7 and into R8 approximately 200 m from the current (2005) location, which is corroborated by the 1947 USGS topographic map (Figure 3-28b).

- Within R6 and R7, comparison of the channel thalweg data from 1901 and 1947 shows maximum of 10 m (30 ft) of incision through R6 and converging channel thalweg elevations through R7 (Figure 3-30). Comparison of channel thalweg elevation within R6 and R7 between 1947 and 2005 shows local incision at the upstream end of R6, downstream aggradation of approximately 3 m (10 ft), and then convergence of channel thalweg elevation through R7 (and a decrease in reach average slope form 0.0174 to 0.0165). Within R8 and the downstream 'channelized reach,' comparison of the channel thalweg data from 1901/1947 and 2005 shows approximately 3 m (10 ft) of incision within both reaches (Figure 3-30).

- The decreased channel slope and increased channel aggradation through R6 and R7 has resulted in increasing bank erosion and channel widening: between 1969 and 2005, the channel width within R7 has increased by a maximum of 150 m (500 ft) and has been suggested to have doubled in average width from 1996 to 2005 (HDR 2006) (Figure 3-31b).

- The channel historically flowed through an alluvial deposit within R8 (as is evident in the 1969 aerial photograph) (Figure 3-32) but is now incising and locked into place with a confined bedrock chute composed of easily-erodible siltstone.

3.4.2 Mechanisms for historic geomorphic change

Understanding the causes of historic channel geomorphic change is an essential precursor for projecting the future channel geomorphic trajectory. Causes of change in Santa Paula Creek include natural (intrinsic) factors related to the geology and tectonics of the watershed, and its historical pattern of storms. Other mechanisms for geomorphic change are linked more closely to human activities in the watershed and include the indirect influence of land cover changes associated with evolving land uses (mostly vegetation clearance for agriculture and urban development), and more direct impacts related to in-channel infrastructure and channel modifications. In combination, these various factors determine the pattern of morphologic change in lower Santa Paula Creek since Euro-American arrival in the watershed, and as (partially) reflected in the historical evidence outlined in Section 3.4.1.

A primary control on channel geomorphic evolution within the Santa Paula Creek watershed is the geology and tectonics of the watershed. Regional faults that run perpendicular to Santa Paula Creek control the locations of confined bedrock reaches and unconfined alluvial reaches. In particular, the overall gradient of lower Santa Paula Creek is likely determined by the regionally

significant San Cayetano fault that parallels the trend of lower Sisar Creek, crossing Santa Paula Creek in a zone of locally uplifted as possibly tilted bedrock blocks just north of the Sisar Creek confluence. Within the study reach, the Sulphur Mountain fault crosses Santa Paula Creek near the confluence with Anlauf Canyon, less than 1 km downstream of the Highway 150 bridge, and has resulted in a bedrock channel constriction that appears to limit the propagation of incision downstream of the Highway 150 bridge in reach 1. More generally, rapid rates of tectonic uplift within the watershed (estimated to be between 1–2 mm a^{-1}) in association with the highly sheared and fractured local shale and sandstone geology result in extremely high erosion rates and consequent high rates of both fine and coarse sediment production, and steep channel gradients throughout the entire watershed. Once sediment is delivered into the channel network, steep channel gradients (1.5–2.5% in the study reach to over 6% in the upper watershed) promote frequent mobilization of the entire bed (including the largest size fraction of bed sediment) and high downstream sediment yield throughout most of the watershed. Geologic restrictions on downstream sediment yield do occur in the watershed and include narrow bedrock gorges and fault-induced bedrock steps that act to impede coarse sediment transport during high flow events. Some version of this mechanism may also be in part responsible for the recent widening of reach 7 above the recently exposed bedrock in reach 8.

Storm sequence and frequency are a second control on the historic channel geomorphic evolution within the Santa Paula Creek. Sediment transport analysis (presented in Section 3.3) from daily mean discharge shows that the days with the highest peak discharges on record (2/25/1969, 2/10/1978, and 1/10/2005) combined to deliver over half of the total sediment yield from WY 1928–2005 through lower Santa Paula Creek (see Figure 3-27). Sediment transport rates of this magnitude are expected (and have been observed) to have significant impact on channel migration/bank erosion, local- and reach-scale incision/aggradation dynamics, and channel slope. Historically, several individual large storm events within the watershed (*i.e.*, 1884, 1969, 1978, and 2005) have likely had persistent impacts on channel morphologic characteristics. Anecdotal evidence suggests that the 1884 event transported a significant amount of sediment through the Santa Paula Creek watershed, causing widespread incision of over 3 m within many Santa Paula Creek tributaries and triggering massive debris flows within the watershed (L.M. Hardison, as cited in USACE 1995). The 1884 storm may have been especially significant in morphologic terms because it occurred after the introduction of extensive ranching in the Santa Clara watershed from the 1820s on, and after a prolonged period of drought during the 1860s and 1870s (which resulted in a dramatic reduction in cattle numbers). As such, we can assume that vegetation cover in the watershed was very low, enabling accelerated rates of runoff through the watershed, and extremely high rates of sediment production. Therefore, this event may have represented a significant period of incision in Santa Paula Creek (*i.e.*, away from the creek operating much closer in elevation to the left bank terrace shown in Figure 3-29) and, potentially, to the exposure of Sulphur Mountain fault in the upstream end of reach 2. Furthermore, because the frequency of large storm events is highly correlated to ENSO climactic phenomenon (see Figure 3-5), significant morphological changes will occur in the creek far more frequently during ENSO wet periods, such as from 1969 to present, when high peak discharges occur statistically every 3 to 8 years (including the especially high flows of 1969, 1978, and 2005).

The morphology of Santa Paula Creek is highly sensitive to flow constrictions that impede sediment transport. The intrinsic expression of this effect is observed at bedrock constrictions, but in-channel infrastructure that acts to impound water and sediment has a very similar effect. Specifically, the Highway 150 bridge and drop structures and the Harvey Diversion Dam have been shown to impact downstream sediment transport and channel bed and bank erosion dynamics. Field observations and comparison of historic (1947) and current (2005) thalweg elevations suggest that the drop structures are causing a backwater effect during high flow events,

which in turn causes upstream sediment deposition and channel aggradation and channel incision directly downstream of the structures. This decrease in sediment supply downstream of the Highway 150 bridge has contributed to significant channel incision in reach 1 which, in combination with aggradation in reaches 2 to 5 largely attributable to sediment impoundment by Harvey Diversion Dam, has caused a reach-scale decrease in channel slope from reach 1 to reach 5. This decrease in slope has caused localized bank erosion and channel widening which is evident in reach 2 (possibly also related to re-deposition of sediment eroded from reach 1). Sediment impoundment by Harvey Diversion Dam has also contributed to significant incision in reach 6, below the dam and subsequently to downstream channel aggradation in recent years through reaches 6 and 7 (following incision from 1901 to 1947) because of the reduction in channel slope. Similar to reach 2, but with a more dramatic morphological impact, channel aggradation has prompted extensive bank erosion and channel widening in reach 7 creating a hazard to homes situated on the right bank of the creek.

Channelization and dredging, and the associated generation of migrating knickpoints, is a second important historic human impact on the morphology of lower Santa Paula Creek. The city of Santa Paula is situated on the alluvial fan of the lowest reaches of Santa Paula Creek, and is a natural zone of sediment deposition. The original form of the creek was recorded as numerous shallow channels spread across the fan and which switched courses during flood events in response to the deposition of sediment and large wood carried from upstream. Early in the history of Santa Paula, the channels were diverted and channelized into one channel on the eastern edge of the city. Efforts at directing the channel may have been initiated by Southern Pacific Transportation Company prior to 1914 in order to reduce the number of railroad bridge crossings. The straight channel reach below reach 8 is clearly established by the time of the earliest air photographs in 1927/1938, but the course of relic distributary channels can still be seen clearly in undeveloped city blocks. Strategic channelization of the creek was facilitated by the Flood Control Act of 1948. However, the first of three planned stages of channel re-sectioning and bank armoring by the USACE (*i.e.*, channelization) was only completed in 1974, and the rest of the scheme was not completed, largely due to environmental concerns. In conjunction with this scheme, the channel thalweg in reaches 7 and 8 is maintained at 1977 elevations by periodic dredging of relatively large volumes of sediment (Table 3-3). Flood damage in 1974 prompted channel re-design and re-structuring to its current configuration in 2000 (see Section 3.2.3.3 for details).

The combination of various channelization and dredging schemes has provided ample opportunity for the creation and upstream migration of knickpoints that result in channel incision. Comparison of the 1901and 1947 thalweg suggest that incision was not widespread in Reach 8 and further downstream prior to 1947, possibly due the large volumes of sediment delivered to the lower parts of Santa Paula Creek at the time. Incision is evident in reaches 6 and 7, but it is unclear whether the response is in relation to upstream-moving knickpoints or downstream-moving erosion resulting from the Harvey Diversion Dam, or some combination of the two. More recently though, incision in Reach 8 seems likely to be, at least in part, related to channelization and dredging since the 1970s. This assessment is based on the observation that Reach 8 contained a significant volume of in-channel alluvial sediments following the 1969 flood. Either knickpoints then eroded through the alluvial sediments to bedrock, or the channel was dredged to bedrock. Currently, there are two "knickpoints" in the lower reaches of Santa Paula Creek. The first knickpoint is now fixed and forms the headwall of the constructed debris basin and fish ladder of the 2000 USACE channelized reach. The second knickpoint forms the boundary between reaches 7 and 8. Comparison of channel thalweg data suggests that after the initiation of channel maintenance within the 'channelized reach,' the first knickpoint began migrating upstream and was stalled when it incised into bedrock (at the USACE fish ladder

location). The second smaller knickpoint then formed and began incise through the in-channel alluvium down to bedrock and migrate upstream through Reach 8. Assuming the smaller knickpoint began in 1969 when channelization efforts begun, the minimum rate of migration for the smaller knickpoint is approximately 26 m a^{-1} (945 m in 36 years). The second knickpoint is anticipated to continue migrating upstream through in-channel alluvial deposits and bedrock until it reaches Harvey Diversion Dam or is artificially stabilized. Several recent disconnections of the foot of the fish ladder at Harvey Diversion Dam suggest that, at least locally, incision is continuing to occur below the dam, possibly in connection with the wing wall constructed in 2000 and serving to further constrain the width of flood flows. It is too soon to determine the potential impact, of any, of the re-designed channel, spur dikes and revetments installed in Reach 7 in 2007.

Overall, the lower Santa Paula Creek has shown historical changes in channel morphology that can be linked to a complex suite of factors including geology, storms, channel infrastructure, channelization and dredging. For the period of available historic data (essentially the last one hundred years), the provision of channel infrastructure channel modifications, and the emergence of a wet ENSO phase since 1969, serve to mask any potential effect of land use changes (through land cover changes). It is assumed that the majority of impact associated with land cover change may have occurred coincident with Euro-American arrival in the watershed in the nineteenth century, and so predates available survey data.

Integrating these elements, it appears that the beginnings of the "modern day" Santa Paula Creek, that is, an incised channel confined to a single thread rather than a wide, possibly braided, channel that flowed in numerous distributary channel across an alluvial fan towards the Santa Clara River, may be coincident with Euro-American occupation of the area including the onset of ranching, the growth of the city of Santa Paula, and the coming of the railroad. The very large flood event of 1884 may have been the "threshold" event necessary to translate these human impacts into channel morphology changes. There are now four major breaks in the channel gradient of Santa Paula Creek whereas, before the Twentieth century, only one, different, slope break existed, at the Sulphur Mountain fault (upper end of Reach 2). This is important because, as illustrated in the upper watershed, breaks in slope affect the connectivity of sediment transport causing upstream aggradation and downstream incision. Three of the new breaks are fixed in location, at the Highway 150 bridge drop structures, Harvey Diversion dam, and the USACE debris basin/fish ladder, while the fourth is a knickpoint eroded into bedrock near the junction of reaches 7 and 8. Lower Santa Paula Creek is, therefore, now a series of segments rather than a continuous river reach, with implications for fish passage. Morphological changes in reaches 1 to 5 seem clearly related to the downstream impacts of the Highway 150 bridge drop structures, to the upstream impact of Harvey Diversion Dam, and potentially to the width constriction in the zone of the Sulphur Mountain. Downstream of the Harvey Diversion Dam, a more complex pattern of mechanisms for change exist. Incision close to the Harvey Diversion and downstream aggradation are presumably related to the dam, and may have become significant following the enlargement of the dam in 1923. The aggrading reach may also be linked to the sequence of large floods since 1969 which have provided several flows large enough to cause bank erosion in reach 7. Alternatively, or in addition, widening is a response to the knickpoint now exposed at the upstream end of Reach 8 following channelization and dredging. Reach 8 has become bedrock confined (although erodible) since 1969, presumably in response to knickpoint progression following the 1974 channelization scheme and/or associated dredging activity. Intriguingly, both reaches 5 and 7 are now close to their 1901 bed elevation possibly suggesting the current wet ENSO period has allowed some form of channel "recovery" to a far less incised state in reaches free of width constraints: but it is unclear whether the 1901 elevation is indicative of some form of near "equilibrium" condition.

4 DISCUSSION

4.1 Summary of Current Conditions

The Santa Paula Creek watershed is characterized by very high sediment yields. Estimates of hillslope sediment delivery rate derived in this study range from approximately 500 to 20,000 t km^{-2} a^{-1}, depending on geology, hillslope gradient, and land cover. Integrating the hillslope sediment yield results for individual process domains (*i.e.*, combinations of geology, gradient and land cover) over sub-watershed areas suggests that Sisar Creek yields on the order 2,000 t km^{-2} a^{-1}, while (for example) the chronically-eroding Mud Creek yields closer to 6,000 t km^{-2} a^{-1}. The hillslope sediment yield for the entire Santa Paula Creek watershed is approximately 2,000 t km^{-2} a^{-1}. Active tectonic uplift in the watershed results in the steep slopes that contribute to the high sediment yield. Over the long-term, the sediment yield is in approximate accordance with the ~1 mm a^{-1} rate of active uplift in the watershed. Our calculated hillslope sediment yield is also consistent with estimates of sediment yields from gaging records for the lower Santa Clara River by Warrick (2002) (although, as it is partly calibrated by this research, such an outcome is expected).

Geologically, in-stream sediment is derived from a combination of easily erodible, fine-grained siltstone beds and more slowly eroding but durable sandstone beds that provide very coarse grained material (boulders to cobbles) that pervasively influence channel morphology. The siltstone beds are the dominant source of sediment, in part because they constitute over 50% of the watershed geology; in contrast, coarse sediment delivery is more a function of fracturing by cross-cutting joints in conjunction with oversteepened bedrock slopes. Coarse sediment reaches the river bed either as large blocks that fall directly into the channel or as material that is entrained from coarse talus accumulations from the base of steep slopes.

Rates of sediment production are also dependent on land cover characteristics, with higher yields emanating from "cleared" land (agriculture and grasslands) than under forest. Because there has not been an extensive land cover change in the upper Santa Paula watershed in the last century, it is probable that the anthropogenic influence on overall watershed sediment yields in the upper watershed largely reflect changes brought about in the period not long following Euro-American land occupation rather than more recent changes. In the lower watershed, continued agriculture and watershed development have likely increased hillslope sediment yields, especially of fine sediment. On shorter timeframes, wildfire has a profound effect on sediment delivery: simulating the impact by decreasing vegetation cover for all hillslopes that are currently well vegetated and have a hillslope gradient >10% results in a seven-fold increase in hillslope sediment delivery for a fire than burns 100% of the watershed. This figure, if accurate, thus represents a likely upper bound on the effect of fire in the watershed.

Santa Paula Creek is characterized by high rates of sediment transport and active channel erosion. The mainstem of lower Santa Paula Creek (*i.e.*, below the confluence of Sisar Creek and "upper" Santa Paula Creek) has very high rates of sediment transport, which is a function of a relatively high gradient (0.0145–0.0229) and the high sediment yields from upstream. The channel bed surface is characterized primarily by cobble deposits, but even the coarsest (90^{th} percentile) of these sediments are estimated to be mobile in floods with a return period of 1–3 years. This is consistent with other evidence for very high rates of sediment transport and significant morphological change in large flood events. The mainstem channel also contributes to the

watershed sediment yield through active channel incision and widening. Evidence from topographic maps, air photographs and recent LiDAR images indicate that the lower mainstem has predominately incised since the earliest records since 1901 (with a maximum of 12 m), although aggradation has occurred behind flow constrictions, and the channel has widened a maximum of 200 m in the past 40 years between Harvey Diversion Dam and the USACE fish ladder. Overall, the dynamics of flow and sediment transport in the creek mean that the largest single flow is also the dominant, channel-forming discharge, whereas in many rivers a more moderate ("bankfull") flood flow usually represents the dominant discharge.

Recent changes in channel morphology in the lower Santa Paula Creek mainstem are driven by both natural and anthropogenic factors. In terms of natural factors and over the long term, the channel morphology shows an adjustment to regional patterns of faulting and tectonic activity, whereby bedrock channel constrictions resulting from upthrust blocks restrict the connectivity of coarse sediment to downstream reaches and thus contribute to local incision. More recently, a strong ENSO climatic signal over the last 40 years has promoted a clustering of large flood events (*i.e.*, 1969, 1973, 1978, 1980, 1983, 1992, 1992, 1995, 1998, and 2005) that have transported more sediment than would otherwise have occurred over the period, and have increased the ability of the channel to erode its bed and banks. Bed erosion is most pronounced where the channel is confined either by bedrock or by levees and bank protection, and bank erosion (widening) is commonly at a maximum upstream of flow constrictions.

Anthropogenic influences include in-channel structures that serve to constrict flow and sediment transport, especially at the Highway 150 bridge and at the Harvey Diversion Dam. Such structures function rather like anthropogenic counterparts of fault-related bedrock outcrops: flow constrictions at the approach to these structures during large flood events result in sediment deposition upstream of the structure, and incision immediately downstream of the structure. The channel is likely to meander as the gradient reduces approaching the structure from upstream (forcing sediment deposition), and downstream the sediment derived from local channel incision will be deposited and may result in aggradation and channel widening.

Removal of in-channel sediment, channel straightening, and bank armoring near the mouth of Santa Paula Creek have served to locally increase channel gradients and confine flood flow widths, resulting an in increased ability to erode the channel bed in flood events and knickpoint migration upstream, which in turn causes further channel incision and bank widening in reaches that are not bedrock-controlled. Several phases of knickpoint migration may have occurred, potentially relating to efforts in straightening and confining the channel in the early twentieth century, following channelization and dredging efforts in the early 1970s, and following recent re-design of the channelized reaches.

4.2 Conceptual Understanding and Trajectory of Channel Morphology

The general morphology of lower Santa Paula Creek (LSPC, below the confluence with Sisar Creek) is largely controlled by regional geological characteristics. The channel receives a high sediment load from the hillslopes as a consequence of high rates of tectonic uplift in the upstream watershed. The delivery of hillslope sediment from the upper watershed to the channel is highly dependent on land cover and hillslope gradient (for fine sediment) and local geologic controls (for coarse sediment). The steep gradient of the creek enables it to transport this load to the Santa Clara River in a series of concentrated pulses occurring during high-intensity rainfall events, especially those associated with the ENSO phenomenon. Paleochannels clearly evident on historic aerial photographs indicate that, under pre-settlement conditions, the lower Santa Paula

Creek would periodically switch courses during flood events, entering the Santa Clara River at different locations. The lower Santa Paula Creek therefore used to operate as an alluvial fan, albeit one affected by regional tectonic activity. While, on millennial timeframes, tectonic uplift has resulted in a series of clearly evident terraces on the margins of the valley of the upper LSPC, photographic and topographic evidence indicates that the mainstem active channel was unlikely to have been incised. Instead, flood flows would disperse across the alluvial fan during high-magnitude events, allowing sediment deposition and preventing significant erosion of the active channel. This condition, which may have existed until the time of extensive Euro-American settlement of the watershed, which probably also resulted in a higher water table that supported riparian vegetation and buffered the creek against the erosive forces of high flows.

In contrast, the morphology of the current LSPC alternates between bedrock-confined reaches and incised alluvial reaches, and it is largely confined to a single high-gradient channel disconnected from its floodplain. Upstream of flow constrictions, local aggradation causes extensive channel widening. Evidence from the upper watershed indicates that bedrock outcrops associated with upthrust faults act naturally as hydraulic constrictions on the channel, reducing coarse sediment connectivity and indirectly causing local scour and downstream incision. In the lower LSPC, bedrock outcrops located near the Highway 150 bridge, the Harvey Diversion Dam, and upstream of the USACE fish ladder have a functionally similar affect; but the lower two of these outcrops were probably buried then exposed by channel bed erosion following in-channel modification and structure installation. Such incision means that flood flows in the LSPC are now flashier and run deeper in the active channel. This allows the mainstem to maintain higher flood flow velocities than would earlier have been the case in earlier times, develop higher shear stresses on the channel bed, and thus transport higher rates of sediment (including sediment scoured from the bed and banks of the channel). In addition, channelization of the lowest reaches of the LSPC appears to have prompted more, or more active, knickpoints, which in turn are further incising the channel bed.

Coincident with these in-channel conditions, a series of large rainfall events over the last 40 years associated with a strong multi-decadal occurrence of the ENSO phenomenon has resulted in numerous high-magnitude flood events. The flood events have caused considerable incision in some parts of Santa Paula Creek, which serves to increase further the sensitivity of the channel to subsequent large flood events. The natural geomorphic control on such incision is for the channel to widen by eroding its channel banks and so create a new floodplain onto which to disperse flood flow energy. A combination of bank revetment and bedrock constraints on the LSPC mean that widening of the channel has only been possible in select locations (*e.g.*, Reach 7), thus perpetuating the condition as a positive feedback loop. Overall, the "morphodynamics" of the LSPC (*i.e.*, the changeability of the channel form) is now far more sensitive to flood flows than prior to significant human settlement.

In Section 3.4.2, available historical data was used to reconstruct historical changes to the morphology of Santa Paula Creek to the extent possible. The primary data sources included long profiles and centerline traces of the channel bed, at approximate 50-year intervals from topographic maps as far back as 1850, and aerial photographs, especially those from 1969, 1998 and 2005. These were used to detail changes in planform and provide further clues to the timing of changes in bed elevation. In conjunction with other analyses in this report, this reconstruction helps us to understand the dominant processes in the Santa Paula Creek watershed and to project a potential scenario of future change in lower Santa Paula Creek.

Reaches 1 and 6 seem unlikely to change from their current trajectory of channel incision while the Highway 150 bridge drop structures and the Harvey Diversion Dam remain in their current

form. Both reaches are now highly incised into bedrock, which reduces the chance of significant channel widening. As such, both creeks will remain as highly efficient conduits for sediment transport downstream of a control on sediment passage, and incision is the most likely continuing response. In Reach 6, incision may be enhanced if knickpoints currently in reaches 7 and 8 migrate upstream into the reach.

Reaches 2 to 5 appear to have their gradient controlled regionally by the crest of Harvey Diversion Dam. Because these reaches have lower gradients and less confinement than those immediately above Reach 1, the limited aggradation and widening in these reaches may continue. Bed levels will also presumably aggrade further were the crest elevation of the Harvey Diversion Dam ever increased.

Future morphological change in Reach 7 may reflect several competing factors. The recent trend of aggradation and channel widening may reverse into incision in moderate flood events, because the flow is now directed towards the channel center by the recently constructed dikes. This trend will be accentuated if the knickpoint currently at the boundary of Reach 7 and 8 erodes upstream and into the reach. Incision during large flood events may be partly controlled by the resistance to flow provided by the constructed dikes, being greater if the dikes retain their form for longer periods. However, because Reach 8 is now a bedrock-influenced reach, further incision in Reach 8 may impart an increasing level of flow constriction in Reach 7 and so encourage upstream sediment deposition, especially at the downstream end of the reach which may then widen.

Reach 8 looks set to continue a trend for slight incision because the exposed erodible bedrock will limit the amount of channel widening possible during flood events, and so focus erosion on the channel bed. If the USACE fish ladder retains its structural stability and so maintains a fixed bed elevation at the downstream end of Reach 8, the amount of incision possible will be limited and, over the longer term, a trend of aggradation may begin.

In every location, the rate of morphological change will be determined by the frequency of large, sediment-laden flood events. Changes will be rapid while frequent ENSO events occur, such as in the period since 1969, or in flood events following fire in the upper watershed.

4.3 Implications for Management

Like all fluvial systems, Santa Paula Creek responds to numerous natural and human influences across its watershed. Here, highly influential factors include geological type, bedrock exposure and active tectonics, the natural function of lower Santa Paula Creek as an alluvial fan, the semi-arid climate and ENSO influence on the frequency of storm events, the frequency of wildfire in the upper watershed, the extent of flow constriction provided by in-channel infrastructure, the history of channelization, and the extent of sediment dredging from the bed of the channel. Arising from our analyses is a series of implications that should assist in managing the lower Santa Paula Creek. These include:

- The connectivity of coarse sediment transport may be the single most important factor in preventing damaging morphological changes, especially associated with channel incision—the most severely incised reaches are the ones just downstream of hydraulic obstructions, both natural (*i.e.,* faults) and constructed (*i.e.,* Highway 150 bridge and Harvey Diversion Dam). Therefore, all channel infrastructure and channel modifications should be designed to retain or improve coarse sediment connectivity. As such, predicted rates and caliber of sediment transported down the mainstem Santa Paula Creek should

constrain the hydraulic design characteristics of any future in-channel structures or modification.

- In alluvial and unconfined river systems, river channels are expected to "recover" (at least partially) from passages of incision through a set of processes that include channel widening, aggradation, and the creation of a new floodplain. In many reaches of Santa Paula Creek, however, incision has persisted for decades or centuries and under current conditions and the channel does *not* have a tendency to recover, despite large volumes of incoming sediment available to facilitate recovery. Recovery is impeded by (1) the channel incising (or being dredged) to exposed bedrock, which does not allow significant additional channel widening; (2) channelization and bank armoring, which prevents channel widening; and (3) the existence of hard points on the channel bed from channel infrastructure, which perpetuate channel bed discontinuities (*e.g.*, Highway 150 bridge drop structures, Harvey Diversion Dam, USACE fish ladder). Therefore, management measures should be designed to function within the context of prospective future channel morphologies, or to promote "assisted recovery" of channel form as part of the project.
- Sediment yields from hillslopes will increase in the years after a major fire event, until such time that vegetation has recovered. Under a hypothetical 100% burn scenario, short-term sediment yields may well increase seven-fold and so the sediment loads carried in floods occur shortly after fires should be expected to result in substantial morphological change to Santa Paula Creek.
- Frequently-mobilized large sediment can cause significant damage to in-channel infrastructure and needs to be considered in future management and design decisions.
- In-channel infrastructure has had, and will continue to have, a profound impact on upstream sediment deposition, and downstream bank erosion and channel widening.
- Channel destabilization and incision will likely persist with in-channel sediment removal practices.
- High-magnitude flood events have been more frequent in the last 40 years due to intense ENSO activity. Periodic revision of flood frequency statistics has been necessary with the 2005 event (~780 m^3s^{-1}; 27,500 cfs), now considered to be about a 50-year flood event. With the continuation of strong ENSO activity, rates of channel morphological change will be enhanced.

From Section 1.1, the purpose of this watershed assessment is to provide the foundations for site-specific, prioritized recommendations for restoration alternatives that return southern steelhead passage throughout historically-accessible reaches in the Santa Paula Creek watershed, mindful of the need to maintain existing water-diversion rights and the desire to accommodate and mediate hazards associated with flooding and channel erosion. From the implications outlined above, it is clear that the general approach should be in the provision of a wide river corridor without infrastructure constraints in which natural river recovery is possible, flood-related hazards are minimized, and fish passage is assured. Such an approach, of course, must be tempered by existing constraints including floodplain development. Where possible, however, management actions should seek opportunities to remove existing constraints. In this regard, priority actions would logically include:

- Removal or re-design of the grade control structures under the Highway 150 bridge to present less impediment to sediment transport;
- Re-design of water diversion facility provided currently by the Harvey Diversion Dam to present less impediment to sediment transport (and also to reduce the maintenance costs associated with repeated damage to the dam crest caused by large boulders in transport);
- Monitoring of bed level changes in reaches 7 and 8 to ensure that knickpoint migration does not create passage impediments.

As the redesign of the Highway 150 bridge drop structures is currently under consideration by the California Department of Transportation, and long-term monitoring is beyond the scope of this project, the highest priority action for this project is to explore alternatives water-diversion opportunities at or upstream of the site of the current Harvey Diversion Dam.

5 REFERENCES

Andrews, E., R. Antweiler, P. Neiman, and F. Ralph. 2004. Influence of ENSO on flood frequency along the California Coast. Journal of Climate 17: 337-348.

Argus, D. F., M. B. Heflin, A. Donnellan, F. H. Webb, D. Dong, K. J. Hurst, D. C. Jefferson, G. A. Lyzenga, M. M. Watkins, and J. F. Zumberge. 1999. Shortening and thickening of metropolitan Los Angeles measured and inferred by using geodesy. Geology 27: 703-706.

Barnes, H. 1967. Roughness characteristics of natural channels. Water Supply Paper 1849. U. S. Geological Survey, Washington, D.C.

Bathurst, J. 1987. Critical conditions for bed material movement in steep, boulder streams. International Association of Hydrological Sciences 165: 309-318.

Benda, L., and T. Dunne. 1997. Stochastic forcing of sediment supply to channel networks from landsliding and debris flow. Water Resources Research 33: 2849-2863.

Blythe, A. E., D. W. Burbank, K. A. Farley, and E. J. Fielding. 2000. Structural and topographic evolution of the central Transverse Ranges, California, from apatite fissiontrack, (U/Th)/He and digital elevation model analyses. Basin Research 12: 97-114.

Booker, F. A. 1998. Landscape and management response to wildfires in California. Master's thesis. University of California, Berkeley.

Buffington, J. and D. Montgomery. 1997. A systematic analysis of eight decades of incipient motion studies, with special reference to gravel-bedded rivers. Water Resources Research 33: 1993-2029.

Burbank, D. W., J. Leland, E. Fielding, R. S. Anderson, N. Brozovic, R. Reid-Mary, and C. Duncan. 1996. Bedrock incision, rock uplift and threshold hillslopes in the northwestern Himalayas. Nature 379: 505-510.

Cayan, D., K. Redmond, and L. Riddle. 1999. ENSO and hydrologic extremes in the western United States. Journal of Climate 12: 2881-2893.

CDF (California Department of Forestry and Fire Protection). 2004. Fire perimeter GIS data. CDF, Fire and Resource Enhancement Program, Sacramento.

Çemen, I. 1989. Near-surface expression of the eastern part of the San Cayetano fault: a potentially active thrust fault in the California transverse ranges. Journal of Geophysical Research 94: 9665-9677.

De Koff, J. P., Graham, R. C., Hubbert, K. R., P. M. Wohlgemuth. 2006. Prefire and postfire erosion of soil nutrients within a chaparral watershed. Soil Science 171: 915-928.

Deser, C., A. Capotondi, R. Saravanan, and A. Phillips. 2004. Tropical Pacific and Atlantic climate variability in CCSM3. Journal of Climate 19: 2451-2481.

Dibblee, T. 1990. Geologic map of the Santa Paula Peak quadrangle, Ventura County, California. Scale 1:24,000. Dibblee Geological Foundation, Santa Barbara, California.

Dibblee, T. 1992. Geologic map of the Santa Paula quadrangle, Ventura County, California. Scale 1:24,000. Dibblee Geological Foundation, Santa Barbara, California.

Duvall, A., E. Kirby, and D. Burbank. 2004. Tectonic and lithologic controls on bedrock channel profiles and process in coastal California. Journal of Geophysical Research 109: 1-18.

Ferguson, R. 1994. Critical discharge for entrainment of poorly sorted gravel. Earth Surface Processes and Landforms 19: 179-186.

Gabet, E. J., and T. Dunne. 2003. A stochastic sediment delivery model for a steep Mediterranean landscape. Water Resources Research 39: 1237.

HDR (HDR Engineering, Inc.). 2006. Emergency streambank protection basis of design, Santa Paula Creek, Ventura County, California. HDR, Ventura County Watershed Protection District Design and Construction Division.

Hooke, J. 2003. Coarse sediment connectivity in river channel systems: a conceptual framework and methodology. Geomorphology 56: 79-94.

Huftile, G. J., and R. S. Yeats. 1995. Convergence rates across a displacement transfer zone in the western Transverse Ranges, Ventura basin, California. Journal of Geophysical Research 100: 2043-2068.

Inman, D., and S. Jenkins. 1999. Climate change and the episodicity of sediment flux of small California rivers. Journal of Geology 107: 251-270.

Kirchner, J. W., R. C. Finkel, C. S. Riebe, D. E. Granger, J. L. Clayton, J. G. King, and W. F. Megahan. 2001. Mountain erosion over 10 yr, 10 k.y., and 10 m.y. time scales. Geology 29: 591-594.

Krammes, J. S., and J. Osborn. 1969. Water-repellent soils and wetting agents as factors influencing erosion. Pages 177-186 *in* L. F. DeBano, and J. Letey, editors. Symposium on water repellent soils, University of California, Riverside.

Lajoie, K. R., D. J. Ponti, II C. L. Powell, S. A. Mathieson, and A. M. Sarna-Wojcicki. 1991. Emergent marine strandlines and associated sediments, coastal California; a record of Quaternary sea-level fluctuations, vertical tectonic movement, climatic changes, and coastal processes. Pages 190-203 *in* R. B. Morrison, editor. The geology of North America. Volume K-2. Quaternary non-glacial geology: coterminous United States. The Geological Society of America, Boulder, Colorado.

Montgomery, D. R., and Buffington, J. M. 1997. Channel-reach morphology in mountain drainage basins. Geological Society of America Bulletin 109: 596-611.

NOAA (National Oceanic and Atmospheric Administration). 2000. Land cover analysis project: 2000 Southern Coastal California Land Cover/Land Use data. Accessed at: http://www.csc.noaa.gov/crs/lca/ca_so2000.html

Orme, A. R. 1998. Late Quaternary tectonism along the Pacific coast of the California: a contrast in style. Geological Society of London Special Publications 146: 179-197.

Parker, G. 1990. Surface-based bedload transport relation for gravel-bed rivers. Journal of Hydraulic Research 28: 417-436.

Peterson, M. D., and S. G. Wesnousky. 1994. Fault slip rates and earthquake histories for active faults in southern California. Bulletin of Seismological Society of America 84: 1608-1649.

Prothero, D. R. 2001. Magnetostratigraphic tests of sequence strategraphic correlations from the southern California Paleogene. Journal of Sedimentary Research 71: 526-536.

Reid, L. M., and T. Dunne. 1996. Rapid construction of sediment budgets for drainage basins. Catena-Verlag, Cremlingen, Germany.

Reneau, S. L., D. Katzman, G. A. Kuyumjian, A. Lavine, and D. V. Malmon. 2007. Sediment delivery after a wildfire. Geology 35: 151-154.

Rockwell, T. 1988. Neotectonics of the San Cayetano fault, Transverse Ranges, California. Geological Society of America Bulletin 100: 510-513.

Schmidt, K. M., and D. R. Montgomery. 1995. Limits to relief. Science 270: 617-620.

Scott, K. M., and R. P. Williams. 1978. Erosion and sediment yields in the Transverse Ranges, southern California. Professional Paper No. 1030. U. S. Geological Survey, Washington, D. C.

Shakesby, R. A., and S. H. Doerr. 2006. Wildfire as a hydrological and geomorphological agent. Earth-Science Reviews 74: 269-307.

Shields, A. 1936. Anwendung der aehnlichkeits-mechanik und der turbulenzforschung auf die geschiebebewegung. Preussische Versuchsanstalt fur Wasserbau und Schiffbau, Berlin, Heft 26. (English translation by W. P. Ott and J. C. van Uchelen, USDA, Soil Conservation Service Cooperative Laboratory, California Institute of Technology, Pasadena).

Stillwater Sciences. 2007. Santa Clara River Parkway floodplain restoration feasibility study – assessment of geomorphic processes. Prepared by Stillwater Sciences, Berkeley, California for California Coastal Conservancy, Oakland.

Stoecker, M, and E. Kelley. 2005. Santa Clara River steelhead trout: assessment and recovery opportunities. Santa Clara River Trustee Council and The Nature Conservancy, Ventura, California.

Tan, S. S., and P. J. Irvine. 2005. Geologic map of the Santa Paula Peak 7.5' quadrangle, Ventura County, California: a digital database. Scale: 1:24,000. California Department of Conservation, California Geological Survey.

Trecker, M. A., L. D. Gurrola, and E. A. Keller. 1998. Oxygen-isotope correlation of marine terraces and uplift of the Mesa Hills, Santa Barbara, California, USA. Geological Society of London Special Publication, 146: 57– 69.

USACE (U. S. Army Corp of Engineers). 1995. Santa Paula Creek, California General Reevaluation Report: final main report and Environmental Impact Statement/Environment Impact Report. USACE, Los Angeles District Office, Los Angeles, California.

USDA Forest Service. 1954. Fire-flood sequences on the San Dimas Experimental Forest. USDA Forest Service, California Forest and Range Experiment Station 6.

VCWPD (Ventura County Watershed Protection District). 2005. Debris and detention basins. VCWPD, Ventura, California.

VCWPD. 2007. Ventura County Watershed Protection District hydrology data. Accessed at: http://www.vcwatershed.org/hydrodata/htdocs/static/.

Ward, R. 1978. Floods: a geographical perspective. Macmillan, New York.

Warrick, J. 2002. Short-term (1997–2000) and long-term (1928–2000) observations of river water and sediment discharge to the Santa Barbara channel, California. Doctoral dissertation. University of California, Santa Barbara.

Wells, W. G., II. 1987. The effects of fire on the generation of debris flows in southern California. Geological Society of America, Reviews in Engineering Geology 7: 105-114.

Wells, W.G., II. 1981. Some effects of brushfires on erosion processes in coastal Southern California. Pages 305-342 *in* T.R.H. Davies and A.J. Pearse, editors. Erosion and sediment transport in Pacific Rim Steeplands Symposium. Association of Hydrological Sciences, Christchurch, New Zealand.

Wells, W.G., II., P.M. Wohlgemuth, and A.G. Campbell. 1987. Postfire sediment movement by debris flows in the Santa Ynez Mountains, California. Pages 275-276 *in* R. L. Beschta, T. Blinn, G. E. Grant, G. G. Ice and F. J. Swanson, editors. Erosion and sedimentation in the Pacific Rim. International Association of Hydrological Sciences, Corvallis, Oregon.

Willett, S. D., and M. T. Brandon. 2002. On steady states in mountain belts. Geology 30: 175-178.

Williams, R. 1979. Sediment discharge in the Santa Clara River basin, Ventura and Los Angeles Counties, California. U.S. Geological Survey, Menlo Park, California.

Wolman, M., and J. Miller. 1960. Magnitude and frequency of forces in geomorphic processes. Journal of Geology 68: 54-74.

Yeats, R. S. 1988. Late Quaternary slip rates on the Oak Ridge fault, Transverse Ranges, California: implications for seismic risk. Journal of Geophysical Research 93: 137-149.

FIGURES

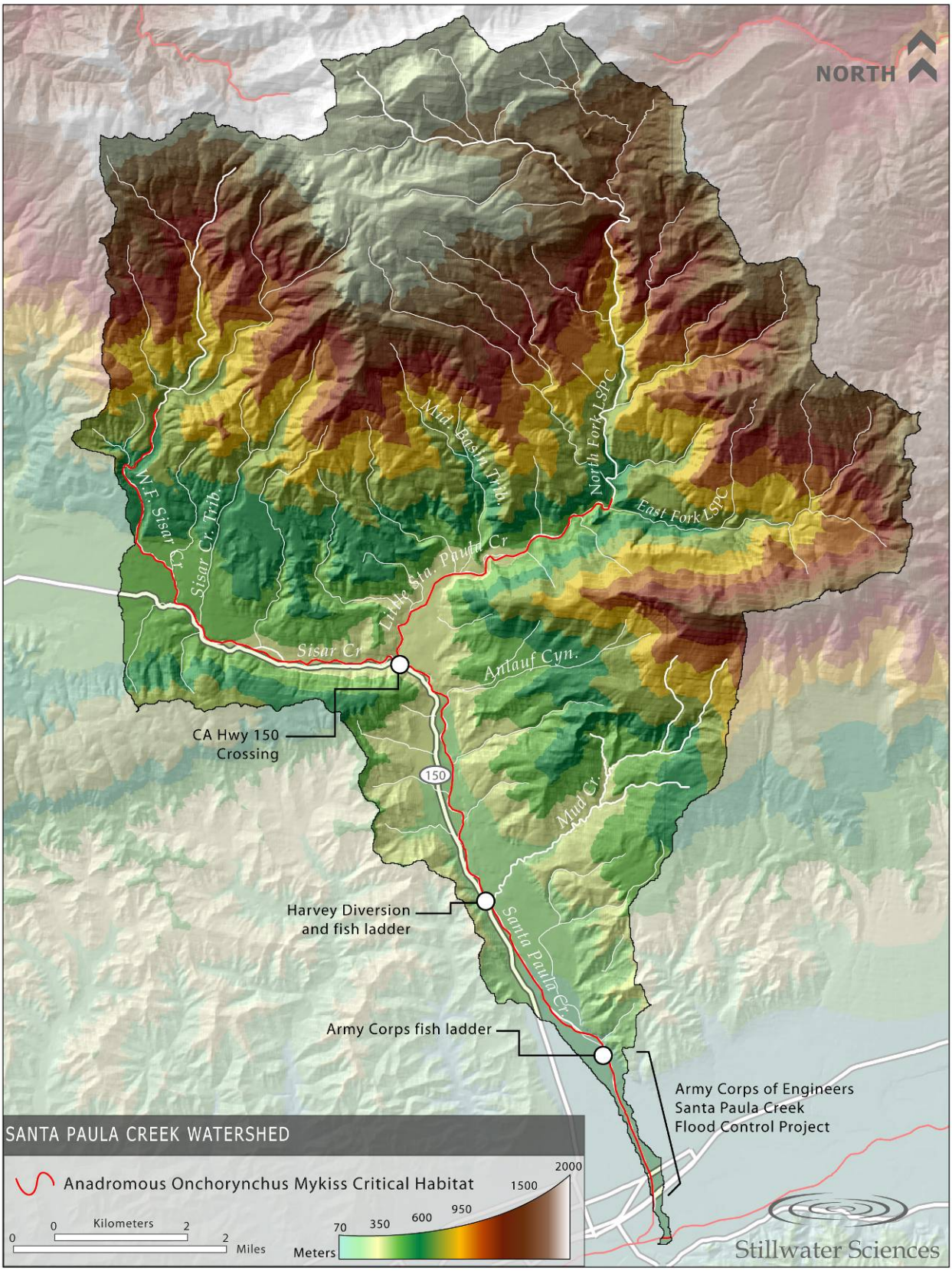

Figure 1-1. Santa Paula Creek watershed.

Figure 2-1. Relief map of southern California, displaying the east–west orientation of the Transverse Ranges relative to the predominant NW grain of the topography along the California coast.

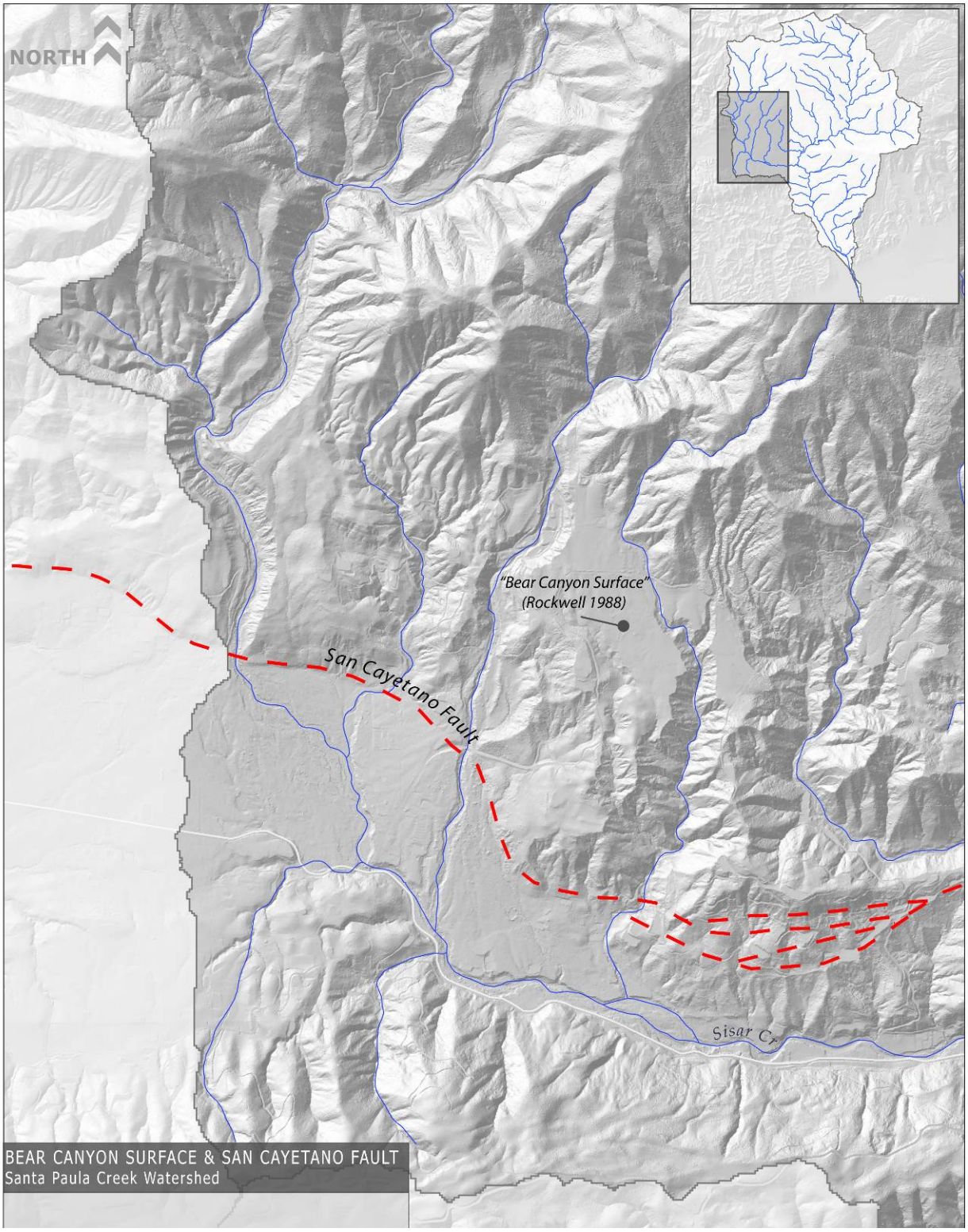

Figure 2-2. The "Bear Canyon surface" (Rockwell 1988) is well-displayed as a remnant uplifted flat in the right-center part of this DEM image (view is 5 km east-west). The San Cayetano fault runs approximately along the southern base of the surface, trending ESE in this area (drawn from Tan and Irvine [2005]).

Figure 2-3. Differential resistance to weathering in sandstone (light-colored boulders) and siltstone (crumbled dark piles).

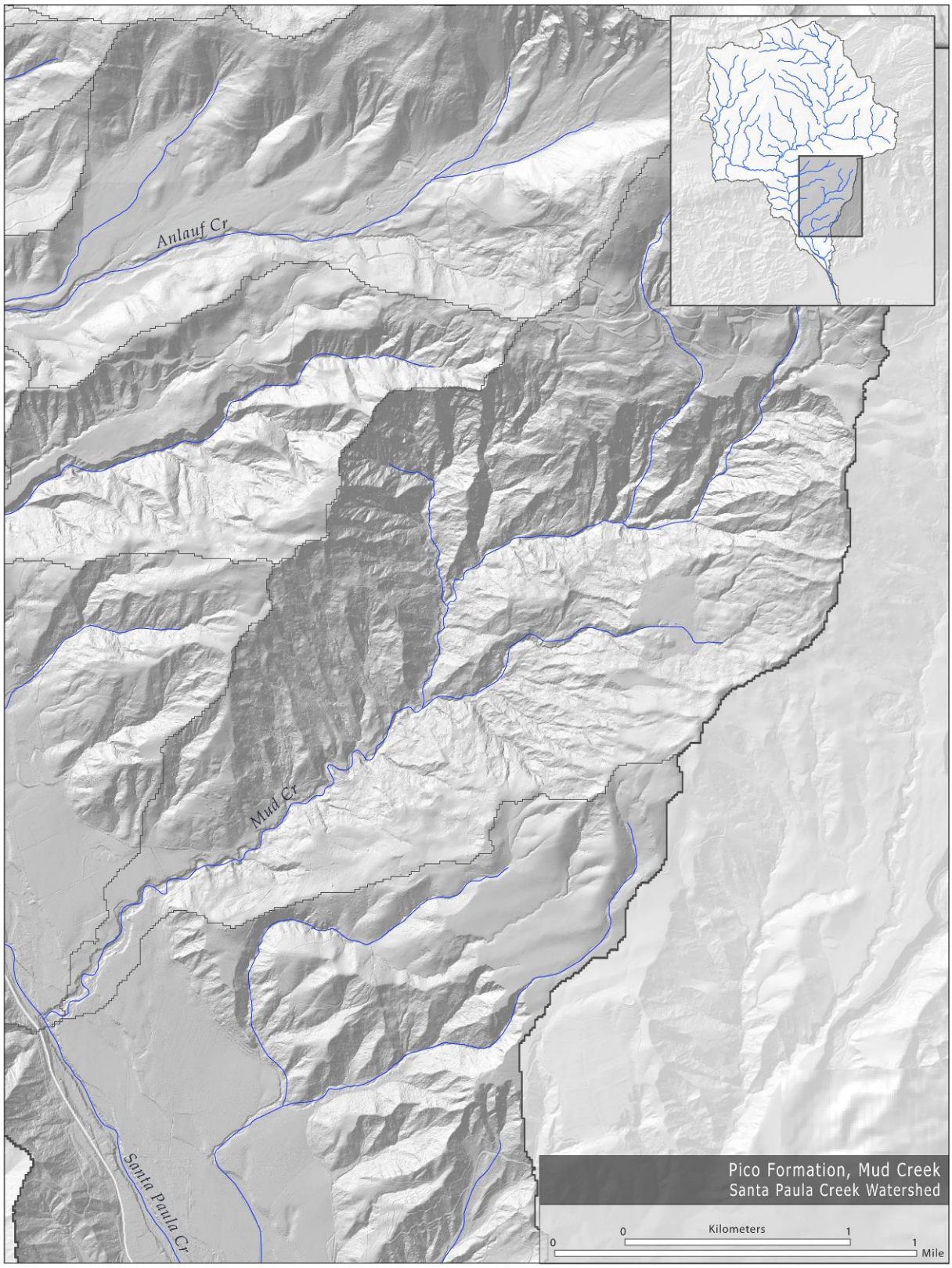

Figure 2-4. Erosional morphology of the Pico Formation, particularly well displayed in the upper watershed of Mud Creek.

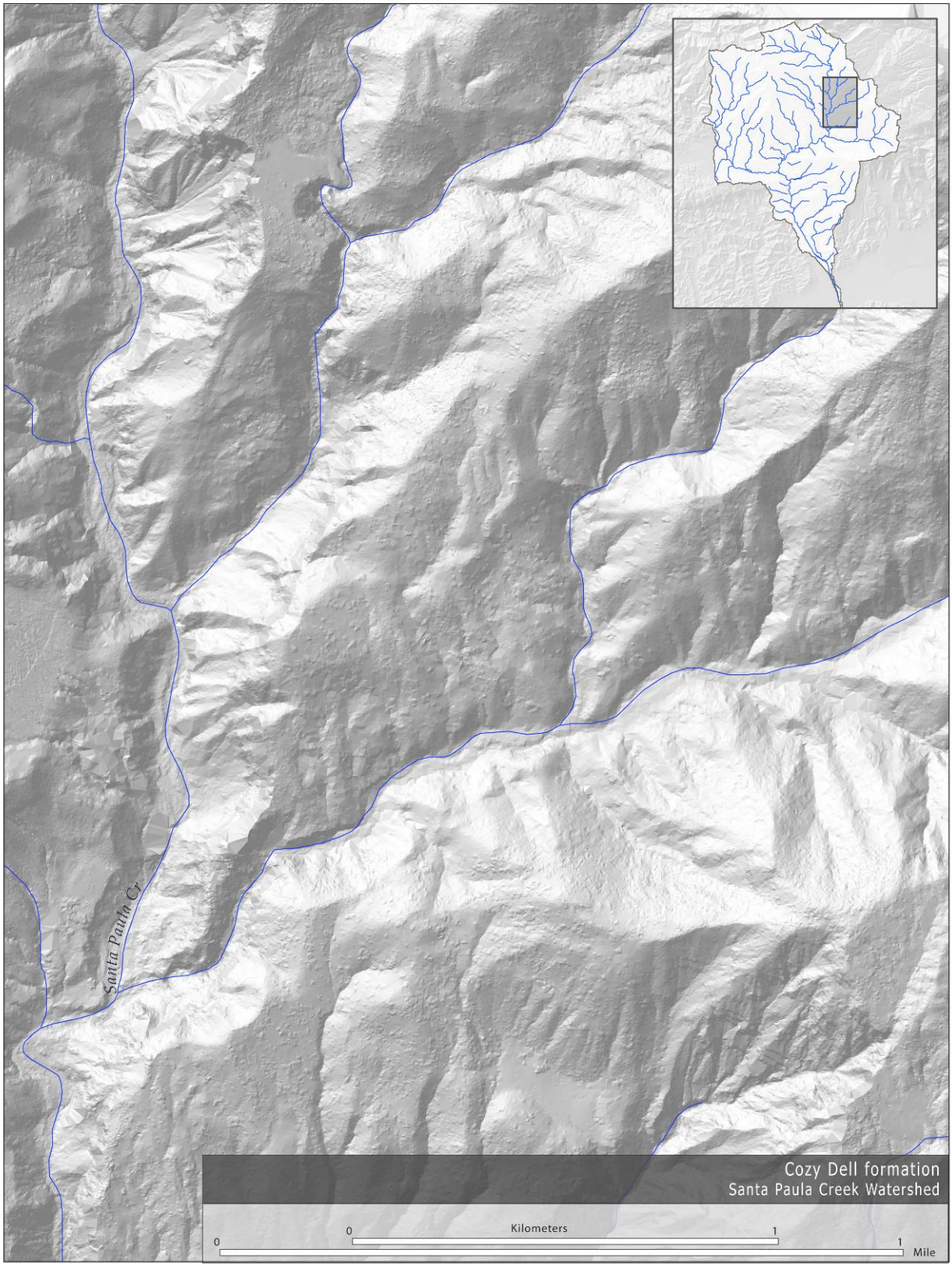

Figure 2-5. Erosional morphology of the Cozy Dell Formation, in the northeastern-most part of the Santa Paula watershed.

Figure 2-6. Alluvial sediment derived from a primarily sandstone-draining channel. Arrow points to notebook (yellow; 10 × 18 cm) in center of picture for scale.

Figure 2-7. Low-sediment-yielding landscape developed on the dip slope of the Matilija Sandstone.

Figure 2-8. The west-facing cliffs of Topatopa Bluff. Bedding in the east-dipping sandstone of the Matilija Formation is evident.

Figure 2-9. Rockfall delivery of sandstone into Santa Paula Creek. Arrow points to notebook (12 × 18 cm); large boulder is ~5 m high.

Figure 2-10. View of Santa Paula Creek a) just upstream of the major sandstone-delivery zone of Figure 2-9 (note the bedrock exposures in the banks and bed of the channel); and b) downstream of sandstone delivery zone.

LOW
Shale Forest 10-20%

MEDIUM
Shale Scrub 10-20%

HIGH
Shale Ag/grass 10-20%

Figure 2-11. Characteristic photographs of vegetation in areas with a) low, b) medium, and c) high sediment-delivery rates.

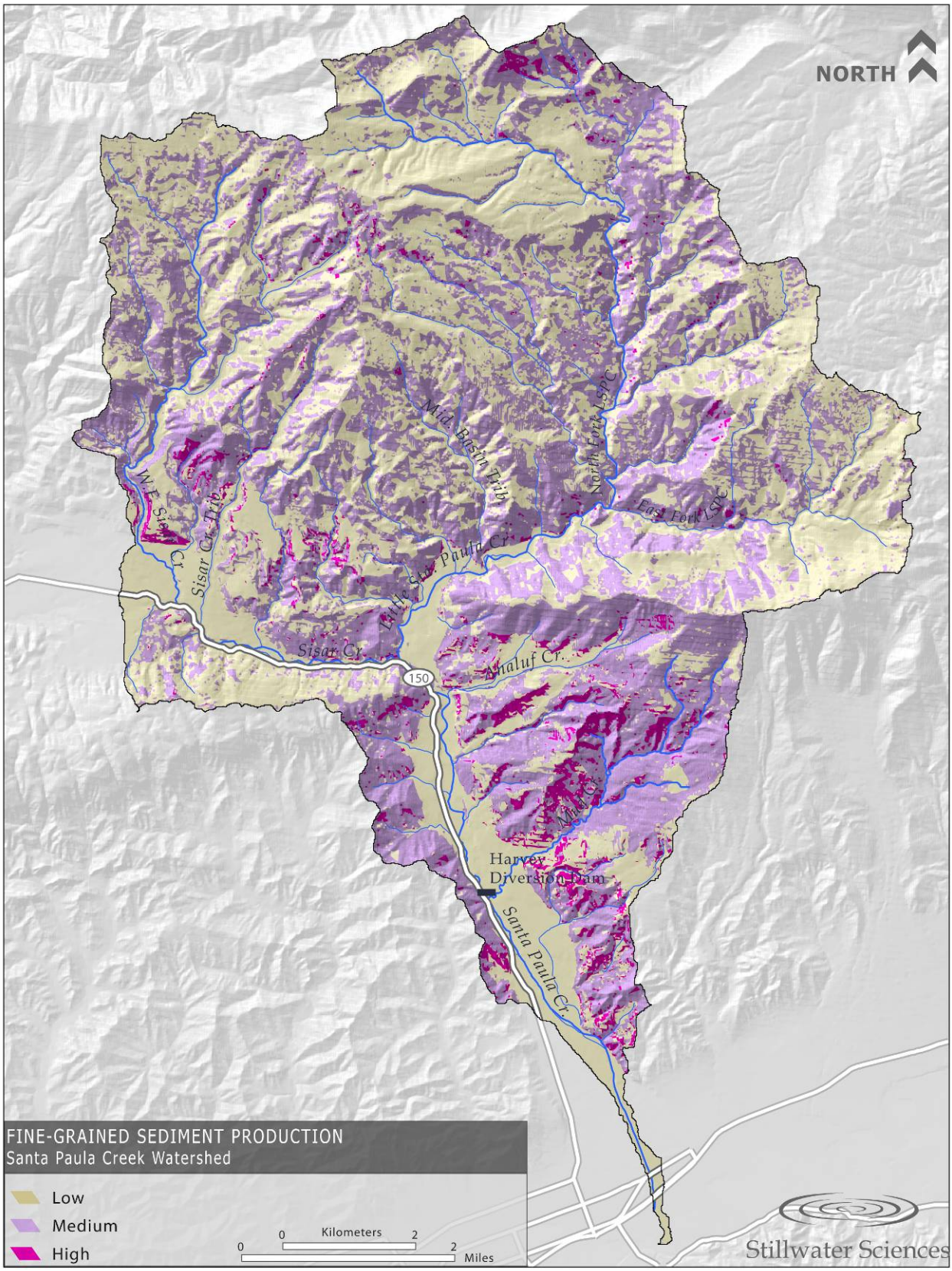

Figure 2-12. Fine grained sediment production in Santa Paula Creek watershed.

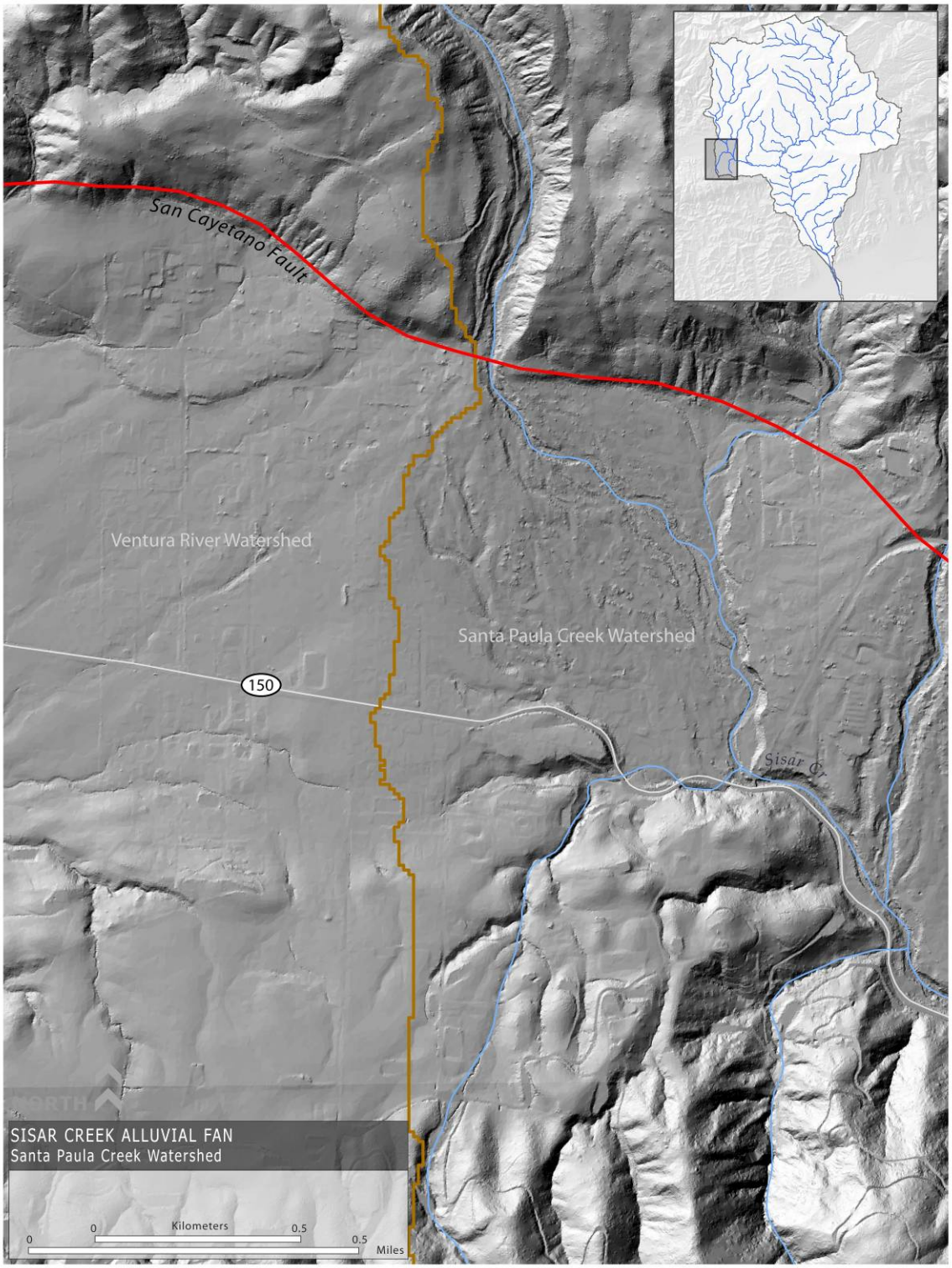

Figure 2-13. Sisar Creek (and, to the east, lower Bear Creek) at their emergence from the rangefront. A broad alluvial fan has developed from the high sediment load of these channels that cannot be transported along the lower gradient of the valley. Based on the pattern of channel features in the western half of this image, Sisar Creek has obviously flowed both east to Santa Paula Creek (as, at present) and to the west across the current watershed divide (irregular north-south brown line in figure).

Figure 2-14. Sandstone source in the eroding unconsolidated terraces flanking lower Santa Paula Creek.

Figure 2-15. Sandstone interbeds of the shale-dominated Cozy Dell Formation (foreground). The Coldwater Sandstone formation is visible in the middle distance along the same ridge.

Figure 2-16. Sandstone production in Santa Paula Creek watershed.

Figure 2-17. Santa Paula Creek crossing of the San Cayetano fault. Dashed lines show mapped strands; the dotted line is unmapped but is strongly suggested by the pattern of bedrock outcrops. Over the course of about 1 km, the transported sediment load of the channel is apparently reduced by a substantial fraction, as indicated by the width of the active meander/braid belt upstream of each valley narrowing. Assessing tectonic-related changes in transport through this reach is confounded by the correspondence of the southern-most fault crossing with the Highway 150 bridge.

Figure 2-18. Recent scour of Santa Paula Creek associated with bedload-transport-restricting structures and presumably expressing an imbalance between transport capacity and sediment supply (a) below the lower Highway 150 crossing; and (b) below the Harvey Diversion Dam.

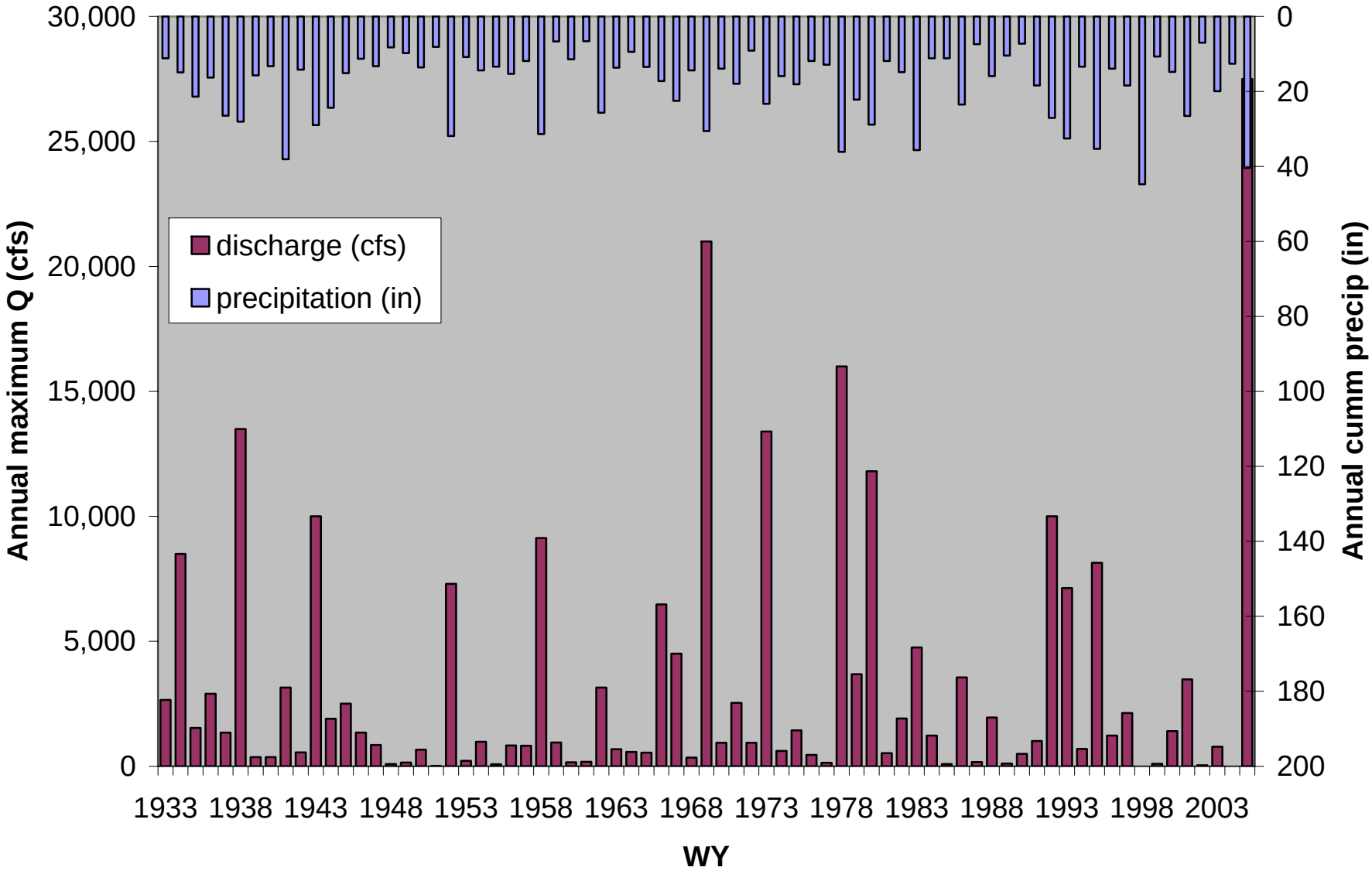

Figure 3-1. Annual discharge and precipitation data for Santa Paula Creek at Santa Paula. Discharge is from USGS gage 11113500 and precipitation is from VCWPD gage 254A.

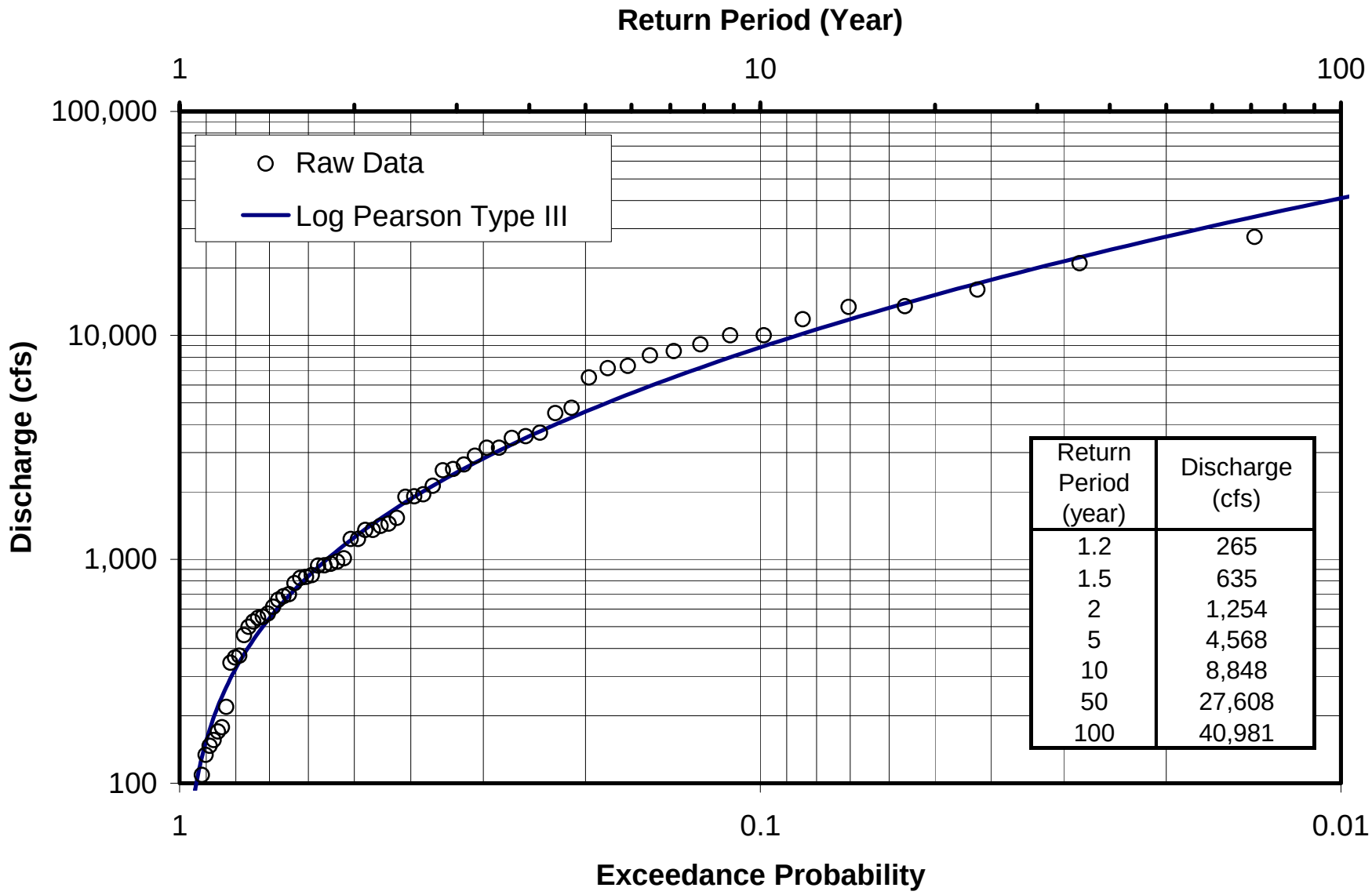

Figure 3-2. Flood frequency curve for Santa Paula Creek at Santa Paula (WY 1933–2005) [USGS gage 11113500].

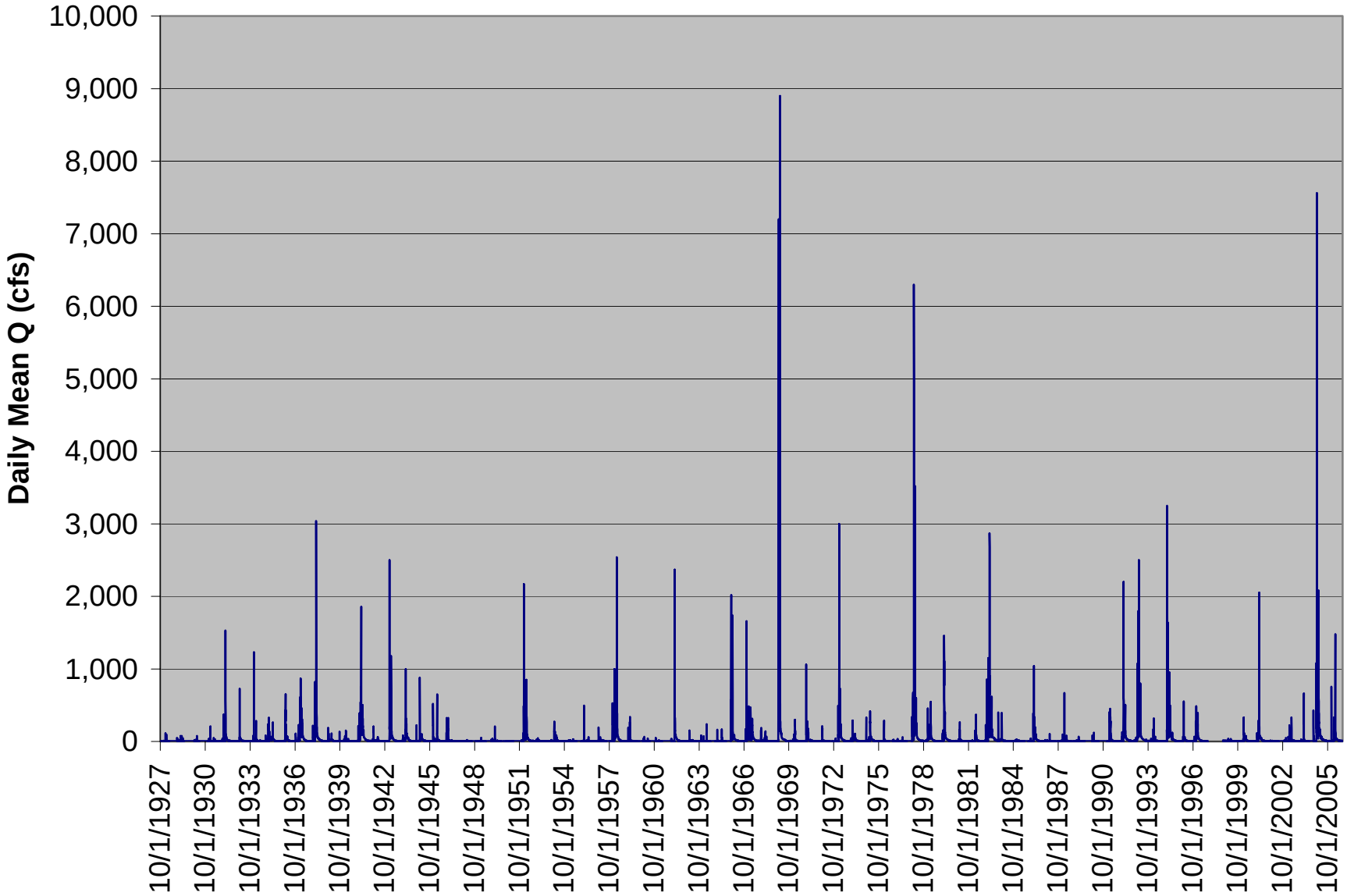

Figure 3-3. Daily mean discharge Santa Paula Creek at Santa Paula [USGS gage 11113500].

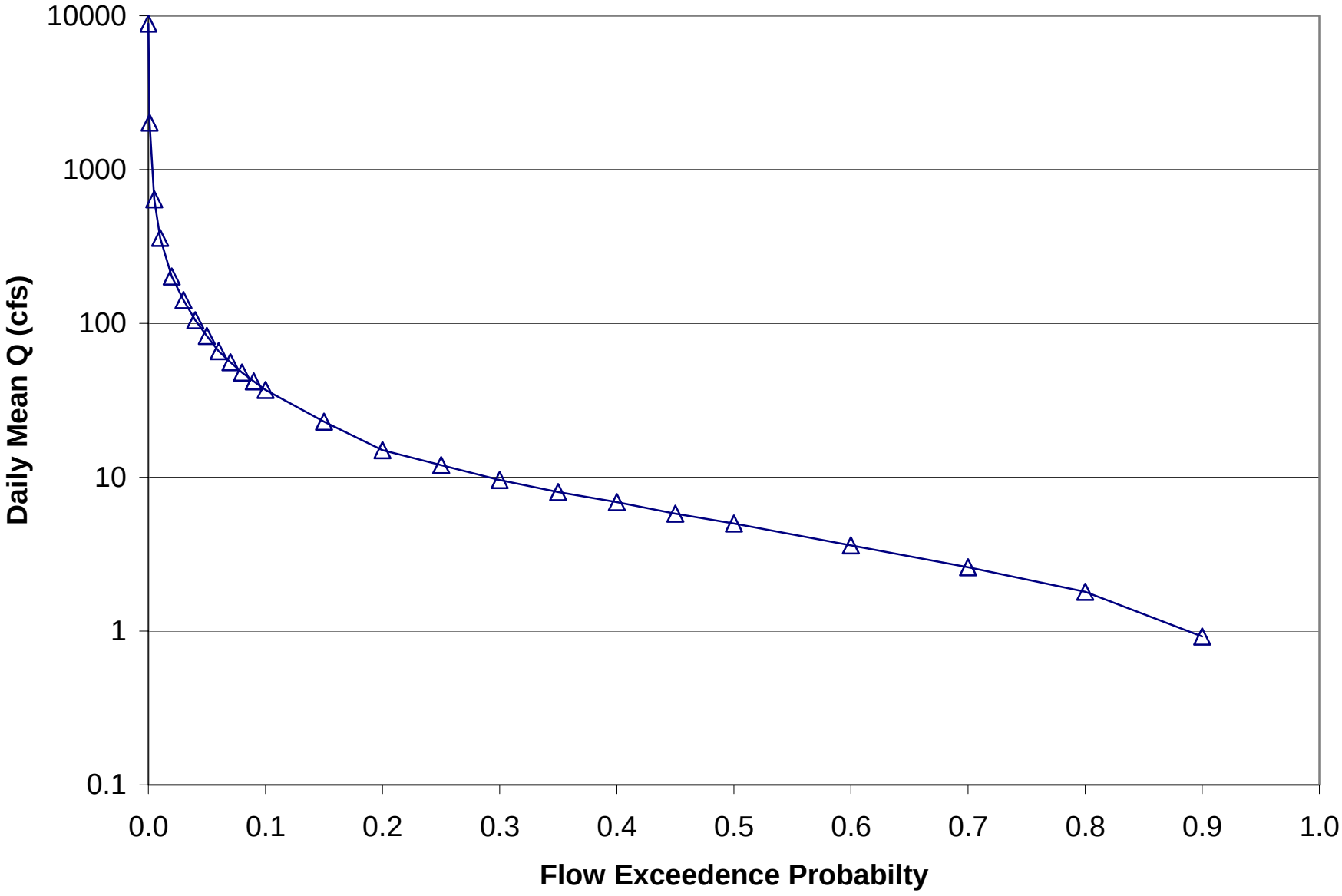

Figure 3-4. Daily mean flow exceedence probability for Santa Paula Creek at Santa Paula [USGS gage 11113500].

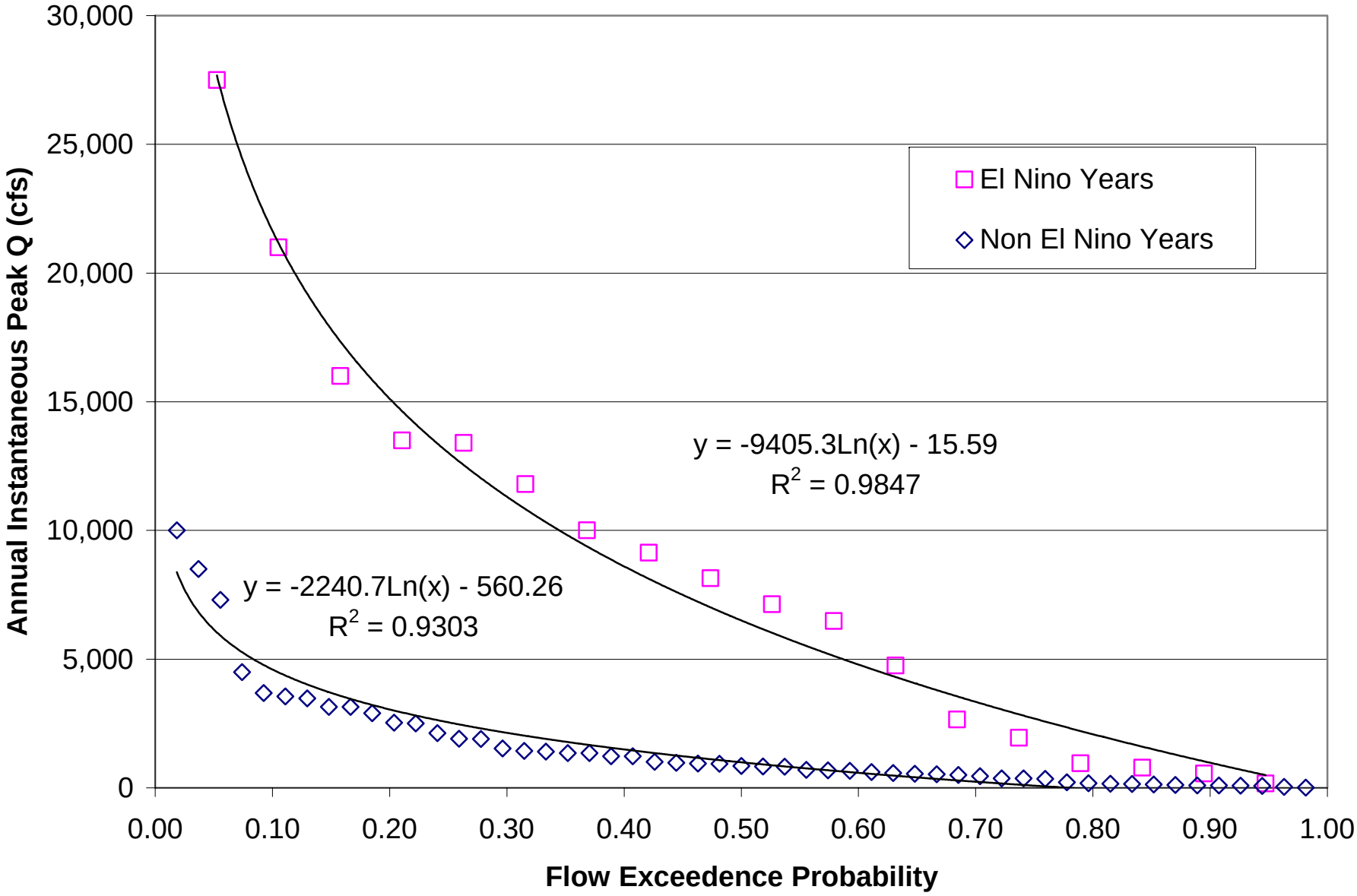

Figure 3-5. Flow exceedence for El Nino/non-El Nino years (WY 1933–2005) for Santa Paula Creek at Santa Paula [USGS gage 11113500].

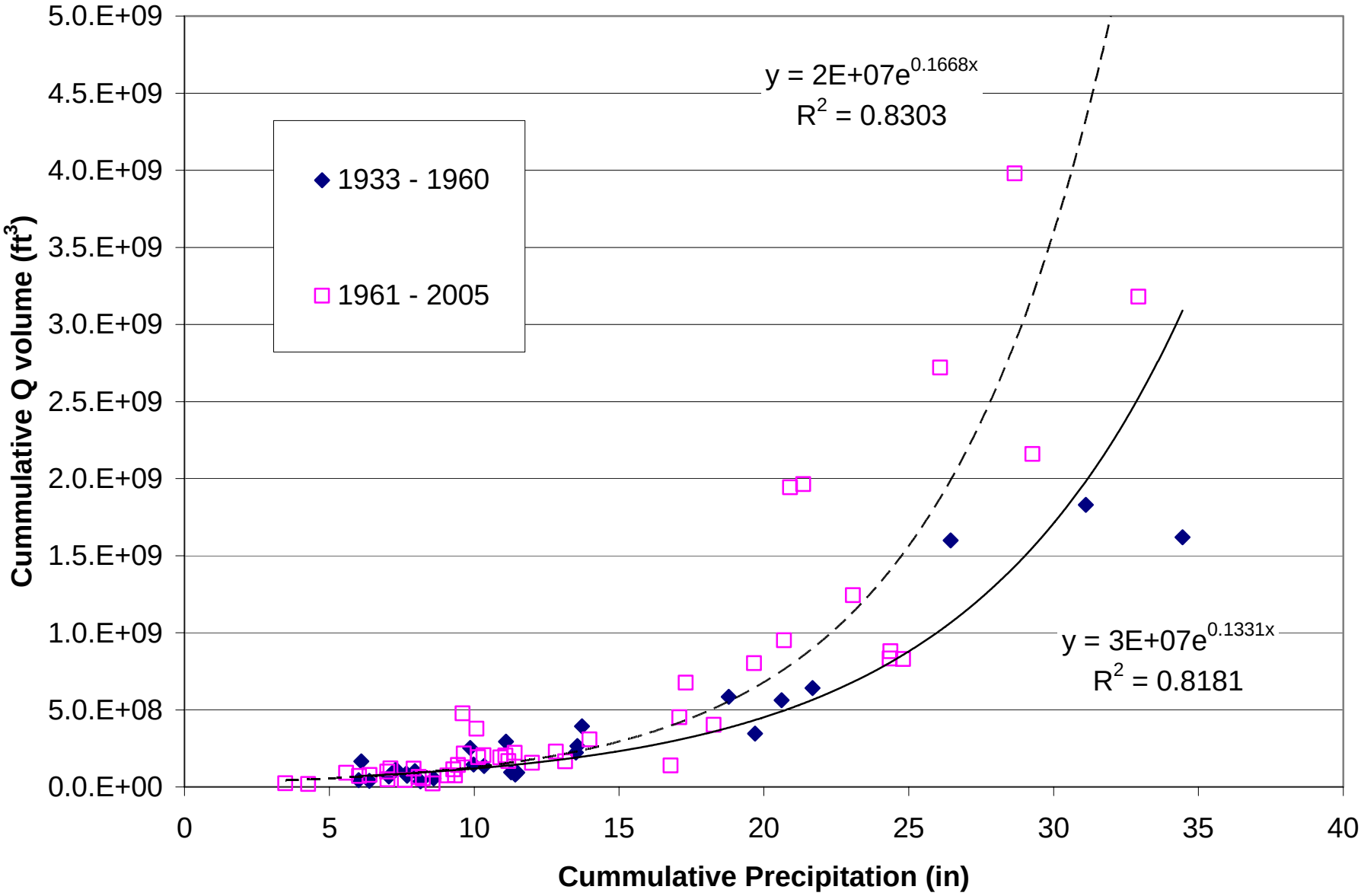

Figure 3-6. Relationship between cumulative discharge and precipitation (WY 1933–2005) for Santa Paula Creek at Santa Paula [USGS gage 11113500].

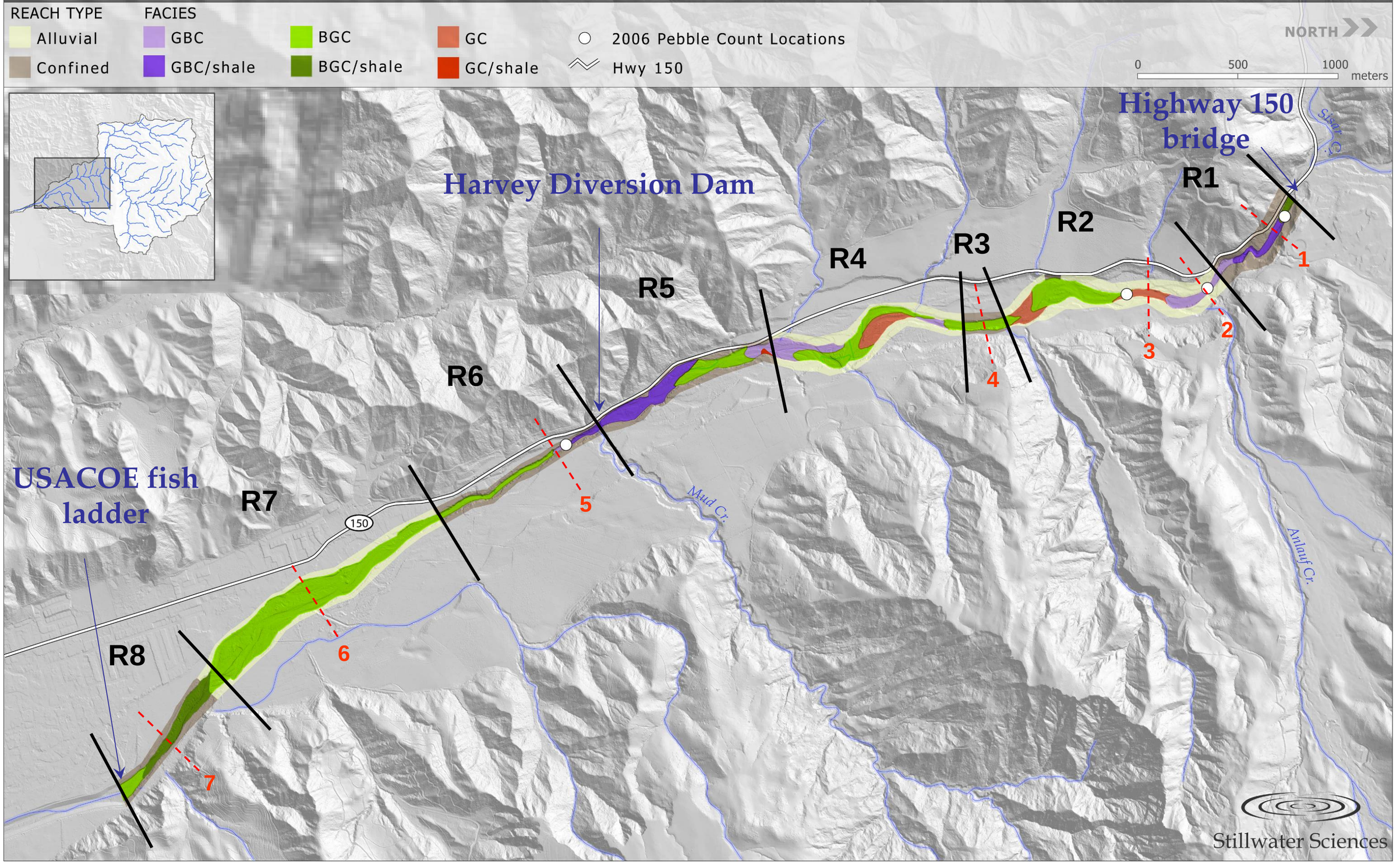

Figure 3-7. Plan view of the Santa Paula Creek watershed from the Highway 150 bridge crossing to the USACOE fish ladder including a facies map and pebble count locations (points), reach delineations (solid lines), and cross-sections where critical discharge for mobilizing coarse sediment was calculated (dashed lines).

Figure 3-8. At the upstream end of R1 looking downstream

Figure 3-9. In the middle of R2 looking downstream.

Figure 3-10. At the upstream end of R3 looking downstream.

Figure 3-11. In the middle of R4 looking downstream.

Figure 3-12. In the middle of R5 looking downstream.

Figure 3-13. At the upstream end of R6 looking downstream.

Figure 3-14. In the middle of R7 looking downstream.

Figure 3-15. At the downstream end of R8 looking upstream.

Figure 3-16. Looking upstream at Highway 150 bridge.

Figure 3-17. Looking upstream at Highway 150 grade control structure and channel incision.

Figure 3-18. Looking downstream at the Southern Pacific Transportation Company (SPTC) truss bridge.

Figure 3-19. Looking downstream at Telegraph Avenue bridge.

Figure 3-20. Looking upstream at damage to Harvey Diversion Dam following 2005 storm event.

Figure 3-21. Looking downstream at Harvey Diversion Dam fish ladder.

Figure 3-22. Looking upstream at US Army Corp of Engineers (USACOE) fish ladder.

Figure 3-23. Looking downstream at right bank spur dikes in R4.

Figure 3-24. Looking downstream at channel realignment in R5.

Figure 3-25. Looking downstream at boulder steps below Harvey Diversion Dam.

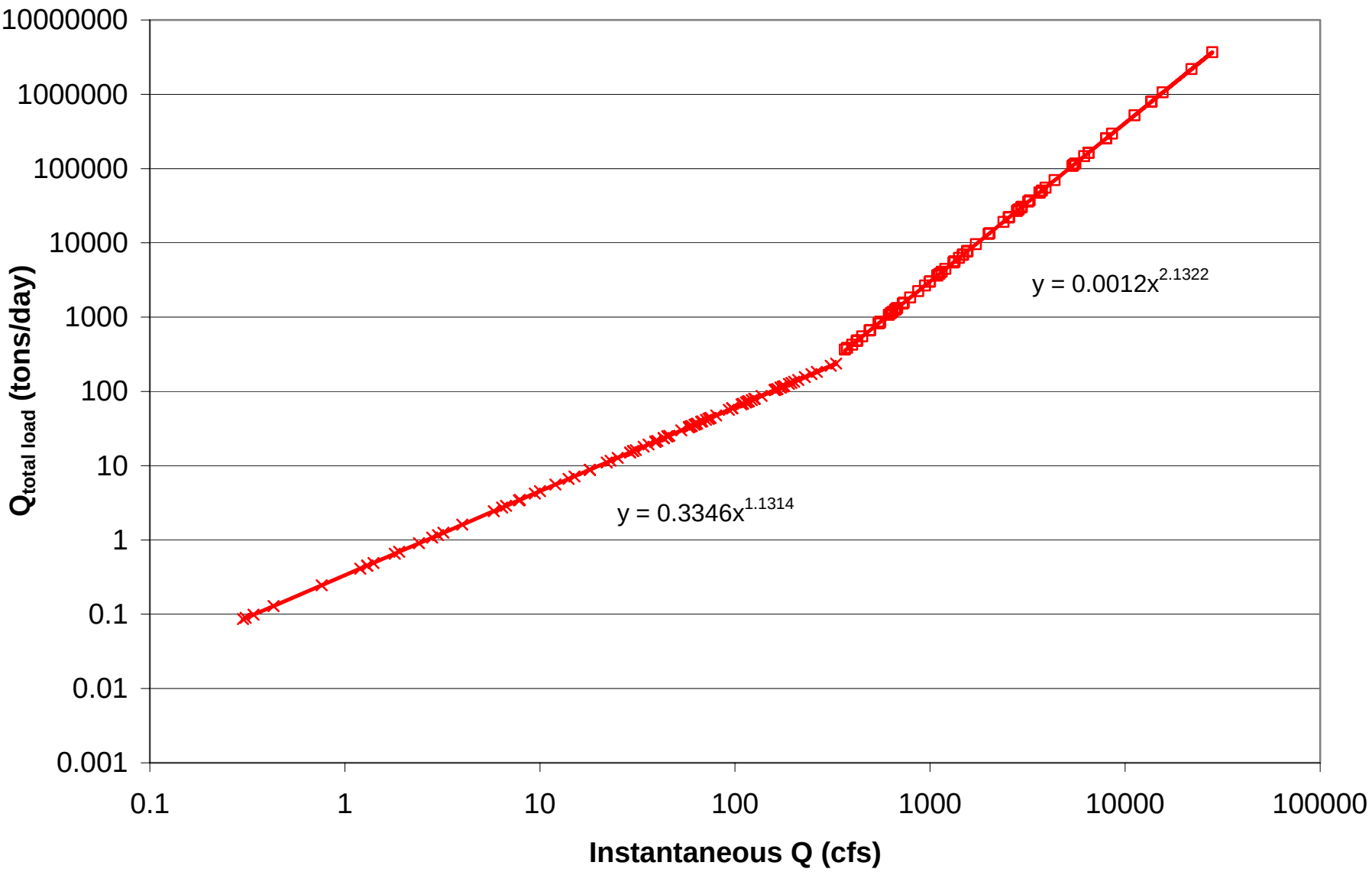

Figure 3-26. Sediment rating curve (suspended sediment load + bedload) for Sespe Creek at Fillmore [USGS gage 11113000] used to determined sediment yield within Santa Paula Creek.

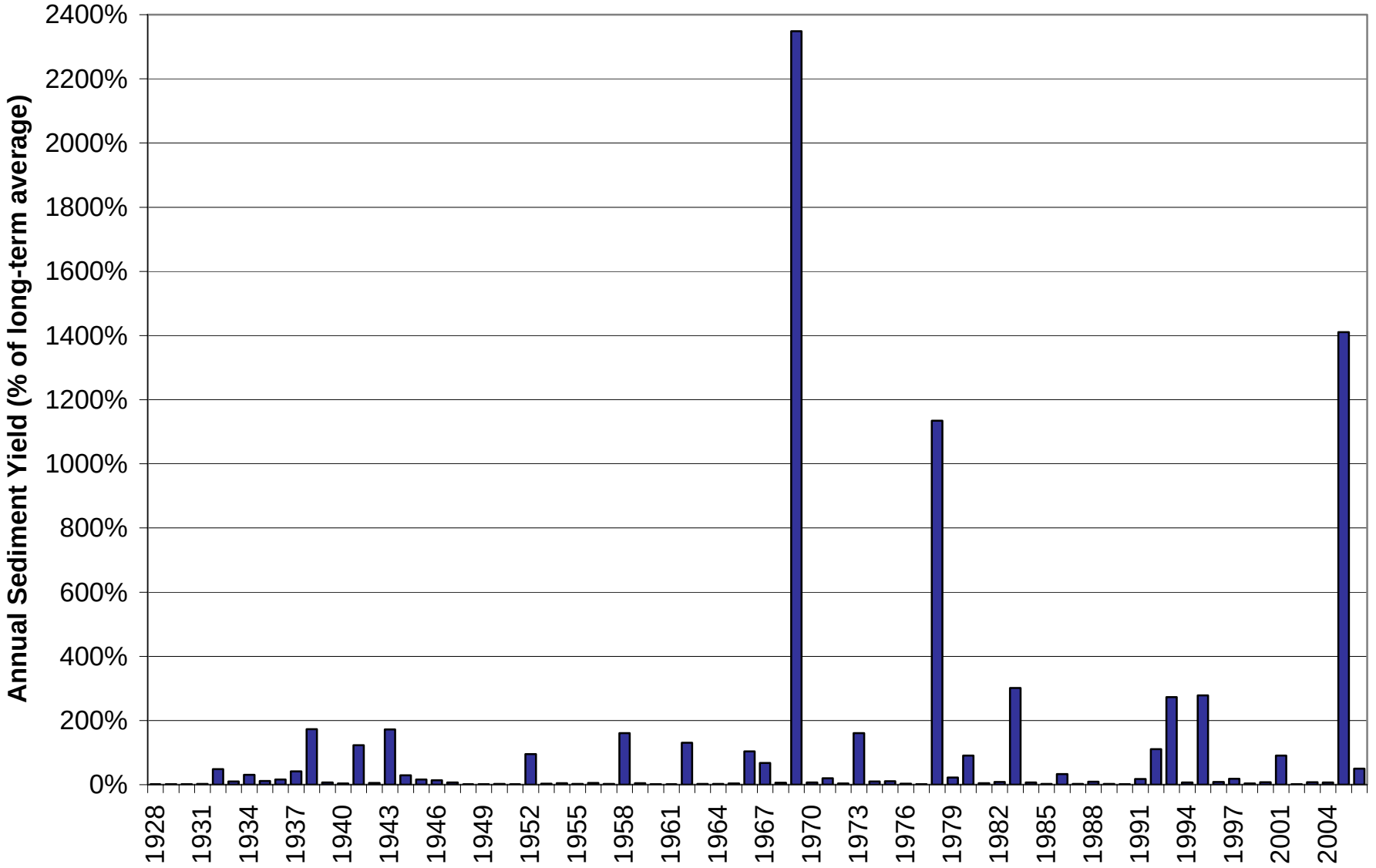

Figure 3-27. Calculated total sediment yield (as percentage of the long-term average) for Santa Paula Creek at Santa Paula [USGS gage 11113500] using Sespe Creek at Fillmore [USGS gage 11113000] sediment rating curve.

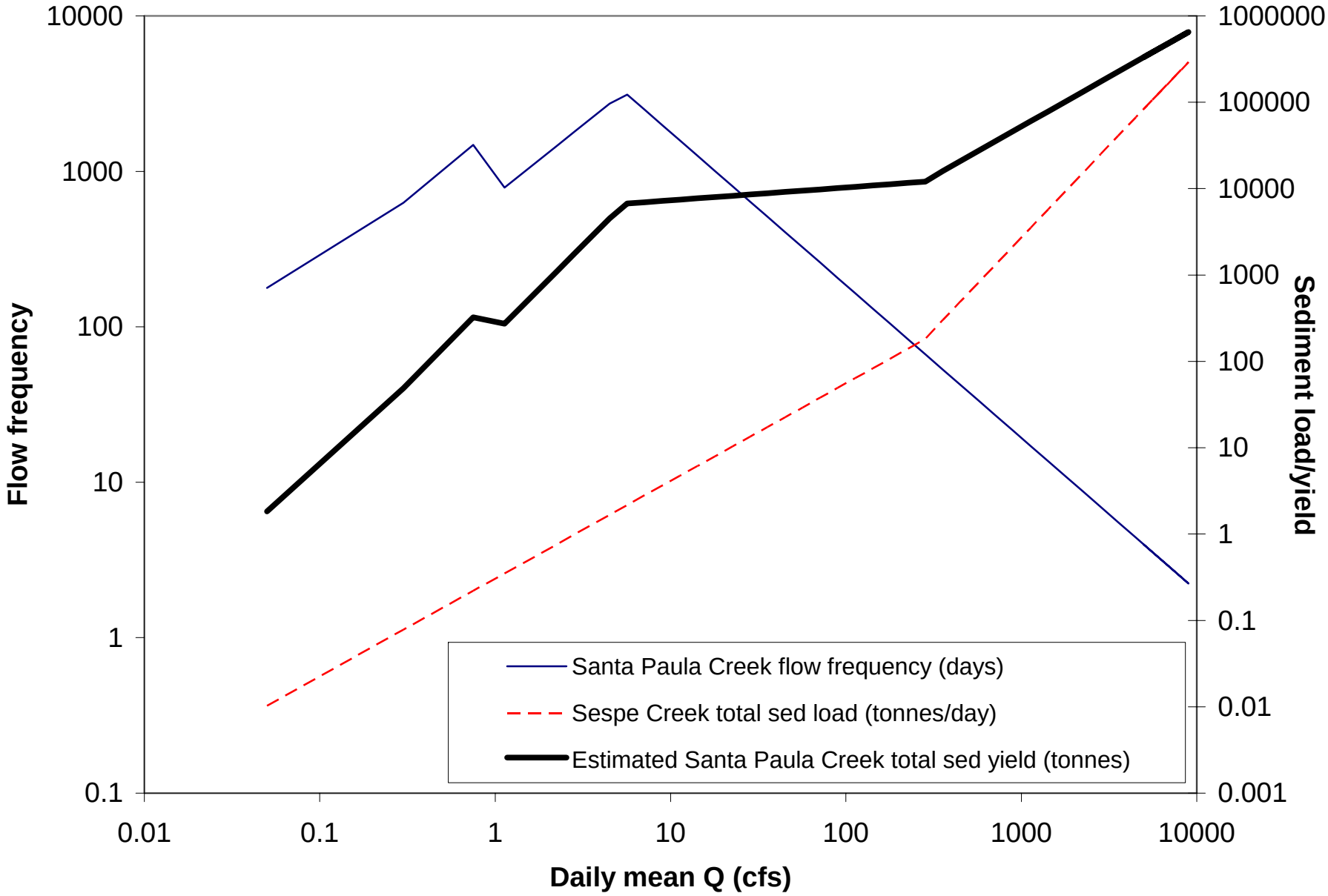

Figure 3-28. Flow frequency and total sediment load (suspended sediment + bedload) as functions of daily mean flow for Santa Paula Creek at Santa Paula [USGS gage 11113500] and sediment discharge for Sespe Creek at Fillmore [USGS gage 11113000].

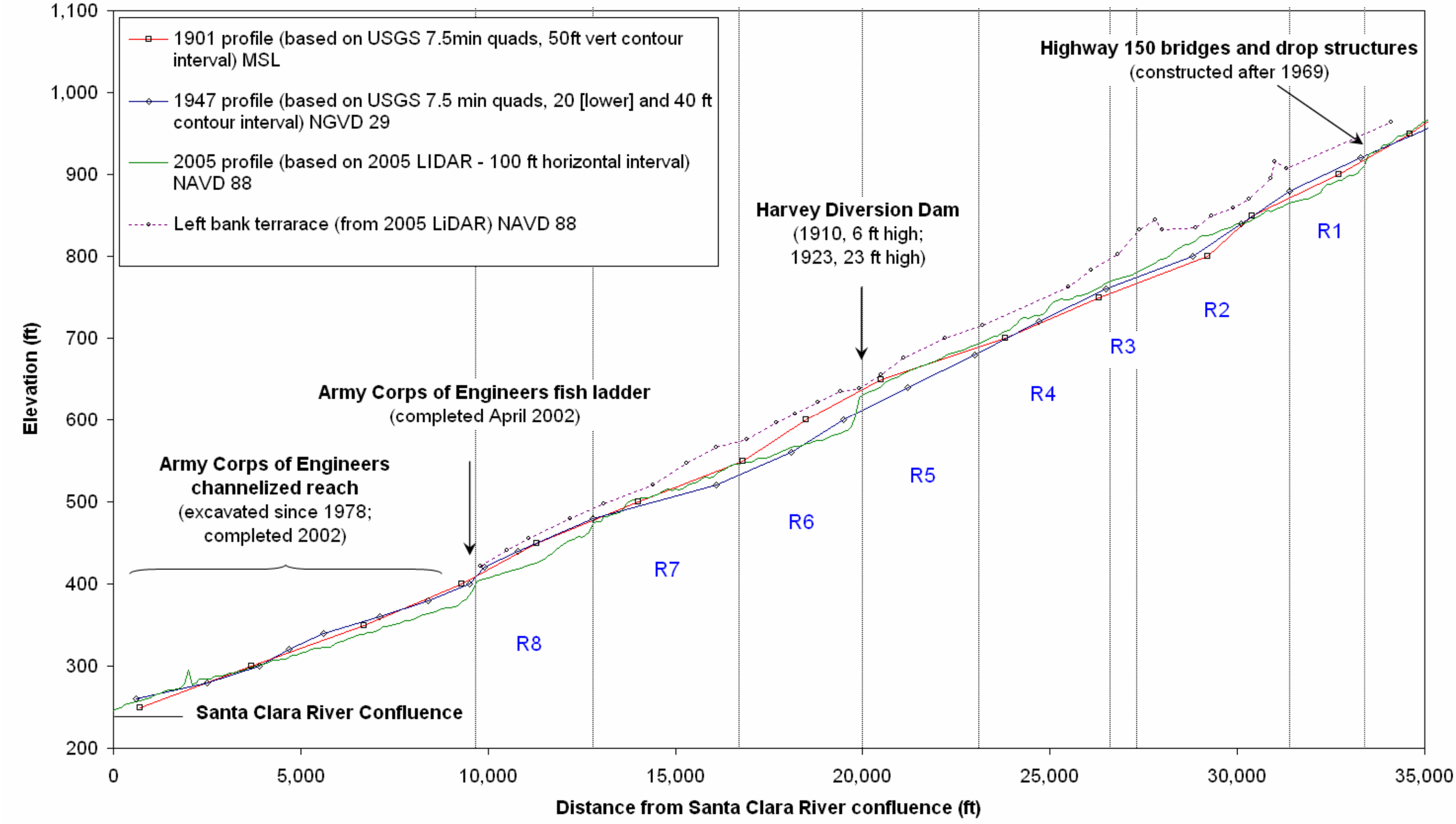

Figure 3-29. Longitudinal profiles (1901, 1947, and 2005) for Santa Paula Creek from the Highway 150 bridge to the confluence with the Santa Clara River.

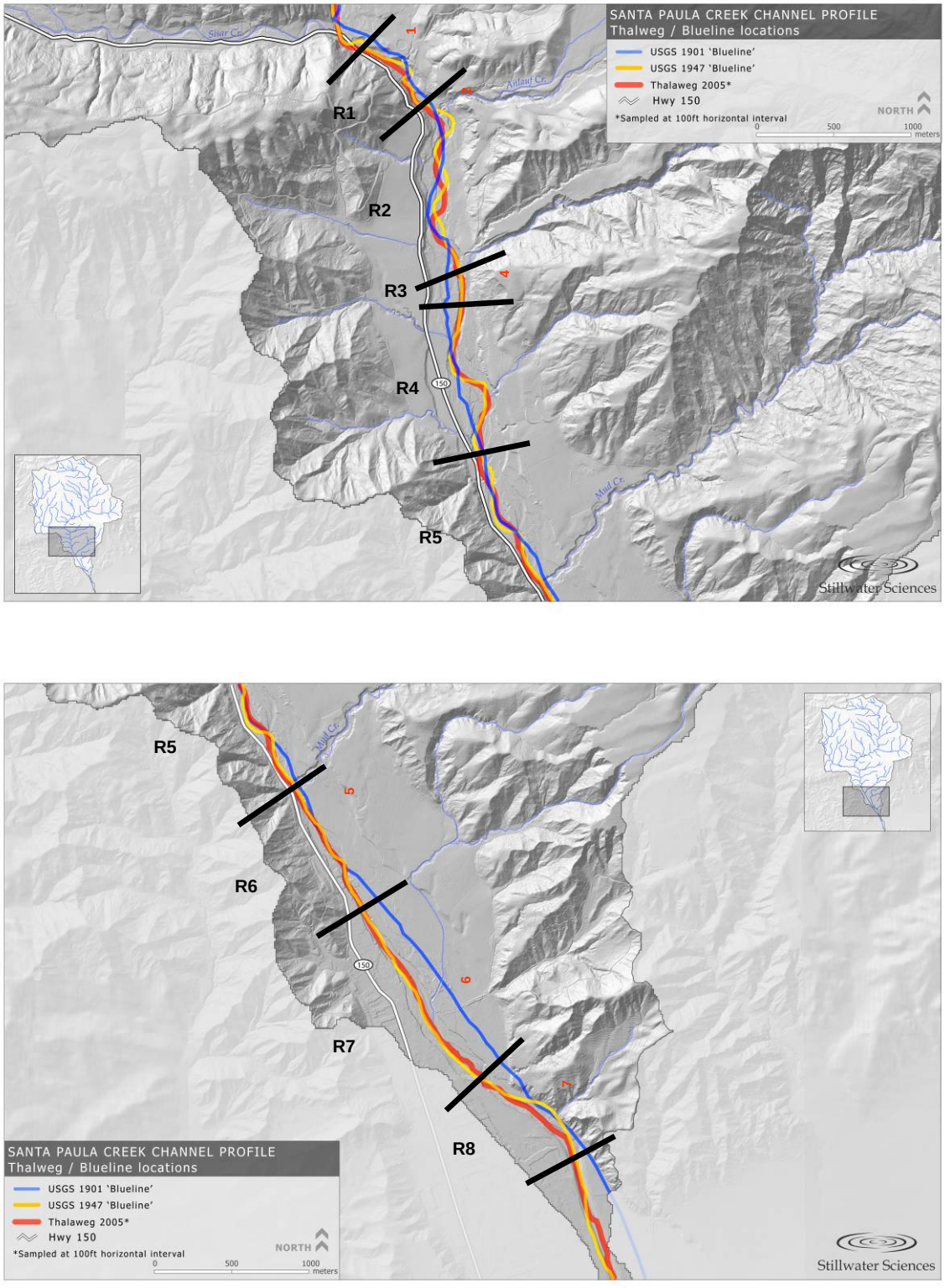

Figure 3-30. Historic (1901 and 1947) and current (2005) channel thalweg location from (a) the Sisar Creek confluence to Mud Creek confluence, and (b) the Mud Creek confluence to USACOE fish ladder.

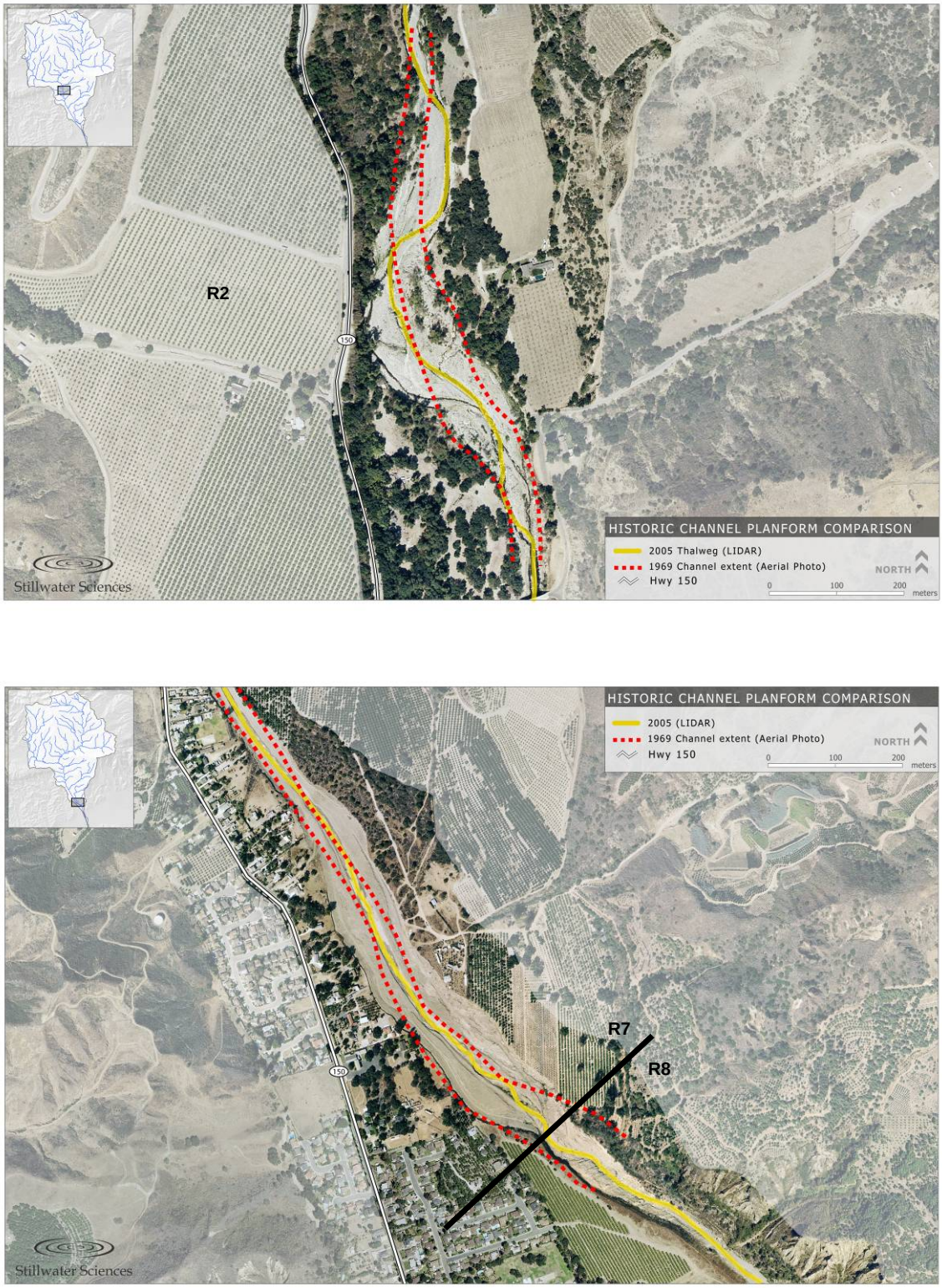

Figure 3-31. Historic (1969) and current (2005) channel width in (a) R2 and (b) R7/R8.

Figure 3-32. Aerial photographs of R8 in (a) 1969 and (b) 2005.

APPENDICES

Appendix A

Process Domain Analysis

Figure A-1. Bedrock units in Santa Paula Creek watershed.

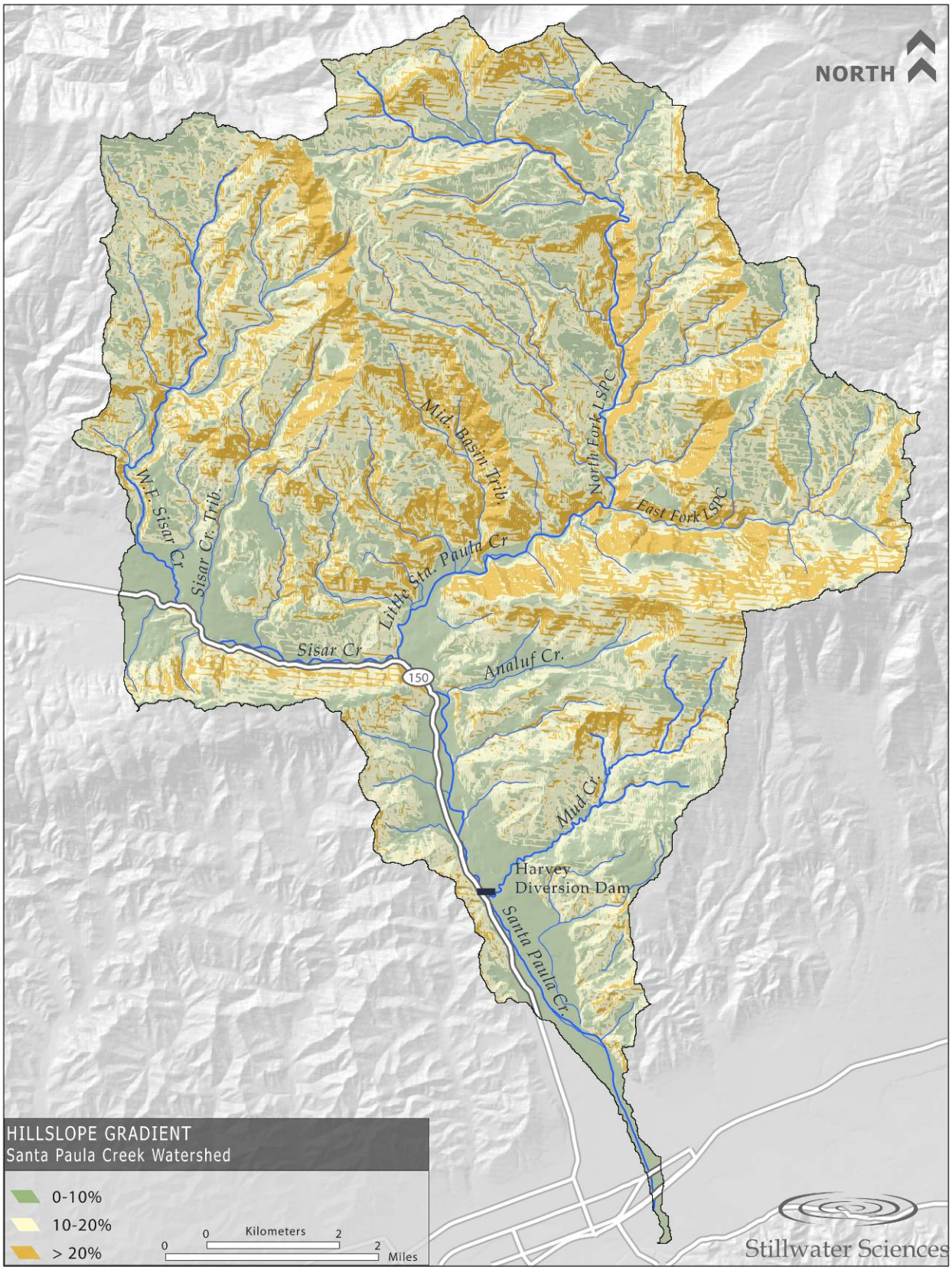

Figure A-2. Hillslope gradient in Santa Paula Creek watershed.

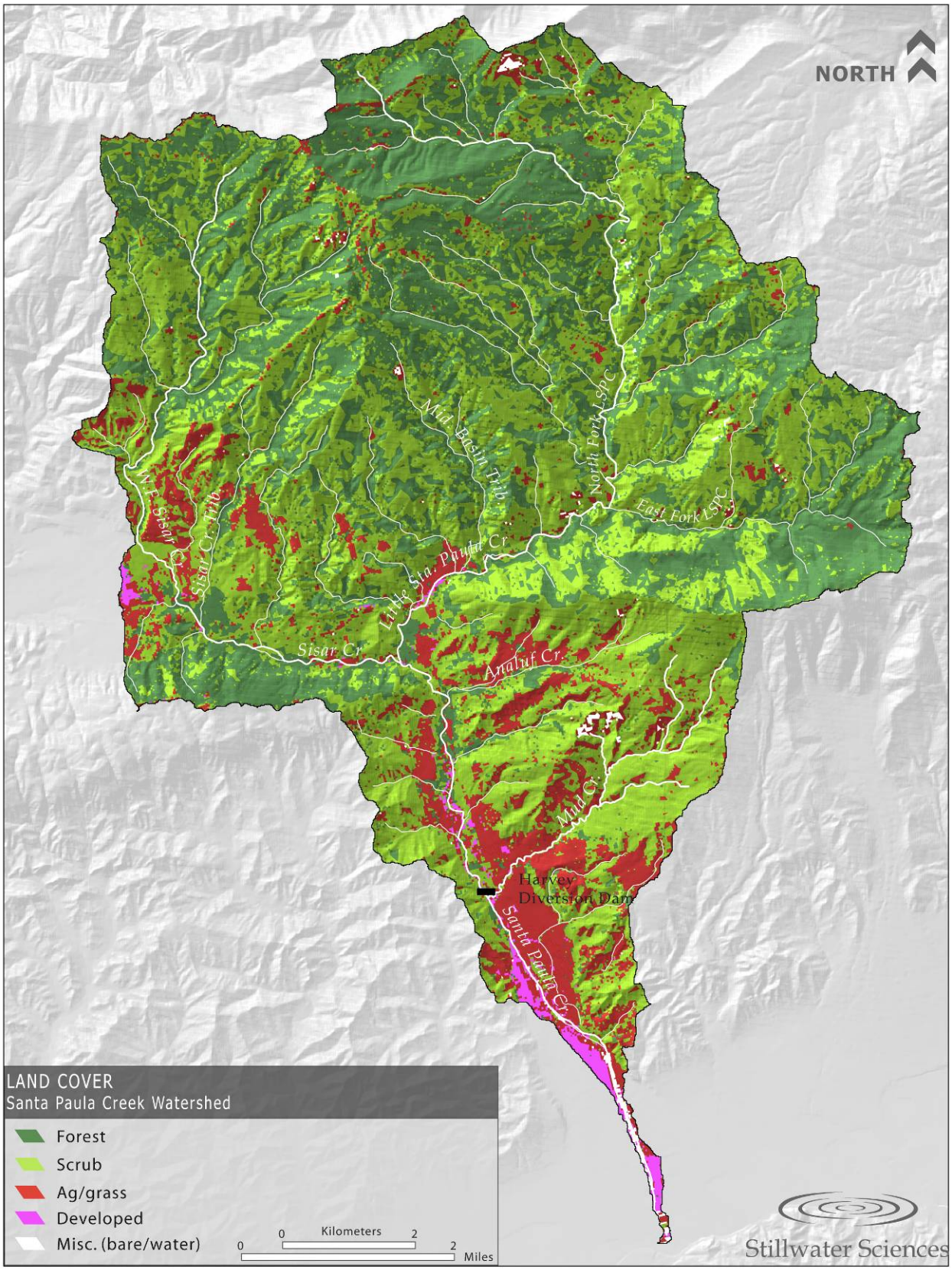

Figure A-3. Landcover in Santa Paula Creek watershed.

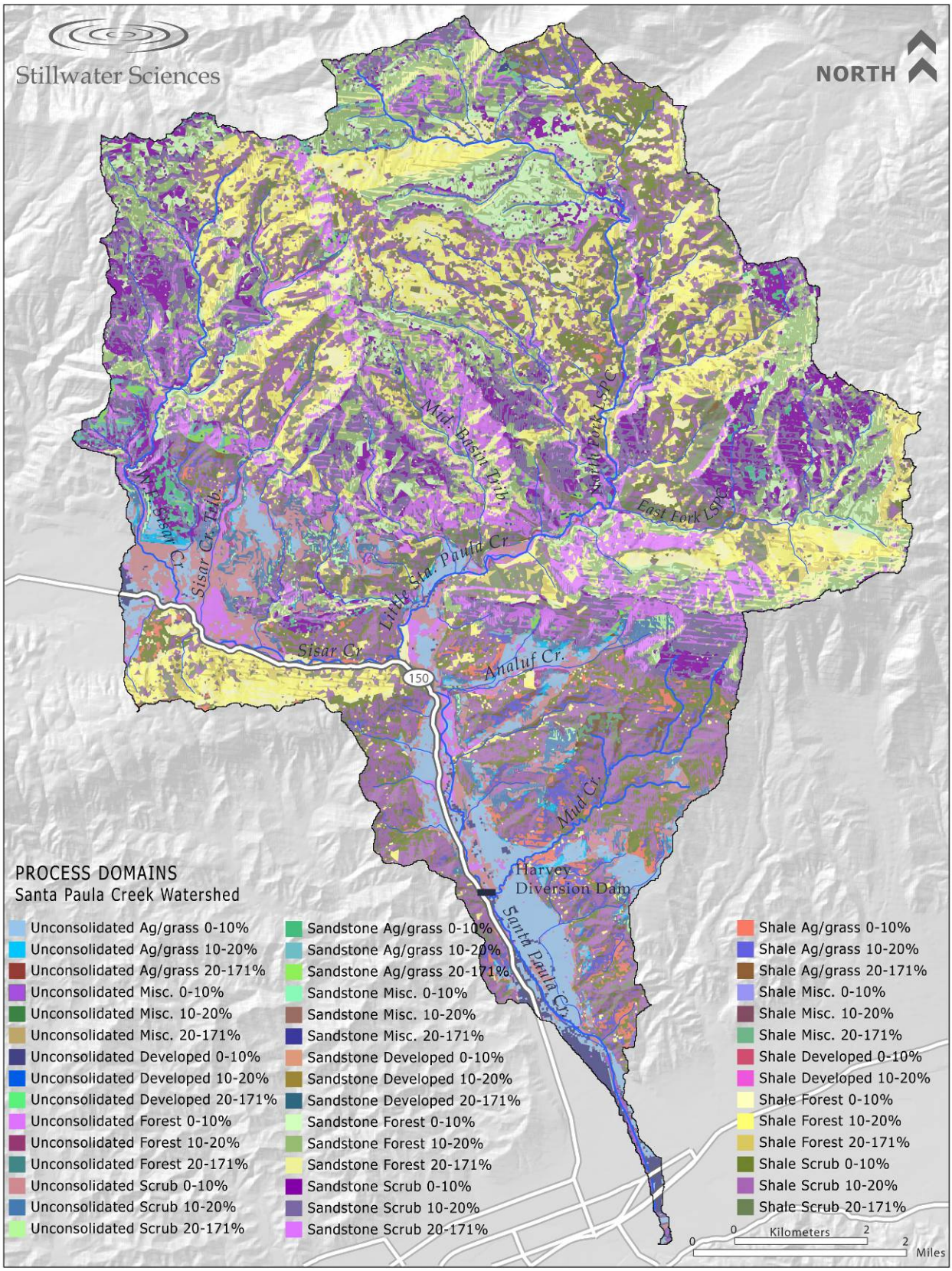

Figure A-4. Process domains in Santa Paula Creek watershed.

Appendix B

Facies Mapping

Mapping of sedimentary facies throughout the Santa Paula Creek study reach (Sisar Creek confluence/Highway 150 bridge to the USACE channelized reach) involved delineating distinct units of surface sediment mixtures. The facies mapping method used for this study was based on the methodology devised by Buffington and Montgomery (1999) for mapping short reaches (20–50 m). To be applicable to a 7.2-km long reach, the Buffington and Montgomery (1999) methodology was modified to capture a coarser classification of sedimentary facies. Within the facies classification, the surface was classified according to the proportional occurrence of the five most prevalent substrate types (sand [S], gravel [G], cobble [C], boulder [B], and bedrock [br]) (see Table B-1). The qualifying criteria for a substrate type to be included in a facie classification were that an individual substrate type comprised ≥5% of the surface facies, or that the two sub-ordinate classes together comprised ≥10%. Where the qualifying criteria were not met, the surface was classified according to the one or two most frequent substrate types, with the dominant substrate type being listed last (*e.g.*, cobble [C] if cobble comprised more than 95% of the material or gravelly cobble [GC] if gravel comprised at least 5% of the bed material and cobble comprised the remaining bed material and no other substrate type represented more than 5% of the surface area).

Table B-1. Size classes for each particle type used for facies mapping.

Size class	Grain size (mm)
Boulder	
very coarse	2048–4096
coarse	1024–2048
medium	512–1024
fine	256–512
Cobble	
coarse	128–256
fine	64–128
Gravel	
very coarse	32–64
coarse	16–32
medium	8–16
fine	4–8
very fine	2–4
Sand	0.0625–2

Wolman (1954) pebble counts were conducted to assist in field determination of sedimentary facies and to chronicle the actual grain size distributions of individual facies within the reach. The intermediate (b) axis of 100 surface bed particles was measured at 4 locations within the study reach. The relative proportion of each grain class was determined in the field to then guide the classification of facies units with the same visual characteristics. The pebble count data for each location were compiled into particle size distributions so that representative grain size fractions could be extracted (see Figure B-1). After filtering the field data, facies and particle size distribution information were entered into a database and transferred to a GIS format.

References

Buffington, J.M., and D.R. Montgomery. 1999. A procedure for classifying textural facies in gravel-bed rivers. Water Resources Research, 35: 1903-1914.

Wolman, G.M. 1954. A method of sampling coarse river-bed material. Transactions of the American Geophysical Union, 35: 951-956.

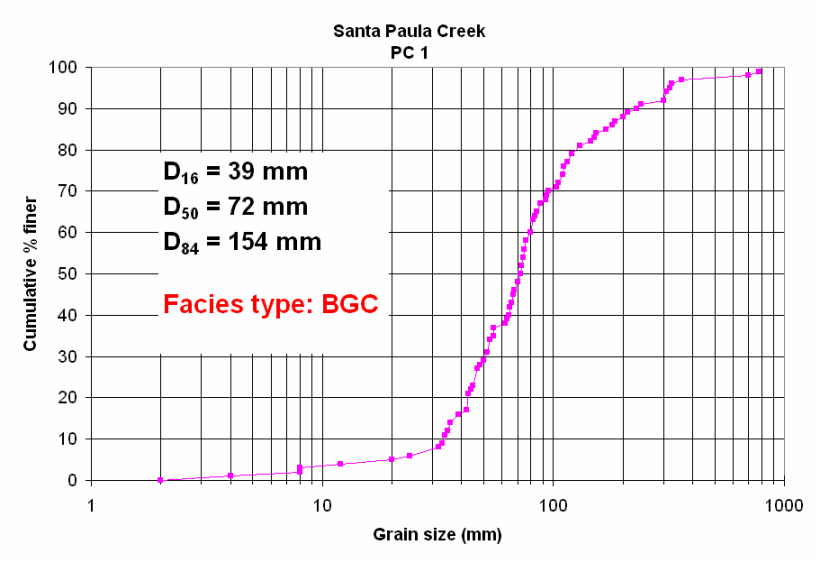

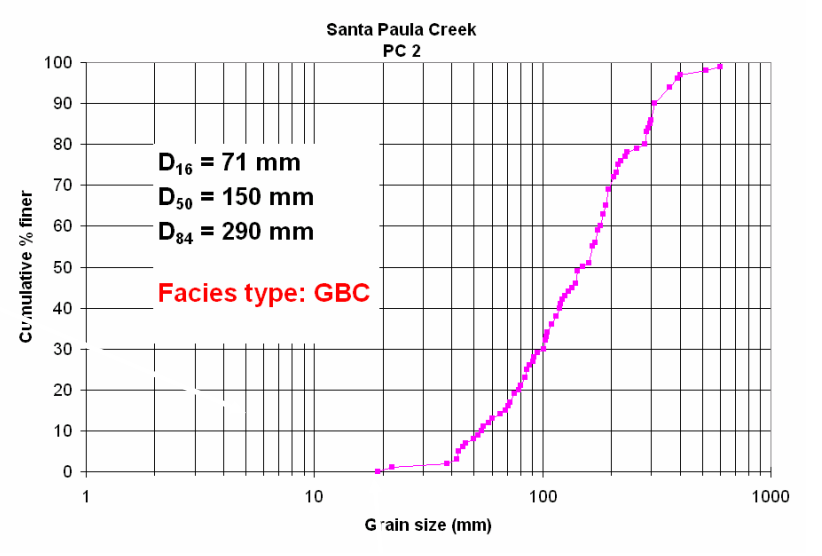

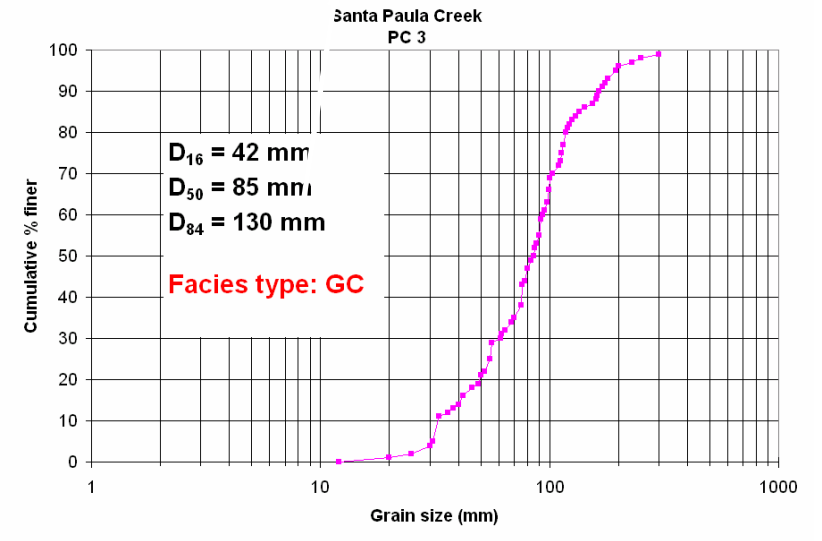

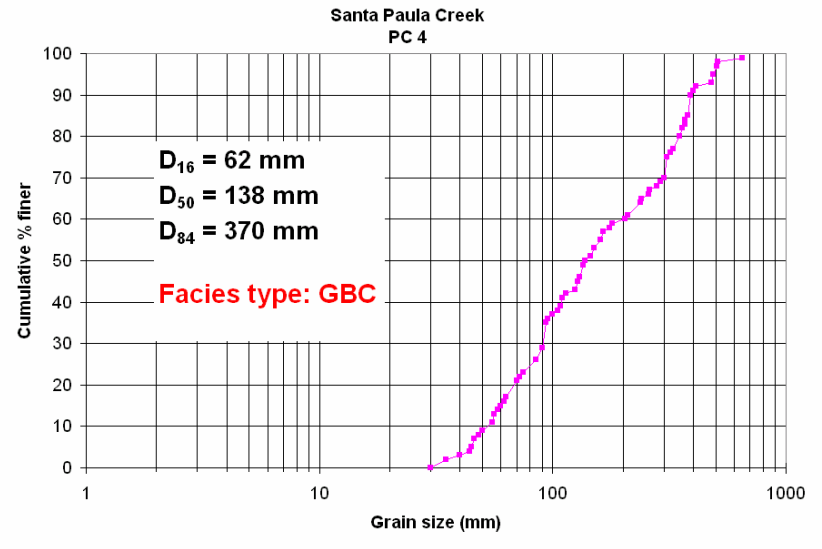

Figure B-1. Particle size distributions derived from pebble count (PC) data. Numbering for pebble counts increases in a downstream direction (*i.e.*, PC 1 is the most upstream pebble count and PC 4 is the most downstream pebble count).